

1-1-2013

# Impact Damage Analysis Of Balsa Wood Sandwich Composite Materials

Suof Abdalslam  
*Wayne State University,*

Follow this and additional works at: [http://digitalcommons.wayne.edu/oa\\_dissertations](http://digitalcommons.wayne.edu/oa_dissertations)



Part of the [Mechanical Engineering Commons](#)

---

## Recommended Citation

Abdalslam, Suof, "Impact Damage Analysis Of Balsa Wood Sandwich Composite Materials" (2013). *Wayne State University Dissertations*. Paper 743.

**IMPACT DAMAGE ANALYSIS OF BALSAWOOD SANDWICH  
COMPOSITE MATERIALS**

by

**SUOF OMRAN ABDALSLAM**

**DISSERTATION**

Submitted to the Graduate School

of Wayne State University,

Detroit, Michigan

in partial fulfillment of the requirements

for the degree of

**DOCTOR OF PHILOSOPHY**

**2013**

MAJOR: MECHANICAL ENGINEERING

Approved by:

\_\_\_\_\_  
Advisor

\_\_\_\_\_  
Date

\_\_\_\_\_  
\_\_\_\_\_  
\_\_\_\_\_

## **DEDICATION**

To my parents who had me in all their prayers.

To my wife and my children for being great pillars of support during the completion of my study.

## **ACKNOWLEDGMENTS**

I have been so lucky to have professor Newaz as my adviser, huge thanks for your guidance and advice throughout the time I spent under your supervision. I would like to thank my committee members' professor E.O. Ayorinde, professor Wen Li and professor Hwai-Chung Wu for giving their valuable time to serve in the examination committee and evaluate my thesis. I would also like to thank Dr. Mohammad Hailat for his helping to conduct the experimental work. My thanks also to all my colleagues in the advanced composite lab and all my friends whose support was very valuable during my Ph.D.'s study at WSU.

This research work was funded through DOE's Lightweight Automotive Materials Program (LAMP) administered by NCMS (Mr. Steven Hale – Program Manager). I acknowledge Jim Dallam and Daniel Allman of MAG-ias for the composite skin prepreg's that were provided. Also, I thank Robert Graybill of Nimbis Services for providing access to OSC HPC portal for the FE analysis.

SUOF OMRAN ABDALSLAM

# TABLE OF CONTENTS

|  |             |
|--|-------------|
| <b>Dedication.....</b>   | <b>ii</b>   |
| <b>Acknowledgments.....</b>  | <b>iii</b>  |
| <b>List of Tables .....</b>  | <b>vii</b>  |
| <b>List of Figures .....</b>   | <b>viii</b> |
| <b>CHAPTER 1: INTRODUCTION .....</b>                                   | <b>1</b>    |
| <b>1.1 SANDWICH COMPOSITES.....</b>                                    | <b>1</b>    |
| 1.1.1 SKIN.....  | 5           |
| 1.1.2 CORE.....  | 6           |
| <b>1.2 MANUFACTURING.....</b>  | <b>8</b>    |
| <b>1.3 LOW VELOCITY IMPACT AND COMPRESSION AFTER IMPACT TESTS...11</b> |             |
| <b>CHAPTER 2: LITERATURE REVIEW AND OBJECTIVES.....</b>                | <b>12</b>   |
| <b>2.1 LITERATURE REVIEW .....</b>                                     | <b>12</b>   |
| 2.1.1 COMPOSITE LAMINATE STRUCURE.....                                 | 12          |
| 2.1.2 COMPOSITE SANDWICH STRUCTURE.....                                | 15          |
| <b>2.2 OBJECTIVES .....</b>  | <b>19</b>   |
| <b>CHAPTER 3: MATRIAL DESCRIPTION AND MATERIAL TESTING .....</b>       | <b>20</b>   |
| <b>3.1 MATERIAL COMPOSITION AND MATERIAL PREPARATION.....</b>          | <b>20</b>   |
| <b>3.2 MATERIAL TESTING .....</b>                                      | <b>22</b>   |
| 3.2.1 MECHANCAL PROPORTIES OF SANDWICH COMPOSITE .....                 | 22          |
| 3.2.2 IMPACT TEST .....  | 24          |
| 3.2.2.1 DROP-WEIGHT IMPACT TOWER .....                                 | 24          |

|  |           |
|--|-----------|
| 3.2.2.2 INSTRON 9250 HV IMPACT TESTING MACHINE.....  | 26        |
| 3.2.3 DAMAGE INSPECTION.....   | 27        |
| 3.2.3.1 END GRAIN SANDWICH COMPOSITE DAMAGE<br>INSPECTION.....                                     | 27        |
| 3.2.3.2 Balsa CORE SANDWICH COMPOSITE DAMAGE<br>INSPECTION.....                                    | 28        |
| 3.2.3.3 IMPACT ENERGY VERSUS DAMAGE AREA.....  | 28        |
| 3.2.4 COMPRESSION AFTER IMPACT (CAI) TEST.....   | 31        |
| 3.2.4.1 COMPRESSION AFTER IMPACT ALONG LENGTH.....   | 31        |
| 3.2.4.2 COMPRESSION AFTER IMPACT THROUGH THICKNESS.  | 33        |
| <b>CHAPTER 4: FINITE ELEMENT ANALYSIS (FEA) .....</b>  | <b>35</b> |
| <b>4.1 PROPERTIES OF SANDWICH COMPOSITE.....</b>   | <b>35</b> |
| <b>4.2 MODEL DEFINITION.....</b>   | <b>35</b> |
| <b>4.3 MODEL CREATION.....</b>   | <b>35</b> |
| <b>4.4 MESH GENERATION AND CONTACT DEFINITION .....</b>  | <b>36</b> |
| 4.4.1 IMPACT TEST SIMULATION FOR QUARTER OF END GRAIN<br>SANDWICH STRUCTURE.....                   | 36        |
| 4.4.2. IMPACT TEST SIMULATION FOR ENTIRE OF END GRAIN<br>AND REGULAR Balsa SANDWICH STRUCTURE..... | 37        |
| <b>4.5 SANDWICH COMPOSITE MATERIAL MODEL .....</b>   | <b>37</b> |
| <b>CHAPTER 5: RESULTS AND DISCUSSION.....</b>  | <b>40</b> |
| <b>5.1 EXPERIMENTAL RESULTS.....</b>   | <b>40</b> |
| 5.1.1 IMPACT TESTING.....  | 40        |

|   |           |
|---|-----------|
| 5.1.1.1 IMPACT TESTING BY DROP WEIGHT IMPACT<br>TOWER.....                                  | 40        |
| 5.1.1.2 IMPACT TESTING BY INSTRON 9250HV MACHINE.....                                       | 43        |
| 5.1.2 COMPRESSION AFTER IMPACT TESTING .....  | 52        |
| 5.1.2.1 FAILURE MODES OF SANDWICH COMPOSITES WITH<br>END GRAIN AND REGULAR Balsa CORES..... | 52        |
| 5.1.2.2 THE EFFECTS OF IMPACT ENERGY AND DAMAGE<br>AREA ON RESIDUAL STRENGTH.....           | 52        |
| 5.1.3 COMPRESSION AFTER IMPACT TESTING THROUGH<br>THICKNESS.....                            | 64        |
| <b>5.2 FINITE ELEMENT RESULTS.....</b>  | <b>67</b> |
| 5.2.1 QUARTER OF END GRAIN SANDWICH SYSTEM<br>SIMULATION.....                               | 67        |
| 5.2.2 END GRAIN AND REGULAR Balsa SANDWICH<br>SYSTEMS SIMULATION.....                       | 71        |
| <b>CHAPTER 6: CONCLUTIONS AND RECOMMENDATIONS.....</b>                                      | <b>74</b> |
| 6.1 CONCLUSIONS.....  | 74        |
| 6.2 RECOMMENDATIONS.....  | 76        |
| <b>References.....</b>  | <b>77</b> |
| <b>Abstract.....</b>  | <b>82</b> |
| <b>Autobiographical Statement.....</b>  | <b>84</b> |

## LIST OF TABLES

|   |    |
|---|----|
| Table 1.1 Structural efficiency of sandwich panels in terms of weight.....  | 3  |
| Table 1.2 Typical skin materials.....   | 6  |
| Table 1.3 Typical core materials.....   | 8  |
| Table 1.4 fabrication process for polymer matrix composites.....  | 9  |
| Table 3.1 sandwich composite core grain orientation.....  | 23 |
| Table 3.2 Material properties of E-glass/epoxy laminate .....   | 23 |
| Table 3.3 Material properties of balsawood .....  | 24 |
| Table3.4 Test matrix for impact test by drop weight impact tower.....   | 25 |
| Table3.5 Test matrix for impact test by Instron 9250 HV machine.....  | 27 |
| Table 3.6 Test matrix of sandwich composite with end-grain core for CAI test.....   | 32 |
| Table 3.7 Test matrix of sandwich composite with end-grain and regular balsa<br>core materials for CAI test.....              | 32 |
| Table 3.8 Compression after impact through thickness test matrix.....   | 34 |
| Table 5.1 Energy absorption of sandwich composite with end grain core.....  | 42 |
| Table 5.2 Energy absorption of sandwich composite with end grain core tested<br>by Instron 9250 HV machine.....               | 50 |
| Table 5.3 Energy absorption of Sandwich composite with regular balsa core.....  | 51 |
| Table 5.4 Summary of damage state and failure load of end grain sandwich<br>composite.....                                    | 61 |
| Table 5.5 Summary of damage state and failure load of end grain sandwich<br>composite.....                                    | 62 |
| Table 5-6 Summary of damage state and failure load of regular balsa<br>sandwich composite.....                                | 63 |
| Table 5.7 Summary of damage state and failure load of end grain<br>sandwich composite after compressed through thickness..... | 67 |



## L.IST OF FIGURES

|  |    |
|--|----|
| Figure 1.1: Sandwich structure components .....  | 1  |
| Figure 1.2: Sandwich panel and I-Beam.....   | 2  |
| Figure 1.3: Simply supported sandwich beam structure.....  | 4  |
| Figure 1.4: Core materials (a) balsa wood (b) honeycomb (c) cellular foam.....   | 7  |
| Figure 1.5: Open mold, hand lay-up composite fabrication.....  | 10 |
| Figure 1.6: Open mold, spray-up composite fabrication.....   | 10 |
| Figure 1.7: Hot-melt prepregging process.....  | 10 |
| Figure 3.1: (a) E-glass/Epoxy pre-preg; (b) Fully cured laminate .....   | 21 |
| Figure 3.2: Balsa wood; Schematic representation of grain direction.....   | 21 |
| Figure 3.3: Curing and post curing equipment.....  | 22 |
| Figure 3.4 : Experimental setup for impact testing of composite sandwich panels.....   | 25 |
| Figure 3.5: Impact testing machine Instron 9250 HV.....  | 26 |
| Figure 3.6:.. Assessment of damage size in impact side of sandwich after impact<br>visually inspection; (a) 17J, (b) 26J.....  | 29 |
| Figure 3.7: Ultrasonic c-scan images of front surface impact damage at<br>(a) 17J, (b) 26J .....   | 29 |
| Figure 3. 8: Extent of damage in impact side of regular balsa core sandwich<br>composite after impact by 26J (a) skin failure, (b) core cracks<br>along fiber, (c) core shear failure..... | 30 |
| Figure 3.9: Impact energy versus delamination area for end grain balsa.<br>The error bars show variation in data.....  | 30 |
| Figure 3.10: Experimental set up for compression after impact test a long length .....   | 31 |
| Figure 3.11: Set up of compression after impact test through the thickness.....  | 34 |

|   |    |
|---|----|
| Figure 4.1: Quarter of the system finite element model.....   | 38 |
| Figure 4.2: Fine mesh of entire sandwich composite plate.....   | 38 |
| Figure 4.3: Entire of the system finite element model .....   | 39 |
| Figure 4.4. Failure model used in Mat 59 of LS- Dyna .....  | 39 |
| Figure 5.1: Typical load-time response comparison of two different impact energy levels.....  | 41 |
| Figure 5.2: Typical load-deflection response comparison of two different impact energy.....   | 42 |
| Figure 5.3: Typical load time response of sandwich composites with end grain core.....  | 44 |
| Figure 5.4: Typical load time response of sandwich composites with regular balsa core.....  | 45 |
| Figure 5.5: Typical load deflection response of sandwich composites with end grain core.....  | 45 |
| Figure 5.6: Typical load deflection response of sandwich composites with regular balsa core.....  | 46 |
| Figure 5.7: Typical load time response from impact tests comparison of sandwich composites with end grain and regular balsa cores at (a) 17J (b) 26J 35J..... | 47 |
| Figure 5. 8:Typical load deflection comparison of sandwich composites with end grain and regular balsa cores at (a) 17J (b) 26J (c) 35J.....                  | 48 |
| Figure 5.9: Impact energy vs. absorbed energy comparison of sandwich composites with end grain and regular balsa cores.....                                   | 51 |
| Figure 5.10: typical velocity time comparison of sandwich composite with end grain and regular balsa core at 17J impact energy.....                           | 52 |
| Figure 5.11: Sandwich composite with end grain failure modes under compression...57   |    |
| Figure 5.12: Compression failure modes for sandwich composite with regular balsa core.....  | 58 |
| Figure 5.13: Residual strength versus delamination area for end grain sandwich composite structures .....   | 59 |

|  |    |
|--|----|
| Figure 5.14: Residual strength versus impact energy for end grain sandwich composite structures. The error bars show variation in data.....                    | 59 |
| Figure 5.15: Residual strength versus impact energy for end grain sandwich composite subjected to 50.8 mm impactor diameter. ....                              | 60 |
| Figure 5.16: Residual strength versus impact energy for regular balsa sandwich composite subjected to 50.8 mm impactor diameter .....                          | 60 |
| Figure 5.17: Typical compressive stress strain curves for damaged and undamaged specimens (CAI).....   | 61 |
| Figure 5.18: Typical compressive stress strain curves along length for sandwich Composite with end grain core.....   | 62 |
| Figure 5.19: Typical compressive stress strain curves along length for sandwich composite structure with regular balsa core.....                               | 63 |
| Figure 5.20: Through thickness compression after impact average failure stress comparison of damaged and undamaged sandwich composite with end grain core..... | 65 |
| Figure 5.21: Through thickness compression after impact maximum failure stress comparison of damaged and undamaged sandwich composite with end grain core..... | 66 |
| Figure 5.22: Residual strength versus impact energy for end grain sandwich composite after compression through thickness.....                                  | 66 |
| Figure 5.23: Comparison of experimental and FEA load- time histories of sandwich composites with end grain core at 17 J.....                                   | 68 |
| Figure 5.24: Comparison of experimental and FEA load- time histories of sandwich composites with end grain core at 26 J.....                                   | 69 |
| Figure 5.25: Comparison of experimental and FEA deflection- time histories of sandwich composites with end grain core at 17J.....                              | 69 |
| Figure 5.26: Comparison of experimental and FEA deflection- time histories of sandwich composites with end grain core at 26J.....                              | 70 |
| Figure 5.27: Comparison of experimental and FEA impactor kinetic energy histories at 26 J impact energy.....   | 70 |

Figure 5.28: Sandwich composite with end-grain core comparison of experimental and FEA load-time histories at 17J.....72

Figure 5.29: Sandwich composite with regular balsa core comparison of experimental and FEA load- time histories at 17J.....72

Figure 5.30: Comparison of experimental and FEA deflection- time histories of sandwich composites with (a) end-grain (b) regular balsa at 17J.....73

## CHAPTER 1

### INTRODUCTION

#### 1.1. SANDWICH COMPOSITE

A sandwich structure is defined as a composed of two face sheets and a core which are bonded to each other. Usually the faces are made from the same material, and the same thickness. The components of sandwich composite structure are shown in Fig.1.1.

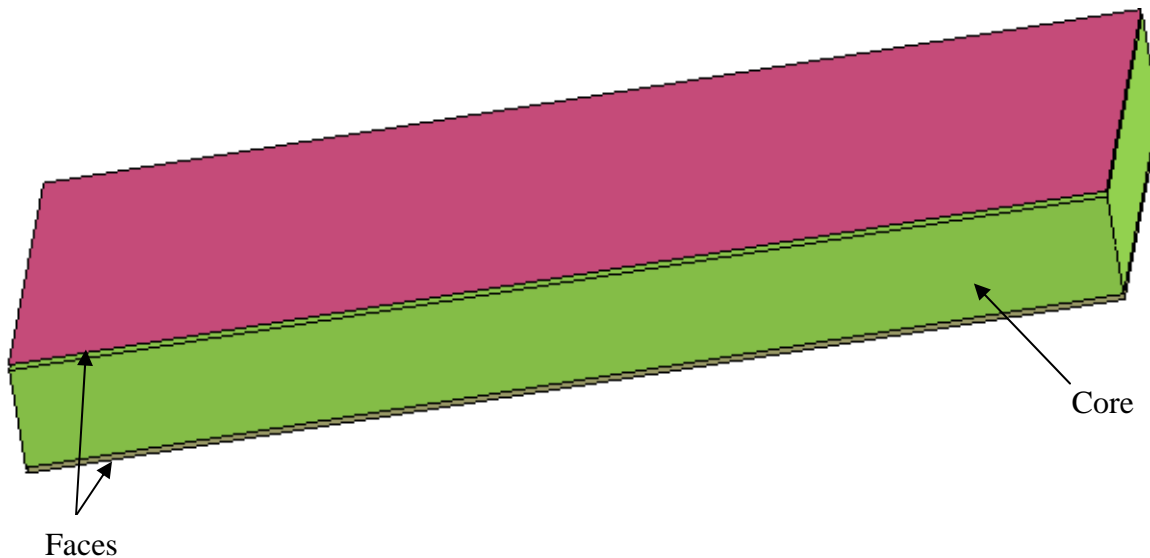


Fig.1.1: Sandwich structure components

In a sandwich composite, in order to transfer the load between the components of the sandwich structure, the skin should be adhesively bonded to the core, thus one skin acts in compression as the other skin acts under tension and the core resists the shear loads. This provides high stiffness, strength-to-weight ratio, bending rigidity and

energy absorbing capability to the structure. The adhesive must rigidly bond the facings to the core material to resist shear and tensile stresses in the sandwich panel. Appropriate adhesives include high modulus, high strength materials available as liquids, pastes or dry films. The sandwich composite structure with low weight can be provided high bending stiffness. The stiff, strong face sheets hold the bending load, while the core resists shear loads. The principal is the same I-beam, where the facing skins of a sandwich panel can be compared to the flanges of an I-beam, and the core corresponds to the web, as shown in Fig.1.2. [1].

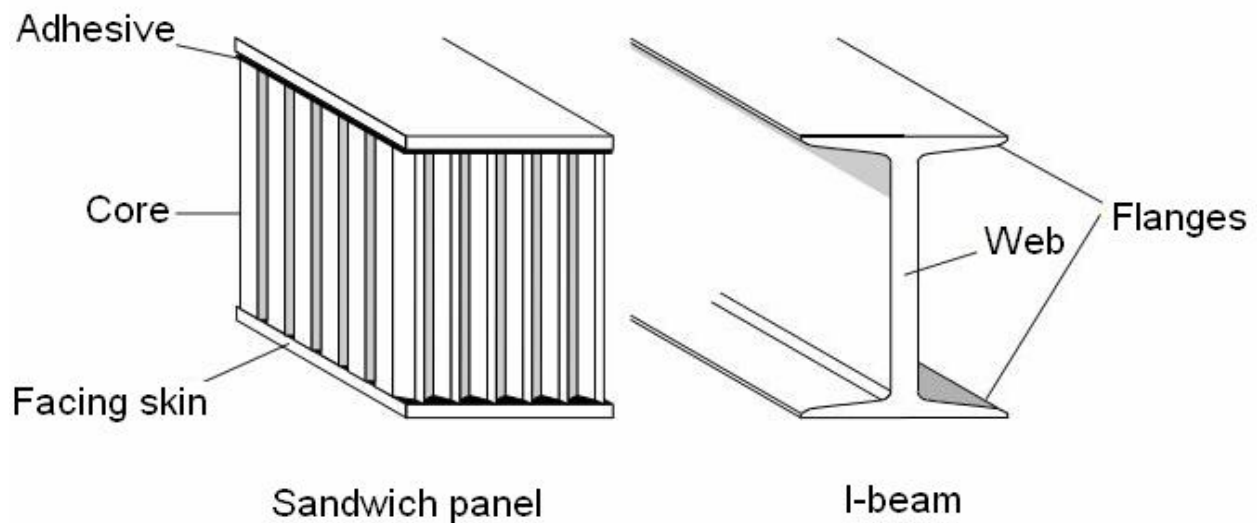
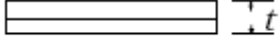

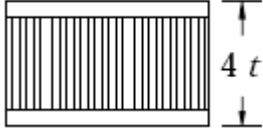


Fig.1.2: Sandwich Panel and I-Beam. (Ref. [1])

The comparison of flexural stiffness and strength advantage for the sandwich panels and solid panels using typical beam theory with typical values of facing skin and core density is tabulated in table 1.1. From the table, it can be seen that the by making the panels thicker, the bending stiffness is increased. [2]

Table 1.1 Structural efficiency of sandwich panels in terms of weight [Ref. 2]

|                   | Solid material  | Core thickness<br>$t$   | Core thickness<br>$3t$  |
|-------------------|---|---|---|
|                   |  |  |  |
| Bending stiffness | 1.0   | 7.0   | 37  |
| Bending strength  | 1.0   | 3.5   | 9.2   |
| Weight            | 1.0   | 1.03  | 1.06  |

The flexural rigidity  $D$  of the sandwich beam that shown in Fig. (1.3) can be determined using beam theory. It is found that the flexural rigidity  $D$  of sandwich beam is given by:

$$D = \frac{E_{fx}bt^3}{6} + \frac{E_{fx}btd^2}{2} + \frac{E_{cx}bc^3}{12} = 2D_f + D_0 + D_c \quad (1.1)$$

Where  $d$  is the distance between the midplanes of the upper and bottom skins.

$E_{fx}$ : the in-plane Young's moduli of the skin for loading in the x direction

$E_{cx}$ : the in-plane Young's moduli of the core for loading in the x direction

$2D_f$ : the bending stiffness of the faces about their individual neutral axis

$D_0$ : the bending stiffness of the faces about the middle axis

$D_c$ : the bending stiffness of the core

The face approximation:

$$\frac{2D_f}{D_0} < 0.01 \text{ if } 3 \left[ \frac{d^2}{t^2} \right] > 100 \text{ or } \frac{d}{t} > 5.77 \quad (1.2)$$

Weak core approximation:

$$\frac{D_c}{D_0} < 0.01 \text{ if } \frac{6E_{fs}t}{E_{cw}c} \left( \frac{d^2}{c^2} \right) > 100 \text{ or } \frac{E_{fs}t}{E_{cw}c} \left( \frac{d^2}{c^2} \right) > 16.66 \quad (1.3)$$

If both above relations are satisfied then the equation 1.1 can be written as

$$D = D_0 = \frac{E_{fs}btcd^2}{2} = E_{fs}I \quad (1.4)$$

Where  $I$  is the second moment of area of the cross-section of sandwich beam.

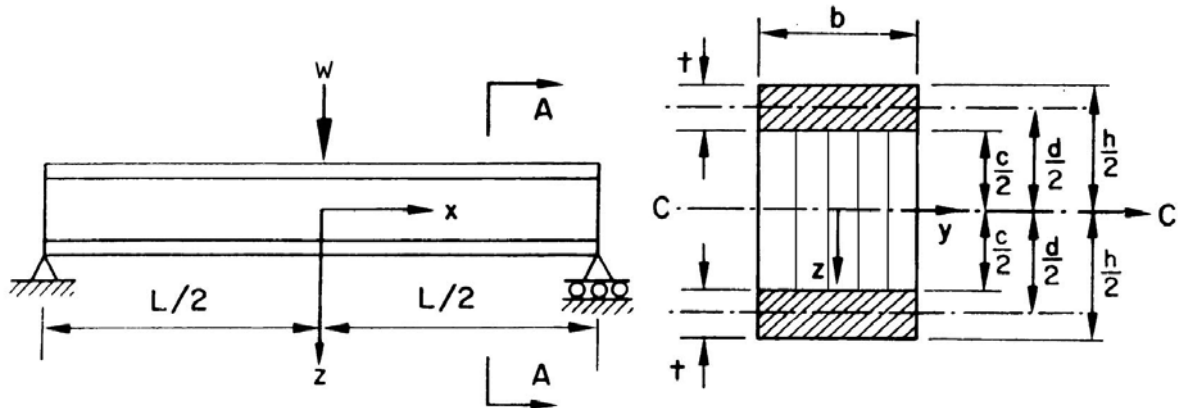


Fig. 1.3: Simply supported sandwich beam structure (Ref. [2])



The sandwich composite structures nowadays are widely used in many applications where lightweight materials with improve in-plane and flexural stiffness are required [3]. These composite materials are being used in a number of applications within the marine, aerospace, and automotive industries because they have desirable properties such as lightweight, corrosion resistance and electrical and thermal insulation which are added advantages of composites over steel in such applications [4].the components of the sandwich system

The configurations of sandwich system materials are unlimited with wide range of skin and core materials. To select right materials some factors should be taken into account such as strength, stiffness, adhesive performance, environmental behavior and economic availability.

#### **1.1.1. Skin**

Skin is known as a thin stiff laminate which is provided flexural stiffness and impact resistance to the sandwich system. The skin can be made from metallic and non metallic materials, some of these materials are tabulated in table 1.2.

The majority of composite materials offer low density along with higher strength properties than metals; however, the stiffness is often lower. So it is found, fiber composite laminates are preferred over the metals for sandwich construction. Also it is found that manufacturing of sandwich composites is much easier than the manufacturing of metal face sandwich structures.

Table 1.2: Typical skin materials (Ref. [1])

| Materials                              | $\rho$ (kg/m <sup>3</sup> ) | E (Gpa) | $\sigma_u$ (Mpa) |
|--|-----------------------------|---------|------------------|
| <b>Metals</b>                          |                             |         |                  |
| Stainless steel                        | 7900                        | 196     | 200              |
| Aluminum alloy 2024                    | 2700                        | 73      | 300              |
| Titanium alloy                         | 4500                        | 108     | 980              |
| <b>Non-metals</b>                      |                             |         |                  |
| Carbon /epoxy (Unidirectional)         | 1600                        | 180/10  | 1500/40          |
| Glass/epoxy (Unidirectional)           | 1800                        | 39/8    | 1060/30          |
| Kevlar/epoxy (Unidirectional)          | 1300                        | 76/6    | 1400/12          |
| Glass weave/polyester (Bi-directional) | 1700                        | 16      | 250              |
| Kevlar/polyester (Bi-directional)      | 1300                        | 17.5    | 375              |

### 1.1.2. Core

In a sandwich composite structure, the core is responsible for separating and fixing the skin, resisting transverse shear, and providing other functions like absorbing energy and insulating heat transfer. There are various types of core materials that have been used in sandwich composite such as balsa wood, honey comb, and foam. Each core has some advantage and some disadvantages, for example, Balsa wood was the first material which was used as cores in sandwich composite structures (Fig. 1.4(a)) and is still used in Marine Industry. Balsa wood Under a microscope shows a high-aspect ratio

closed cell structure. Balsa wood is light core material and has high strength; however, balsa wood can rot with exposure to moisture. Honeycomb core material has been developed and used in aerospace applications because it provides good shear strength, and it provides stiffness-to-weight ratio. The honeycomb core (Fig. 1.4(b)) is more expensive comparing with the other core materials like balsa wood and foam. The cellular foam (Fig. 1.4(c)) has lower stiffness and strength to weight ratio than honeycomb but has other advantages such as less expensive than honeycomb, easy manufacturing and easy to bond to the skins. In addition, the cellular foams have high thermal insulation and they are impervious to moisture. Some types of core materials which are widely used in composite industries are tabulated in table 1.3.

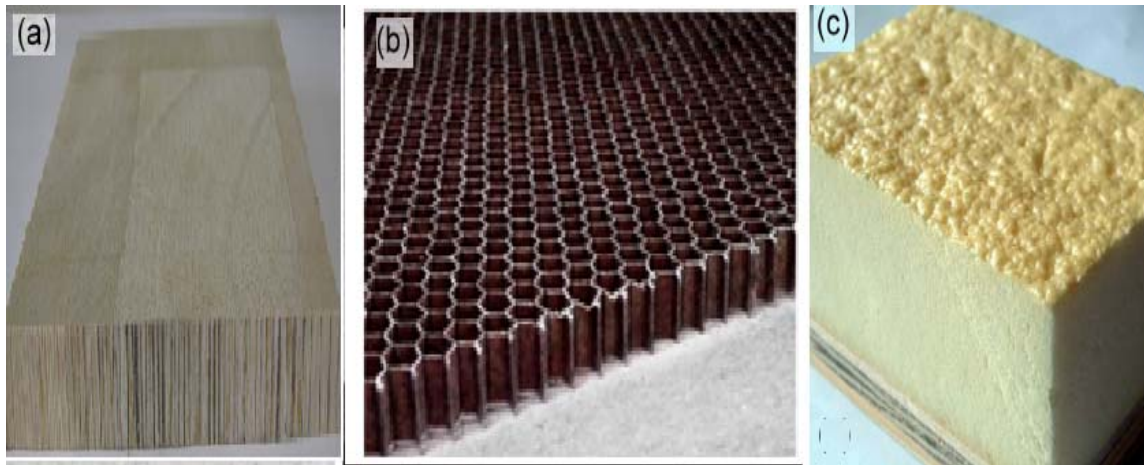


Fig.1.4: Core materials (a) balsa wood (b) honeycomb (c) cellular foam

Table 1.3: Typical core materials (Ref. [1])

| <b>Material (Density, kg/m<sup>3</sup>)</b> | <b>G<sub>c</sub> (Mpa)</b> | <b>σ<sub>u</sub> (Mpa)</b> |
|---|----------------------------|----------------------------|
| Balsa wood (96)                             | 72.85/12.5                 | 10.1/0.81                  |
| Honeycomb:                                  |                            |                            |
| Aluminum alloy (92)                         | 620/260                    | 3.1/2.0                    |
| Aluminum alloy (130)                        | 930/370                    | 5.0/3.1                    |
| Nomex honeycomb (80)                        | 96/44                      | 2.2/1.0                    |
| Paper honeycomb (56)                        | 141/38                     | 1.3/0.48                   |
| Cellular foam:                              |                            |                            |
| Polyurethane foam (40)                      | 4                          | 0.25                       |
| Polystyrene foam (60)                       | 20                         | 0.6                        |

## 1.2. MANUFACTURING

Panels of sandwich composites can be manufactured by different manufacturing techniques, for example, Liquid molding, vacuum bag and autoclave molding and adhesive bonding.

For the sandwich composite adhesive bonding is the simplest manufacturing process, where the adhesive layers are supplied between the skin and core and the whole sandwich composite system is subjected to high temperature and pressure depending on requirements of adhesive material. To obtain good adhesion between skin and core, bonding surface should be rugged or abraded. Fabrication processes that used for polymer composites with various types of fiber reinforcement are

summarized in table 1.4. The open mold process with hand lay-up (Fig.1.5) or spray-up (Fig.1.6) is utilized for large production of components. A major breakthrough in composite manufacturing technology was development of prepreg tape, where the most prepreg tape is made by the hot-melt process [4], as shown in Fig. (1.7).

In this study, a TMP vacuum press molding is used for producing sandwich panels. The prepreg's are layered directly onto both sides of the core in the mold and is placed in a vacuum chamber and subjected to heat and pressure. The temperature and pressure are controlled for certain amount of time for resin cross-linking and temperature is slowly reduced after curing.

Table 1.4 fabrication process for polymer matrix composites. (Ref.[4])

| process                   | Type of reinforcement |         |       |        |
|---------------------------|-----------------------|---------|-------|--------|
|                           | Continuous            | Chopped | Woven | Hybrid |
| Open mold:                |                       |         |       |        |
| <i>Hand lay-up</i>        |                       | X       | X     |        |
| <i>Spray-up</i>           |                       | X       |       |        |
| Autoclave                 | X                     |         | X     |        |
| Compression molding       | X                     | X       | X     | X      |
| Liquid composite molding  | X                     | X       | X     | X      |
| Automated fiber placement | X                     |         | X     |        |

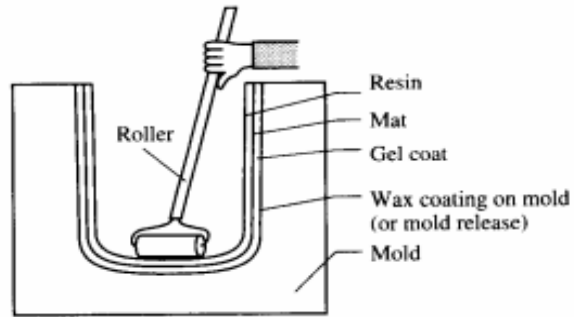


Fig.1.5: Open mold, hand lay-up composite fabrication

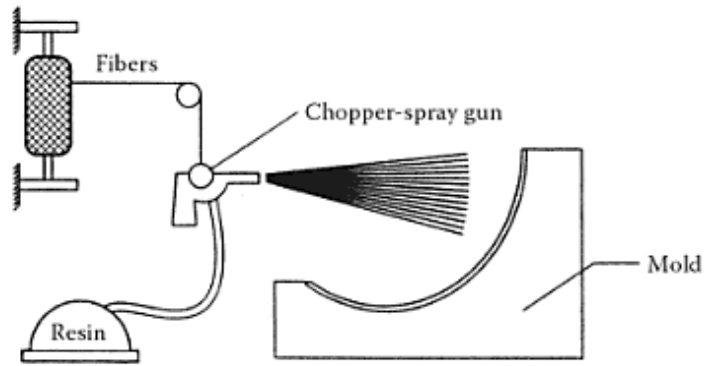


Fig. 1.6: Open mold, spray-up composite fabrication

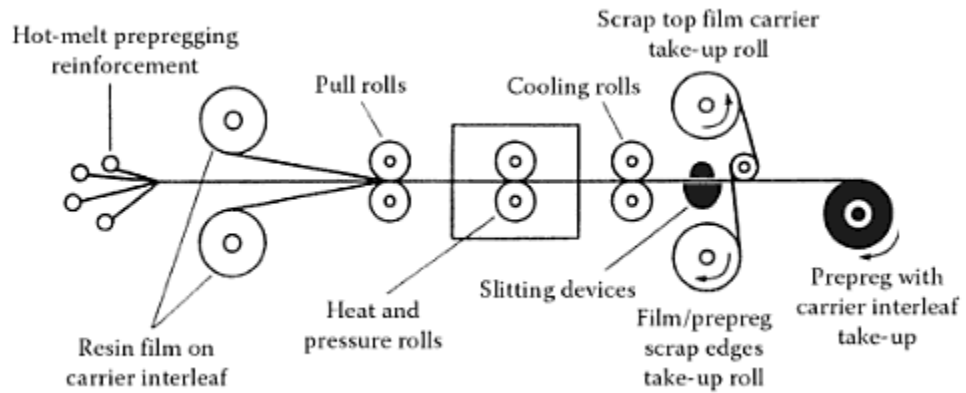


Fig.1.7: Hot-melt prepregging process (Ref.[3])

### **1.3. Low velocity impact and compression after impact tests**

The different types of cores have different damage accumulation behavior when subjected to a low velocity impact. [5]. Impact by foreign object can be expected to occur such as tool drop on sandwich structure. In this case impact velocity is small but the mass of the tool is large. Impact also can occur due to high energy events such as ballistic penetration. Low velocity impact may induce damage in sandwich composite structures like matrix cracks, fiber fracture, fiber kinking, and delamination, which may significantly reduce the strength of the material and finally cause the material to fail without any warning. For this reason, it is very common practice to do compression–after–impact (CAI) testing on composite materials [6].

Low velocity impact test by the Dyna Tup 9250HV impact machine as well as utilizing a manual drop tower were used to evaluate the impact response of sandwich composite panels. The sandwich panel was impacted at the center with different energy levels. Compression after impact (CAI) test was performed by MTS machine to evaluate the residual strength. The damage size was investigated by visual inspection as well as destructive techniques. A finite element analysis per LS-dyna was utilized to predict the response of sandwich composite under dynamic loading.

## CHAPTER 2

### LITERATURE REVIEW AND OBJECTIVES

#### 2.1. Literature Review

##### 2.1.1. Composite Laminate Structure

Many authors have presented experimental investigation on the damage response of composite laminates [7-8]. Strait et al. [9] have performed impact test on composite laminate with varies stacking sequence. It is found that the stacking sequence has a big effect on the impact resistance. The finite element analysis was conducted by Wu and Chang [10] to understand the response of composite laminate under impact force. The displacements, the stress and the strain distributions along the thickness of laminate have been determined during the impact event. Choi and Chang [11] proposed a model to predict damage in graphite/epoxy laminated composite under low velocity point impact. They concluded that there exists an impact velocity threshold for laminated composite below which no delamination occurs but above which significant damage is produced. The damage resistance and residual strength for composite laminates under low velocity impact have been studied by Dost et al. [12].it is found that the laminate stacking has significantly effect on compression after impact results. Caprino et al. [13] have conducted low-velocity impact tests on carbon/epoxy laminates with different thicknesses. They have tested the load and absorbed energy at the point where the delamination started, the peak load and related energy, and penetration energy. A model for predicting the residual strength of laminates with an



indentation law has been presented by Caprino and Lopresto [14]. The residual strength as a function of the depth of indentation was well predicted and good agreement was obtained when compared with the experimental data. However, the internal damage was not well predicted. Luo et al.[15] have studied an approach to evaluate the impact damage initiation and propagation in composite plate. They have shown by introducing both threshold strength and propagation strength for matrix cracking, the main characteristics of impact damage can be predicted. They have found from both simulation and experiment that there is small zone of no matrix failure at the center of impact area. Low velocity impact characteristics of different E-glass fibers reinforced thermoplastic and thermosetting matrix composites have been investigated by Sadasivam and Mallick [16]. The effects of material and geometric parameters on mechanical response of graphite epoxy composite laminate under low velocity impact have been investigated by Cho and Zhao [17]. Aslan et al. [18, 19] have studied experimentally and numerically to understand the effects of the projectile velocity, thickness and in-plane dimensions of target, and projectile mass on the response of laminated composite plates under low-velocity impact. They found have that the peak force increases with the thickness of the composite laminate and the duration time decreases. the effects of different impact energy levels and the thickness of the laminate on the low-velocity impact damage tolerance of GFRP composite laminates have been studied by Datta et al. [20]. Hosur et al. [21] studied experimentally the low velocity impact responses of four different combinations.the results show that the hybrid composites offer better load carrying capability than the carbon epoxy laminates with small reduction in stiffness. Saez et al. [22] have done

experimental and numerical analysis to investigate the damage tolerance of thin carbon/epoxy laminates. Compressions after impact (CAI) tests were conducted for different carbon/epoxy laminate lay ups, and values of residual strength of the laminates were obtained as a function of the impact energy. Its found that the woven laminate was offer the highest residual strength under all the impact energy. Hossenzadeh et al. [23] investigated four different fiber reinforced composite plates after being impacted by standard drop weight with different energies. Their study showed carbon fiber reinforced composite plates the best structure behavior under low velocity impact, meanwhile the hybrid composite plates showed suitable behavior under high impact energy. The threshold damage in all the plates was predicted by using ANSYS LSDYNA code and the damage shape was not as the same test results. Tiberkak et al. [24] studied fiber-reinforced composite laminates under low-velocity impact numerically. The effect of projectile shape during ballistic perforation of carbon /epoxy composite panels under high velocity impact has been studied by Ulven et al. [25]. Conical projectile high velocity impact resulted in the greatest amount of energy absorbed at ballistic limit, followed by flat, hemispherical, and fragment simulating projectile impact. Composite laminates made of E-glass/epoxy (0, 90) have been studied experimentally and numerically under low velocity impact by Aslan and Karakuzu [26]. The resulting data in terms of load-time histories from the impact tests and computer code offer specific information about the effect of the projectile velocity and projectile mass.

### 2.1.2. Composite Sandwich Structure

A number of studies in literature have been focused on the impact response of sandwich composites under low velocity impact. Among these Kim and Jun [27] have investigated the effect of the lay-up of the facing and density of the honey comb core on the impact damage area of the facing. This investigation was shown that a small relative orientation results in a smaller delamination area than for a laminate with exactly the same lay-up. This effect was attributed to the existence of the core. In addition, a higher density core results in a smaller delamination area than a lower density core for the same level of absorbed impact energy. Abrate [28] have performed an extensive literature review on the impact behavior of sandwich structure with laminate face sheets. The most important conclusion that can be drawn from that study is that results from many of the reviewed investigations were often in conflict with each other. A possible explanation is that the majority of experiments performed by the various researchers consider only a limited number of sandwich configurations. Since the impact behavior is influenced by a large number of parameters, results of various experimental studies cannot easily be compared. Anderson and Madenci [29] have examined the low-velocity impact characteristics for sandwich composites with a Rohacell foam core. They have concluded that the damage resistance of a sandwich structure can be improved by increasing the thickness of the face sheets and increasing the density of the (foam) core. However, even though the damage resistance is increased, the damage in the specimens was comparable for similar levels of residual indentation. Hosur et al. [30] have presented a work on the manufacturing and low-velocity impact characterization of foam filled 3-D integrated core sandwich composites. Impact parameters were

evaluated and compared for different types of hybrid face-sheets. Low velocity impact and post impact behavior of composite sandwich panels have been studied experimentally by Schubel et al. [31, 32], where sandwich panels consisting of woven carbon/epoxy face sheets and a PVC foam core. Experimental results were compared with analytical and finite element model analysis to determine their effectiveness in predicting the indentation behavior of the sandwich panel. They have also compared the strength of the damaged and undamaged samples with each other and made useful discussions. Vaidya et al [33] performed experiments to study the behavior of composite sandwich plate with laminate face sheet (glass/fiber carbon) and aluminum foam core under low velocity and medium velocity impact. The vibration response of sandwich composite structure was also studied. From the impact test results, they concluded that the sandwich construction with S2-glass face sheet in conjunction with aluminum foam core was optimal for resisting low and intermediate velocity impact. The effect of manufacturing on impact damage behavior in E-glass/polyester–PVC foam core sandwich structures has been studied by Imielinska et al. [34]. Low velocity impact response of sandwich plates was also investigated by using impact drop tower. Damage initiation and failure mechanisms were recorded by high-speed photography and related to the load–time plots. Ulven and Vaidya [35] have examined impact response of fire damaged E-glass/vinyl ester laminates and balsa wood core sandwich composites with E-glass/ vinyl ester face-sheets. The response of sandwich structure consisting of S2-glass/epoxy face sheets and end grain balsa core under high velocity impact has been studied experimentally and numerically by Deka and Vaidya [36]. Energy absorption and delamination from high velocity impacts were discussed and FE modeling was used

to predict the damage in sandwich composite structure. The results of FE modeling were compared with experimental data and good agreement had been obtained. Leijten et al [37] have experimentally investigated of damage tolerance of composite sandwich panels consisting of carbon Non-Crimp Fabric/epoxy facings and Rohacell foam core. Instrumented low velocity impacts were performed on sandwich specimens and both internal and external damage resulting from these tests was evaluated. They concluded from compression after impact (CAI) test that the residual compression strength only depends on the damage inflicted on the upper and lower face sheets and that the planar damage area as observed from C-scan includes a reasonable amount of core damage. Atas and Sevim [38] have experimentally investigated on the impact response of sandwich composites with cores of balsa wood and PVC foam. A number of tests under different impact energies were conducted where the results of these tests showed that the sandwich with balsa wood core absorbed energy better than panel with PVC core and were showed the damage modes are fiber fracture at upper and lower skins, delamination between adjacent layers of glass-epoxy, shear fractures of the core and face/core depending. In addition to the single impacts, repeated impact response of the specimens was also investigated. Wang et al [39] investigated low velocity impact characteristics and residual tensile strength of carbon fiber composite lattice core sandwich structure, experimentally and numerically. Tests of low velocity impact and residual tensile were performed using a drop weight machine and a static test machine respectively. Impact force and residual tensile strength of carbon fiber composite lattice core sandwich structure were predicted well by finite element model.

Most of the investigations that have been done in the literature were focused on sandwich composite where the skin is made of carbon fiber composite and different core materials as previously mentioned in the literature review. Although balsawood was utilized as a core material in some of these investigations, but mostly this was done under high velocity impact. Nevertheless, in the literature review there many researchers have studied the response of sandwich composite under low velocity impact, but it was from experimental view point only.

In this study, we explore new sandwich composite systems (E-glass /epoxy with balsa). These composites were not investigated under low velocity impact. Besides, the experimental data was utilized to build a finite element model. These composite sandwich panels are chosen as the subject structure because they can be used in many applications primary in automotive industries. For example, new sandwich composites can be utilized for trunk floor, under body, truck bed and other applications in cars. These systems of sandwich composites offer low cost solutions. These composites have high strength to stiffness ratio and can provide weight saving if compared to steel or aluminum structures.

## **2.2. Objectives**

The primary goal of this study is to focus on low velocity impact response of new composite sandwich plates comprising E-glass/epoxy composite laminate face sheets

and core made from two different materials, end-grain and regular balsa wood, and conduct thorough damage analysis to understand the role of failure modes on composite strength. In common practice after the impact test, the damage in sandwich structure should be investigated by visual inspection, non-destructive (C-scan) and destructive techniques. Compression after impact test was conducted to correlate the impact damage to residual strength. This investigation was done experimentally using drop weight impact tower for impact test and MTS machine for CAI and numerically using finite element code LS-DYNA to predict load-time and deflection-time response.

## CHAPTER 3

### MATERIAL DESCRIPTION AND MATERIAL TESTING

#### 3.1. Material Composition and Material Preparation

The facing material was cross ply E-glass/epoxy (Fig. 3.1), and the core materials used in the sandwich structure were end grain and regular balsa. Balsa wood are the two types of balsa sheets available, regular balsa and end grain balsa ,where the grain is oriented along the length of the sheet in the regular balsa, and the grain is maintained along thickness in the case of the end-grain balsa. Schematic representation of grain direction is illustrated in Fig.3.2. The density of the core and facings were  $96 \text{ kg/m}^3$  and  $1723 \text{ kg/m}^3$ , and the dimension of the sandwich plate was  $100 \times 100 \times 11.5 \text{ mm}$ . The skin layers are 1mm on top and on bottom and the core is 9.5 mm thick. To get good adhesion between the skin and the core, whole sandwich structure should be cured. A TMP vacuum press was used to cure the sandwich composite plate  $100 \times 100 \times 11.5 \text{ mm}$  dimension. Four plies of E-glass/epoxy prepreg were used as skin on each side of the balsa core. The pressure utilized in the press was 344 KPa and the temperature was  $135 \text{ }^\circ\text{C}$  for 20 minutes. The sandwich panel was then post cured in an oven at  $80 \text{ }^\circ\text{C}$  for 5 hours. Curing and post curing equipments is presented in Fig.3.3. The prepreg was directly bonded to the core. No adhesive was used between the prepreg a glass fiber laminate and the balsa core.



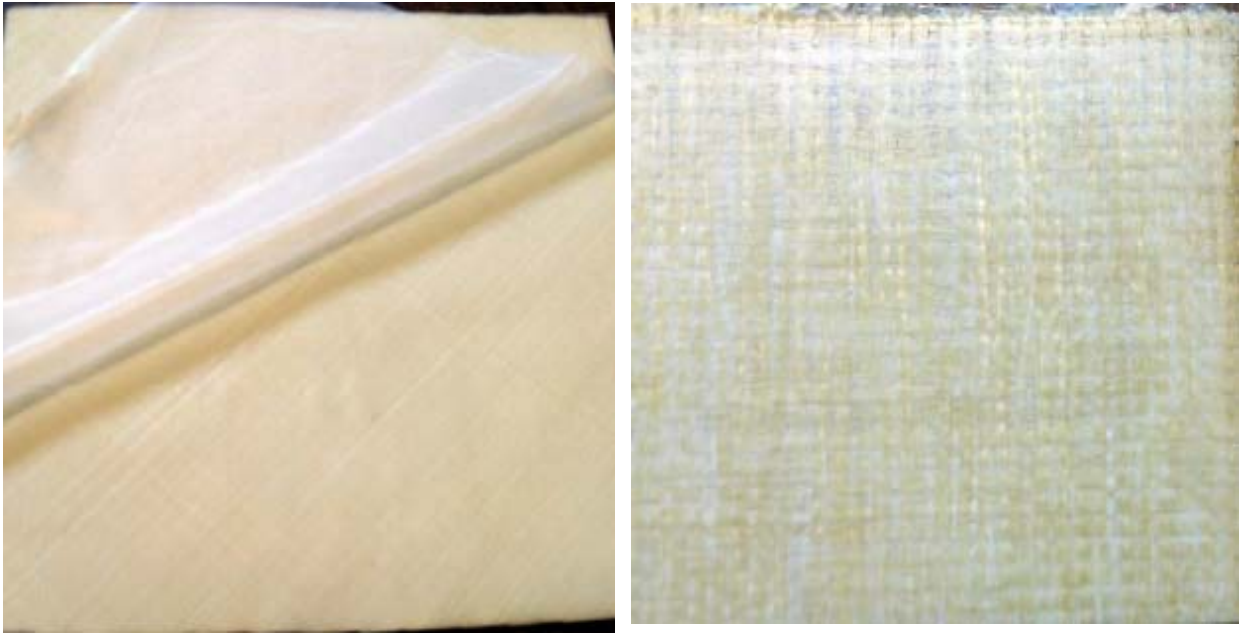


Fig. 3.1: (a) E-glass/Epoxy pre-preg.

(b) Fully cured laminate.

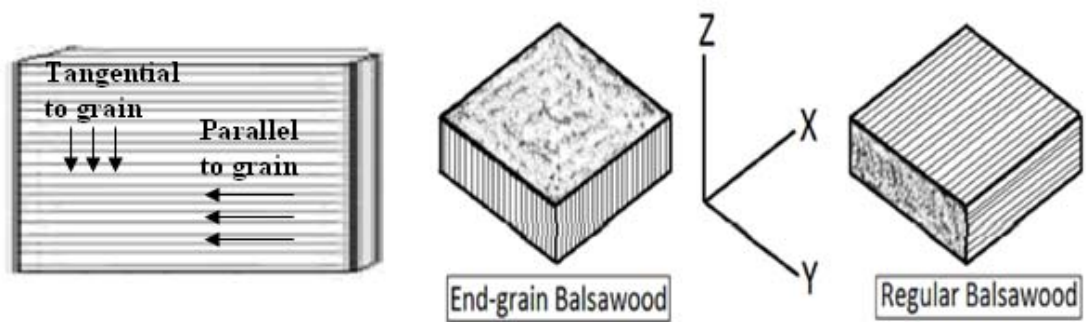


Fig. 3.2: Balsa wood; Schematic representation of grain direction (source [40]).



Fig. 3.3: Curing and post curing equipments.

## 3.2. Material Testing

### 3.2.1. Mechanical Properties of Sandwich Composite Structure

In order to get the parameters for the constitutive models and to validate these models, extensive material testing was conducted on the sandwich composites. Tensile and compression testing for both cores and face sheets in fiber and cross fiber as well as determining the shear properties were conducted to obtain shear modulus, young's modulus tensile and compression strength in both cross and along fiber direction, shear and Poisson's ratio. The core grain orientations with respect to loading for three different cases are shown in table 3.1. The properties of E-glass fiber/epoxy and balsa wood core are summarized in table 3.2 and table 3.3 respectively.

Table 3.1: sandwich composite core grain orientation

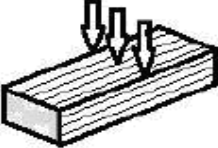
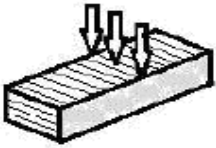
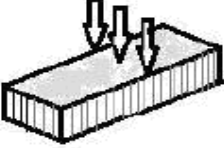
| Core grain orientation | X-axis  | Y-axis  | Z-axis   |
|------------------------|---|---|--|
| Balsa type used        | Regular   |   | End-grain  |
|                        | Radial  | Tangential  | parallel   |
|                        |  |  |  |
|                        | Loading with respect to grain   |   |  |

Table 3.2: Material properties of E-glass/epoxy laminate

| Material specifications<br>(GPa)                 | E glass/epoxy |
|--|---------------|
| $E_x$ Elasticity modulus in fiber direction      | 19.8          |
| $E_y$ Elasticity modulus in cross direction      | 19.8          |
| $E_z$ Elasticity modulus in thickness direction  | 12.6          |
| $G_{xy}$ In-plane shear modulus                  | 4.04          |
| $G_{xz}$ Out-plane shear modulus                 | 3.37          |
| $G_{yz}$ Out-plane shear modulus                 | 3.37          |
| $S_{xc}$ Compressive strength in fiber direction | 0.28          |
| $S_{xt}$ Tensile strength in fiber direction     | 0.55          |
| $S_{yc}$ Compressive strength in cross direction | 0.28          |
| $S_{yt}$ Tensile strength in cross direction     | 0.55          |
| $S_{xy}$ In-plane shear strength                 | 0.031         |

Table 3.3: Material properties of balsa wood core.

| Material specifications  | (MPa)               |
|--|---------------------|
| Parallel normal modulus, EL, MPa                                     | 1683                |
| Perpendicular normal modulus, ET, MPa                                | 54                  |
| Parallel shear modulus, GL, MPa                                      | 72                  |
| Perpendicular shear modulus, GLR, MPa                                | 12.5                |
| Parallel major Poisson's ratio, $\nu_{xy}$ , $\nu_{yz}$ , $\nu_{xz}$ | 0.007, 0.479, 0.007 |
| Parallel tensile strength, XT, MPa                                   | 10.12               |
| Perpendicular tensile strength, YT, MPa                              | 0.82                |
| Parallel compressive strength, XC, MPa                               | 8.05                |
| Perpendicular compressive strength, YC, MPa.                         | 0.707               |
| Parallel shear strength, Sxy, MPa                                    | 1.35                |
| Perpendicular shear strength, Syz, MPa                               | 1.35                |

### 3.2.2. Impact Test

#### 3.2.2.1 Drop-Weight Impact Tower

Low velocity impact tests are performed by drop-weight impact tower as shown in Fig. 3.4. Test specimens are positioned on the load cell has diameter 10 cm and the specimens were clamped along all edges. The steel impactor with weight 2 kg was used for the impact tests which has hemispherical tup with 25.4mm diameter. The drop mass was held manually to prevent repeated impacts. Low velocity impact test was carried out at different impact energy, nevertheless, only two energy levels (17J and 26J) were thoroughly investigated. The test matrix for the impact test study is summarized in table 3.4.

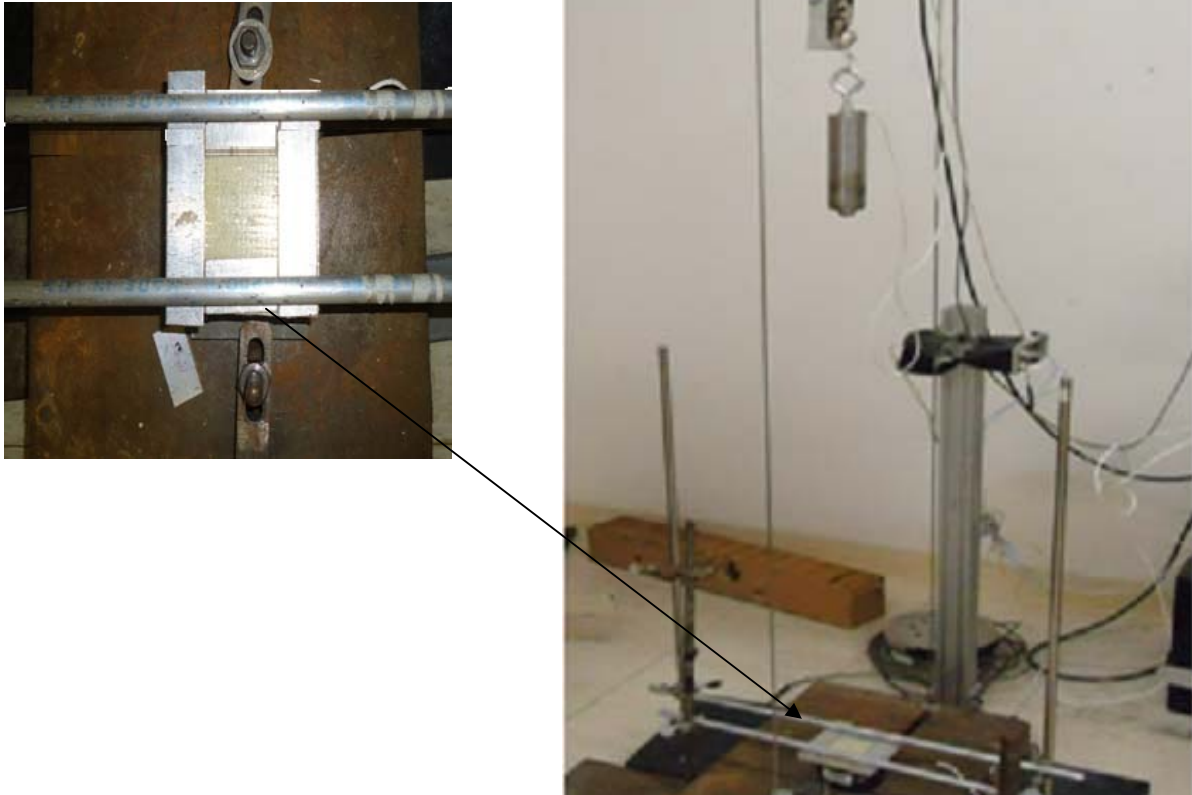


Fig. 3.4: Experimental setup for impact testing of composite sandwich panels.

Table3.4: Test matrix for impact test by drop weight impact tower

| Core material | # of samples tested | Impact energy(J) | Sample dimension |
|---------------|---------------------|------------------|------------------|
| End-grain     | 6                   | 17               | 100mm×100×11.5mm |
| End-grain     | 6                   | 26               | 100mm×100×11.5mm |

### 3.2.2.2 Instron 9250 HV Impact Testing Machine

An instrumented Instron drop tower impact testing machine equipped with dynatup impulse data acquisition system, and pneumatic clamping fixture to hold the specimen during impact test was used. End grain and regular balsa core with E-glass/epoxy laminate were tested under low velocity impact. Impact testing machine is shown in Fig.3.5. Specimens of dimension 100×100×11.5 mm were clamped along all edges leaving unexposed circular opening of 76.2 mm diameter. A hemispherical impactor with 50.8 mm diameter was used for all tests and the total mass of the dropped carriage was 7.7 kg. The drop height was adjusted to control the impact velocity. In this work only three energy levels were used in the impact tests (17 J, 26J, 35J) for both end grain and regular balsa core of sandwich plate. The test matrix by using this impact testing machine is tabulated in table 3.5.

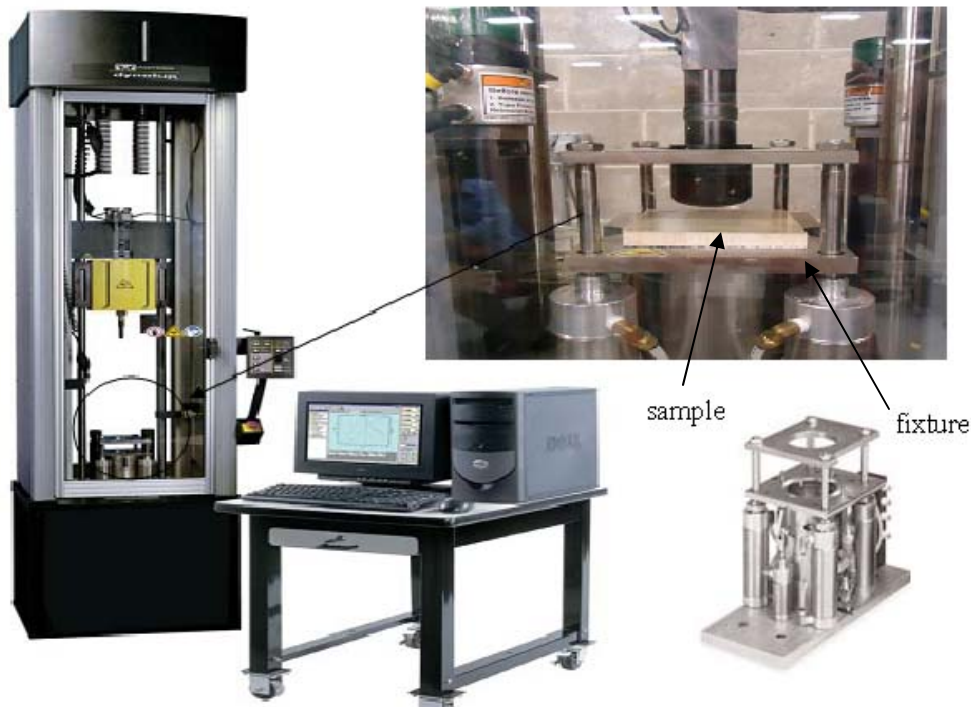


Fig.3.5: Impact testing machine Instron 9250 HV.

Table 3.5: Test matrix for impact test by Instron 9250 HV machine

| Core material | #of samples tested | Impact Energy(J) | Dimension(mm) |
|---------------|--------------------|------------------|---------------|
| End-grain     | 6                  | 17               | 100×100×11.5  |
| End-grain     | 6                  | 26               | 100×100×11.5  |
| End-grain     | 6                  | 35               | 100×100×11.5  |
| Regular balsa | 6                  | 17               | 100×100×11.5  |
| Regular balsa | 6                  | 26               | 100×100×11.5  |
| Regular balsa | 6                  | 35               | 100×100×11.5  |

### 3. 2.3. Damage Inspection

#### 3.2.3.1. End Grain Core Sandwich Composite Damage Inspection (visual and C-scan)

The delamination area was one of the parameters that were used in the evaluation of the impact response of composite sandwich panels. Therefore, it was necessary to use precise methods to estimate the size of damage, in our case the damage was very clearly, and therefore visual inspection was possible and best for end grain balsa/glass fiber sandwich composites. Infrared (IR) inspection using flash thermography was used, but was not effective in our system. Images of the damaged area (brighter area) were taken by a digital camera then edited by image-J software to estimate the average delamination area as shown in Fig. 3.6. In addition to the visual inspection, ultrasonic C-scan images were used to show the extent of damage to the plate. The results of C-scan with impact energy 17J and 26J are shown in Fig.3.7. It can

be seen from these two figures the dark black regions indicate material state changes due to near surface delamination, while the rest of the impact surface indicate regions of uniform signal reflection from the deepest regions of the face sheet i.e. there is no damage reported in this region. As with IR technique, ultrasonic c-scan is not as effective for this sandwich composite structure.

### 3.2.3.2. Balsa Core Damage Inspection

Since we got core shear with energy level of 26 J, we conducted damage inspection of the regular balsa sandwich composite. Destructive method was used to evaluate the damage area of this sandwich system. The face sheets were separated and core cross section was taken. The results show the upper skin was cracked and the core has shear failure mode as shown in Fig. 3.8.

### 3.2.3.3. Impact Energy versus Damage Area

At least six specimens were impacted at each level of energy. After the test the delamination area was recorded. The impact damage area for the end grain balsa core with cross ply E-glass/epoxy composites that were subjected to 8J, 17J, 26J, and 35 J impact energy levels are presented in Fig.3.9. It is found that the higher impact energy produced higher damage area as expected.



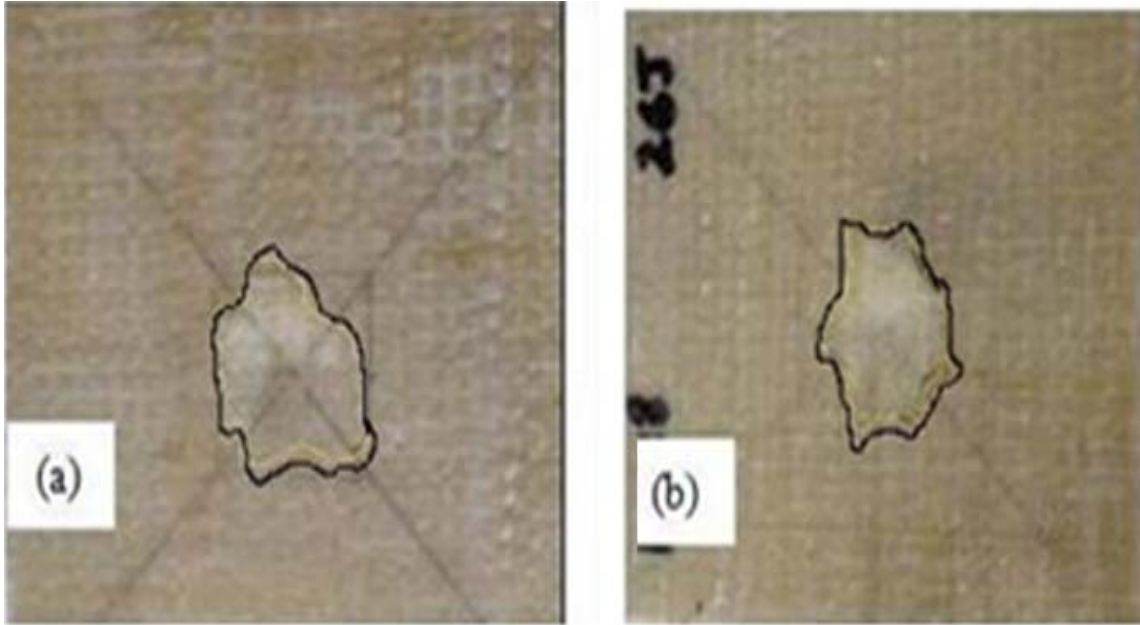


Fig. 3.6. Assessment of damage size in impact side of sandwich after impact visually inspection; (a) 17J, (b) 26J.

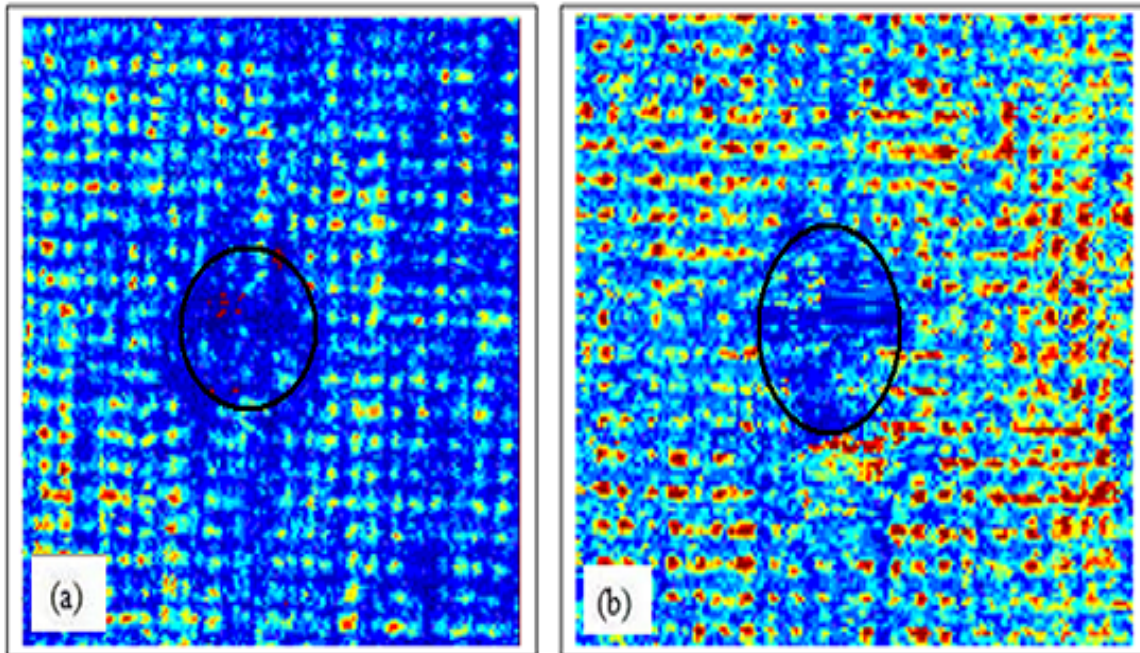


Fig. 3.7: Ultrasonic c-scan images of front surface impact damage at (a) 17J, (b) 26J

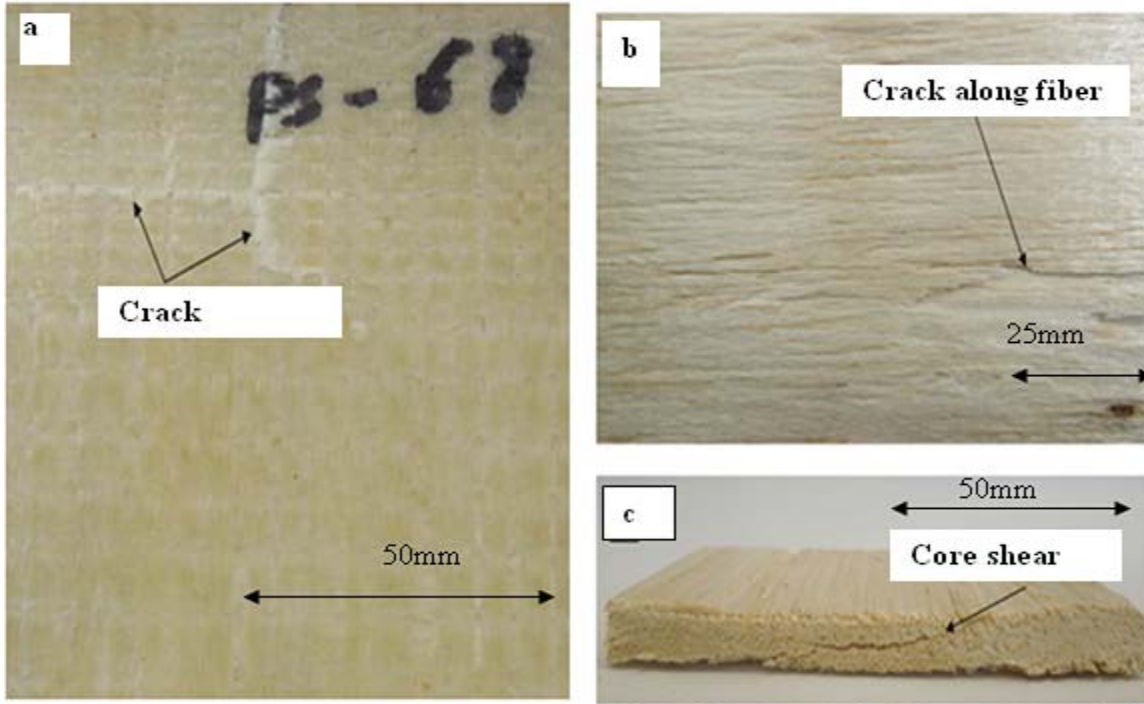


Fig.3. 8: Extent of damage in impact side of regular balsa core sandwich composite after impact by 26J (a) skin failure, (b) core cracks along fiber, (c) core shear failure.

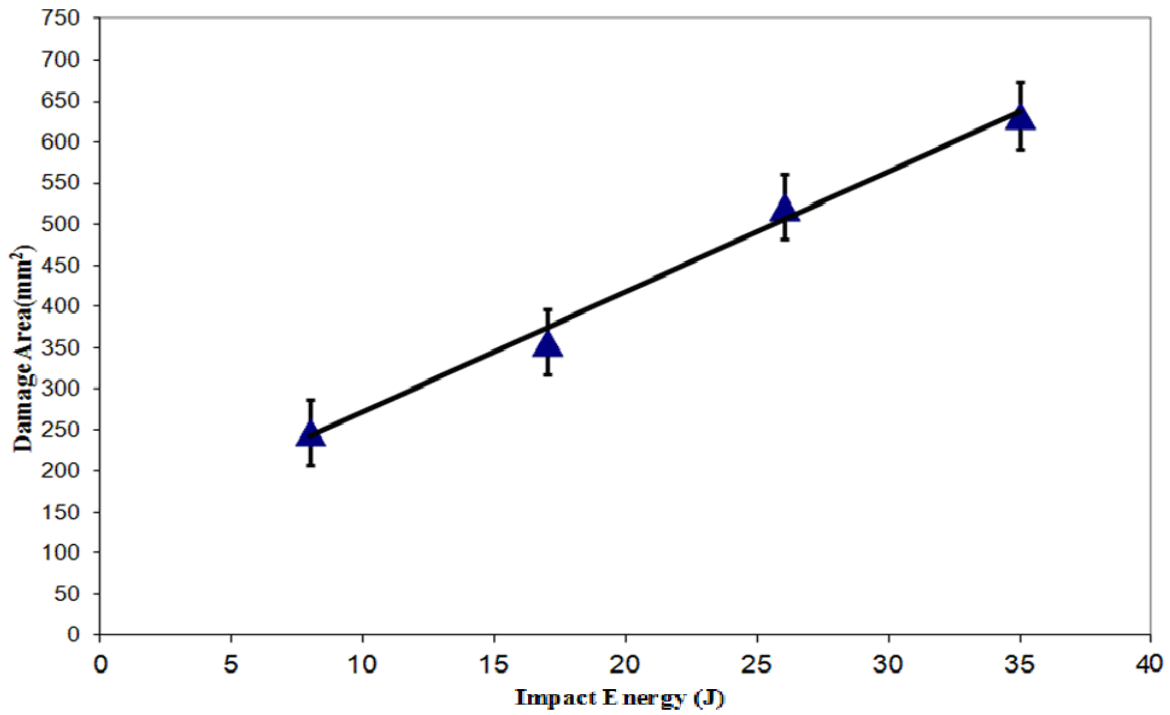


Fig. 3.9. Impact energy versus delamination area for end grain balsa. The error bars show variation in data.

### 3.2.4. Compression after Impact (CAI) Test

#### 3-2-4-1. Compression after Impact a long length

Impacted test specimens are subjected to CAI testing. The CAI tests were done at room temperature using MTS machine as shown in Fig.3.10 with a loading cell of 220 KN. The impacted specimens of sandwich composite with end grain and regular balsa cores which were subjected to three different energy levels (17J, 26J, 35J) were compressed along the length direction at a constant displacement rate 0.05 mm/sec. To obtain the loss of residual strength caused by the impact damage, virgin specimens should be also tested and comparing with the compressed damaged specimens. The test matrix for the samples that were impacted by Drop-weight impact tower is summarizes in table 3-6, and the test matrix for the samples which were impacted by Instron 9250 HV impact testing machine is summarized in table 3-7.

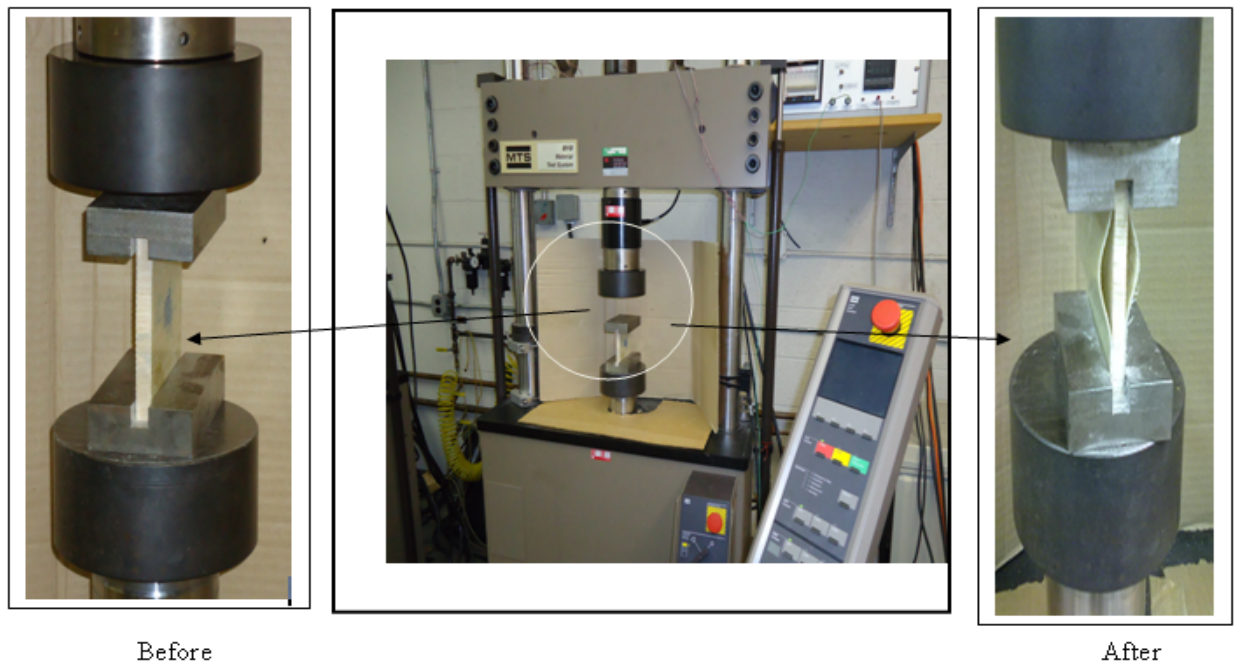


Fig. 3.10: Experimental set up for compression after impact test a long length.

Table 3.6: Test matrix of sandwich composite with end-grain core for CAI test

| Core material | # of tested samples | Impact energy(J) | Sample dimension |
|---------------|---------------------|------------------|------------------|
| End grain     | 6                   | undamaged        | 100mm×100×11.5mm |
| End grain     | 6                   | 8                | 100mm×100×11.5mm |
| End grain     | 6                   | 17               | 100mm×100×11.5mm |
| End grain     | 6                   | 26               | 100mm×100×11.5mm |
| End grain     | 6                   | 35               | 100mm×100×11.5mm |

Table 3.7: Test matrix of sandwich composite with end-grain and regular balsa core materials for CAI test

| Core material | #of tested samples | Impact energy(J) | Sample dimension |
|---------------|--------------------|------------------|------------------|
| End grain     | 6                  | 17               | 100×100×11.5     |
| End grain     | 6                  | 26               | 100×100×11.5     |
| End grain     | 6                  | 35               | 100×100×11.5     |
| Regular balsa | 6                  | 17               | 100×100×11.5     |
| Regular balsa | 6                  | 26               | 100×100×11.5     |
| Regular balsa | 6                  | 35               | 100×100×11.5     |
| Regular balsa | 6                  | undamaged        | 100×100×11.5     |

### 3.2.4.2. Compression after Impact through Thickness

Compression after impact (CAI) test through the thickness of sandwich composite with end grain core was conducted to investigate the characteristics of sandwich composite structure. Fig. 3.11 illustrates the test setup in advanced composites lab. In this test 76.2x76.2x11.5 mm impacted specimens of sandwich composites which were subjected to two different energy levels (17J, 26J) were compressed along the thickness direction with a constant displacement rate 0.05mm/sec. Undamaged specimens should be also tested and comparing with the compressed damaged specimens .The load was concentrated on the damage area by using steel cylindrical bar with diameter 20.5 mm. The specimens are compressed under displacement control on MTS machine until it is crushed to about of 50% of its original thickness. The test matrix for the damaged and undamaged specimens is tabulated in table 3.8.



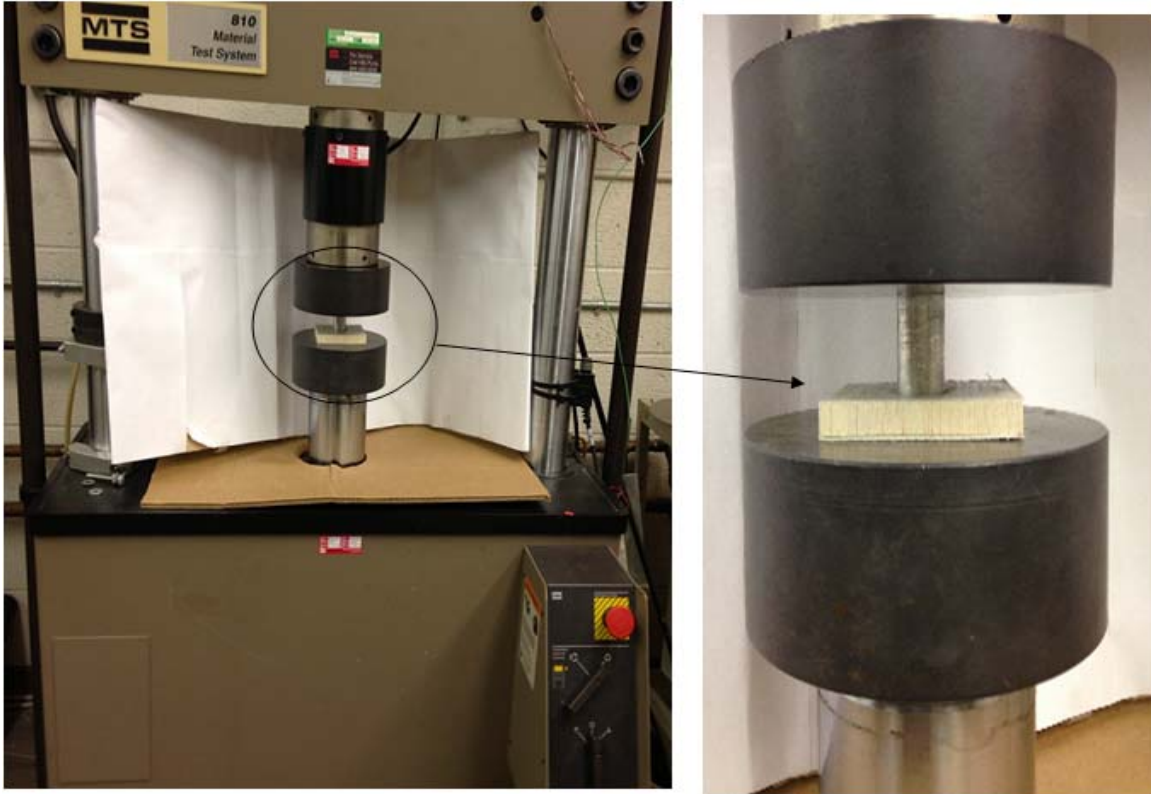


Fig. 3.11: Setup of compression after impact test along the thickness

Table 3.8: Compression after impact through thickness test matrix.

| Core material | No. of tested samples | Impact energy | Sample dimension  |
|---------------|-----------------------|---------------|-------------------|
| End grain     | 6                     | undamaged     | 76.2x76.2x11.5 mm |
| End grain     | 6                     | 17 J          | 76.2x76.2x11.5 mm |
| End grain     | 6                     | 26 J          | 76.2x76.2x11.5 mm |

## CHAPTER 4

### FINITE ELEMENT ANALYSIS (FEA)

#### 4.1. Properties of Sandwich Composite

Tensile and compression testing for both cores and face sheets in fiber and cross fiber direction were conducted to determine the properties of glass fiber/epoxy and balsa wood (regular balsa and end-grain) core. The properties that were used for the simulation are tabulated in table 3.2 and table 3.3.

#### 4-2. Model Definition

A sandwich composite specimen comprises of E-glass/epoxy face sheets with two different core materials, end grain and regular balsa wood were tested and simulated. The impact tests were carried out by two different weight impact towers, the first one has small impactor weight and small diameter (2kg and 25.4mm) and the second one has large impactor weight and large diameter (7.7kg and 50.8mm) and both cases were simulated.

#### 4.3. Model Creation

Hypermesh v 10.0 is used as a pre-processor to create the grid geometry of samples. Ls-Dyna 971 is utilized as a solver and Ls-Pre-post is utilized as a post-processor to process the results from LS-DYNA analysis. The produced composite plate consists of two layers each for the top and bottom layers of E –glass /epoxy face sheet and balsa wood core (end grain and regular balsa).

#### 4.4. Mesh Generation and Contact Definition

##### 4.4.1. Impact Test Simulation for Quarter of The Sandwich Composites with End-grain

###### Core Material:

Due to symmetry of sandwich composite plate geometry, boundary conditions and loading, only 1/4th of the model has been considered. The final load is corrected by considering 4 times the attained result. The grid geometry of E –glass /epoxy was designed as one layer of shell elements and the grid geometry of end grain core was designed as six layers of brick elements. The impactor was modeled with 11563 tetra4 solid elements, and each face sheet and balsa wood core had 672 shell and 4032 brick elements, respectively. The load cell was created as 5 layers of 2295 brick elements. More fine mesh was used in impact region as shown in Fig.4.1 to obtain more accurate results. In Ls-Dyna, using an appropriate hourglass energy (HGE) coefficient type on skin and core is necessary to avoid a negative element volume error. Type 4 and 5 hourglass control with a HGE coefficient (QM) =0.01 was applied to balsa wood core and composite face sheets, respectively.

Eroding\_Single\_Surface contact type, which was defined using a penalty method, was used between the composite plate and the impactor. The same contact type was also used between the composite plate and the load cell. When solid elements in the contact definition are subjected to element deletion, this contact type is highly preferred.



#### 4.4.2. Impact Test Simulation for Entire Sandwich Composites with End-grain and Regular Balsa Core Materials:

In this case the whole sandwich system was modeled. The grid geometry of E-glass /epoxy was designed as one layer of shell elements and the grid geometry of balsa wood core was designed as four layers of brick elements. Each face sheet and balsa wood core had 4864 shell and 19456 brick elements, respectively. The 2 caliber steel spherical impactor was modeled with 13489 tetra4 solid elements. More fine mesh was used in the impact region as shown in Fig.4.2 to get more accurate results. The entire sandwich composite finite element model was shown in Fig. 4.3. The same type 4 and 5 hourglass control with a HGE coefficient 0.01 was applied to balsa wood core and composite face-sheets, respectively. Automatic\_Surface\_To\_Surface contact type was used between the upper skin of composite plate and the impactor, and Tied\_Nodes\_To\_Surface\_Offset was given between the skins and core.

#### 4.5. Sandwich Composite Material Model

*Composite faces:* There were three main failure mechanisms observed, including delamination, fiber breakage and matrix cracking, after the specimens were subjected to impact. The face sheets material model #59 (Composite \_Shell \_Failure \_Model) of the LS-DYNA material model library was used for shell elements, where Schweizerhof et al [41] have presented this material and they have shown this type of material has faceted failure surface as shown in Fig. 4.4. Ply-by-ply orientation of skin is not available in this model and laminate properties were directly applied.

*Wood core:* The wood properties were different in longitudinal, tangential, and radial directions. Therefore for analytical purposes it can be used as an orthotropic material [42]. The wood model was developed by Murray et al. [43] to simulate the deformation and failure of wooden guard rail posts impacted by vehicle. This type of material is currently available in LS-DYNA library as MAT 14 [44].

*Projectile:* Rigid model (MAT 20) was used for the impactor.

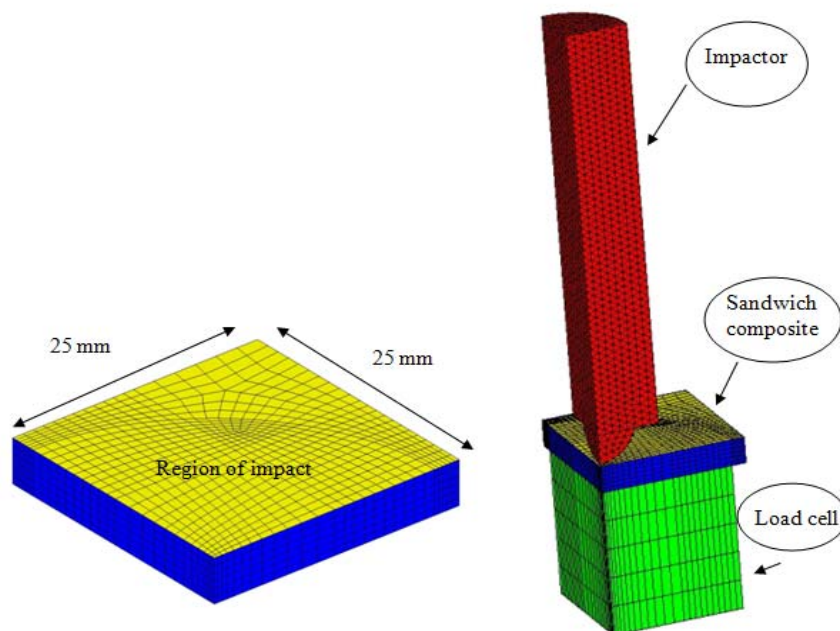


Fig.4.1: Quarter of the system finite element model

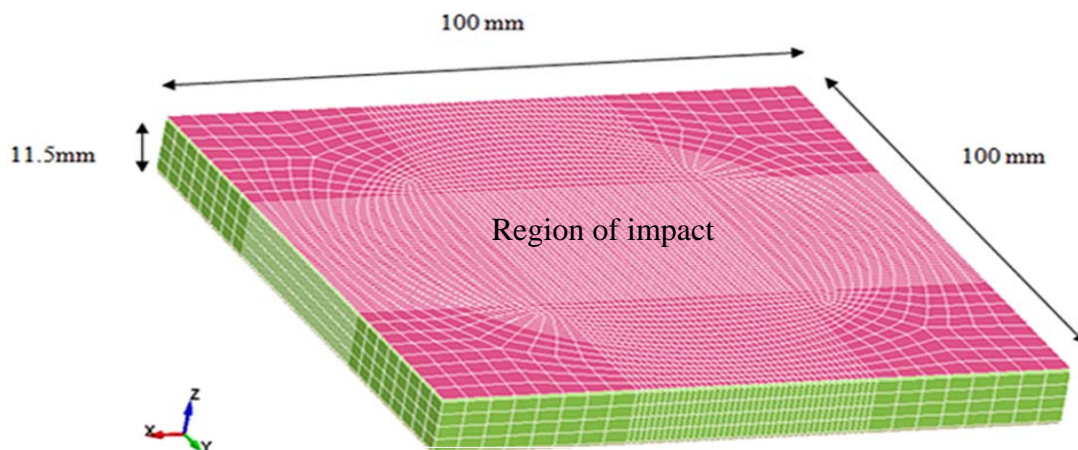


Fig.4.2: Fine mesh of entire sandwich composite plate.

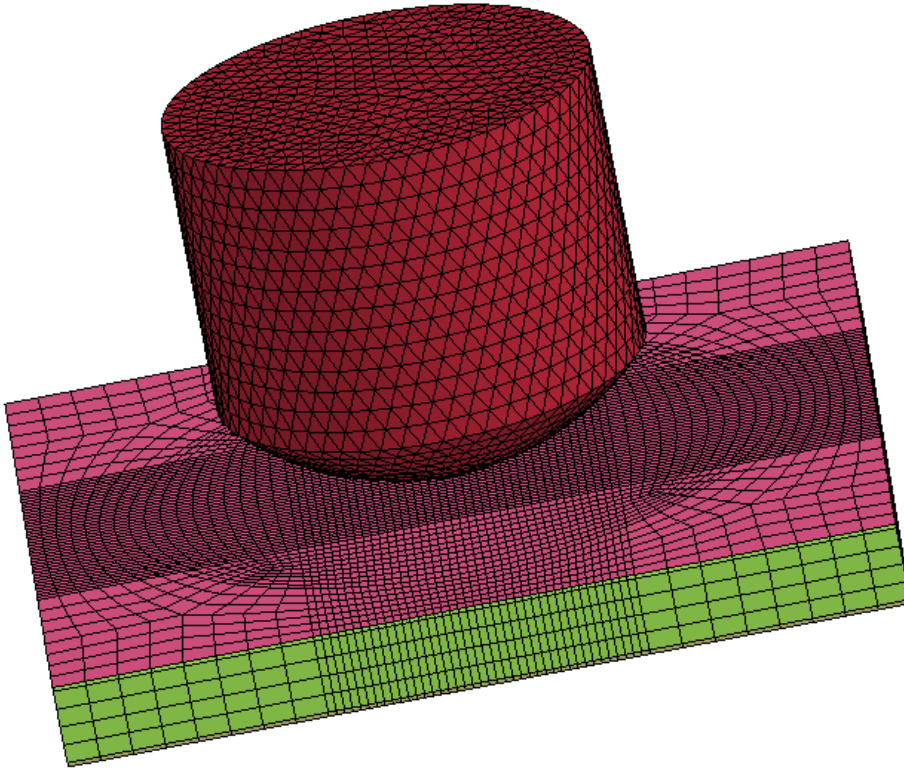
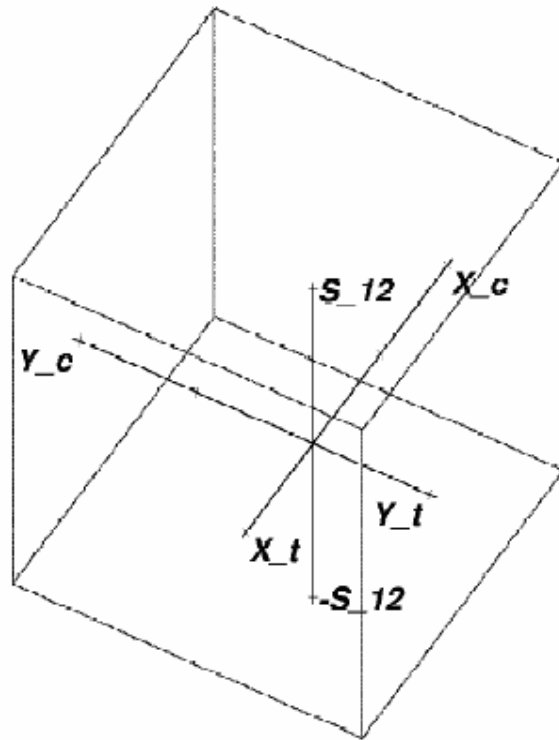


Fig.4.3: Entire of the system finite element model



$$\sigma_{1T} = X_T$$

$$\sigma_{1C} = -X_C$$

$$\sigma_{2T} = Y_T$$

$$\sigma_{2C} = -Y_C$$

$$\sigma_{12} = \sigma_{23} = \sigma_{13} = \pm S_C$$

Fig. 4.4. Failure model used in Mat 59 of LS- Dyna. (Ref. [44]).

## CHAPTER 5

### RESULTS AND DISCUSSION

#### 5.1. Experimental Results

##### 5.1.1. Impact Testing

Impact testing was performed by two different drop weight impact towers. Even though the impact energy levels which were used in both towers were the same, the results were completely different due to impactor mass weight and its size. The values of these evaluations were that sandwich impact responses under two different conditions were obtained. For this reason the results for each impact tower will be discussed separately.

##### 5.1.1.1. Impact Testing by Drop Weight Impact Tower

A typical load - time history graph for the sandwich composites with end grain core which are subjected to 17J and 26J impact from a 2 kg impactor is presented in Fig.5.1. A peak impact loads of 8200 N and 9620 N were recorded by a load cell for the both specimens at 1.5 ms. It is found that larger impact energy causes higher contact force and slightly increase the contact duration. However, Fig. 5.2 shows the recorded load versus deflection from experimental for two sandwich plates which were impacted at two different energy levels, where the projectile tip displacement as a function of time

$x(t)$  is obtained by a double integration:  $x(t) = \int_0^t (v_0 + \int_0^t a.dt).dt$  where  $v_0$  is the initial

velocity and  $a$  is the acceleration that was recorded by accelerometer. A plot shows closed loop in which the area inside the loop represents the energy absorbed by which was calculated by ORIGON software. The energy absorption results for the sandwich composites with end grain core were summarized in table 5.1. The primary damage modes observed are; matrix crack, fiber fracture at the upper skin, and delamination between adjacent glass /epoxy layers. The plot of the load versus deflection shows slightly change in the slope of the curve is due to damage that in composite sandwich plate starts with matrix cracking and fiber breakage and finally delamination. The maximum calculated displacements were around 4.8 and 6.2 mm at impact energy 17J and 26 J respectively.

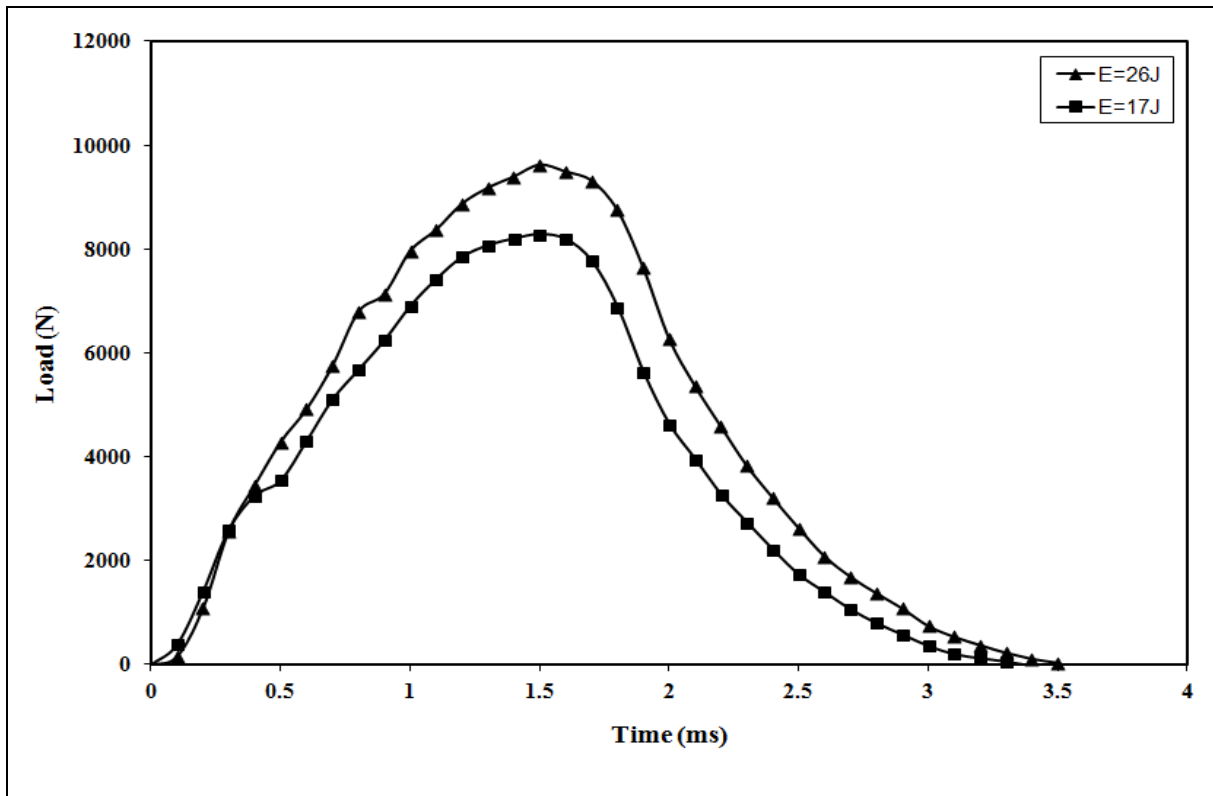


Fig.5.1: Typical load-time response comparison of two different impact energy levels.

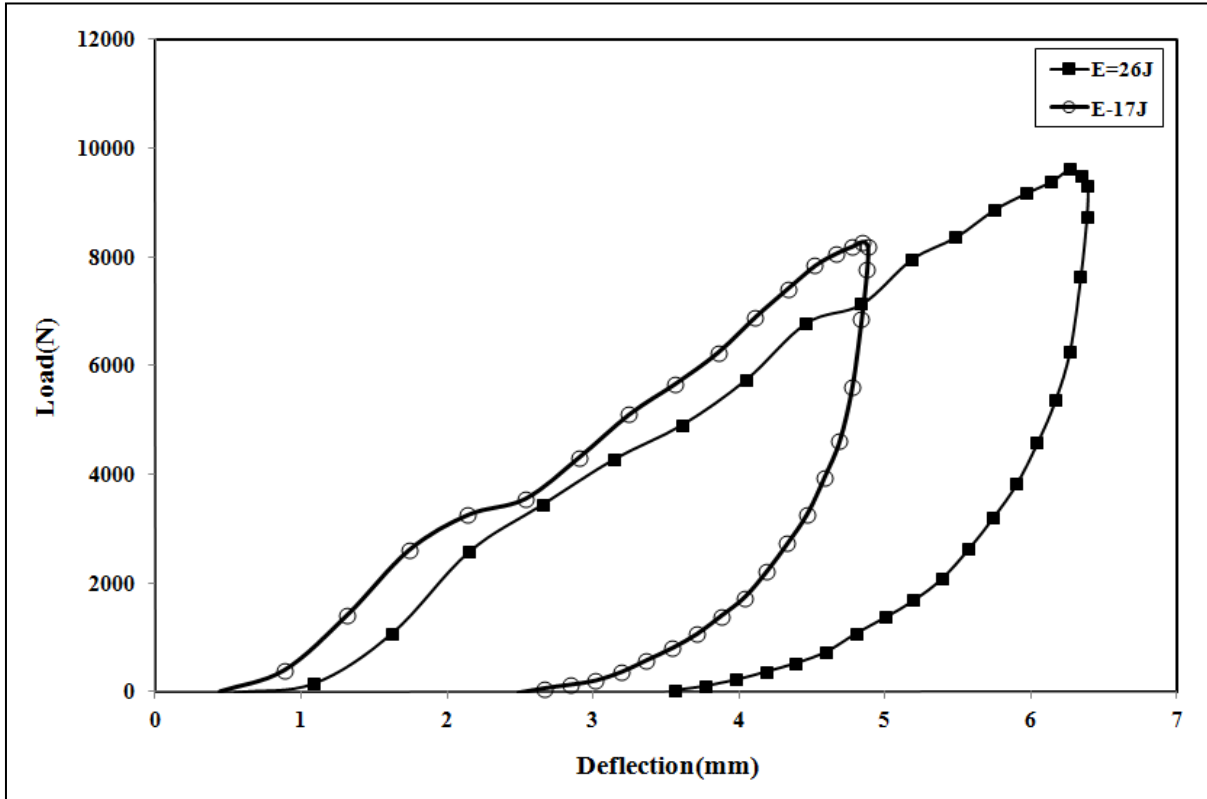


Fig.5.2: Typical load-deflection response comparison of two different impact energy.

Table 5.1: Energy absorption of sandwich composite with end grain core

| Damage state (J) | Peak load (N) | Energy absorption (J) |
|------------------|---------------|-----------------------|
| 17J              | 8200          | 14.24                 |
| 26J              | 9620          | 22.11                 |

### 5.1.1. 2. Impact Testing by Instron 9250 HV Impact Testing Machine

Effects of impact energy on contact force history for two different cores of sandwich structure, end-grain and regular balsa wood, which were subjected to three different energy levels, 17J, 26J, and 35J impact from a 7.7 kg impactor, are given in Fig. 5.3 and Fig. 5.4 respectively. Evidently peak impact loads of 4700 N, 6700 N, and 8500 N were recorded by the load cell at 4.1ms upon impacting the end-grain sandwich structure, and 3600 N, 4200 N and 5700 N were recorded at 4.8 ms upon impacting the regular balsa sandwich structure. Those loads were obtained when the sandwich structure was impacted with energy levels of 17J, 26J, and 35J, respectively. Therefore, the contact force was proportional with the impact energy; the higher impact energy produced higher impact force for both cores. Figures 5.5 and 5.6 present typical force vs. displacement curves for sandwich composites with end grain and regular balsa cores conjunction with E-glass/epoxy face sheets, when both sandwich systems were subjected to the three different energy levels, 17J, 26J and 35J. Here, the systems exhibit a steady increase in the load followed by a change in the slope of the curve showing non linear behavior until the maximum load in the system was reached. It is found that the deflection of the sandwich composites with end-grain and regular balsa cores proportional with the impact energy.

Comparison of both sandwich systems was achieved in terms of load time and load deflection history. Fig. 5.7a, Fig. 5.7b and Fig. 5.7c show the typical load vs. time comparison for sandwich composite specimens made from two different core materials, end grain and regular balsa with the same face sheets. Both specimens were tested under the same conditions and subjected to three energy levels (17J,26J and 35J). It is

observed that the sandwich composite with the end grain core has higher contact force than regular balsa core due to higher stiffness of end-grain core.

The force vs. displacement comparison for both sandwich composites is presented in Figures 5.8a, 5.8b, and 5.8c. It is obvious that the deflection of the sandwich composite with regular balsa core has higher deflection than end grain core because of higher stiffness of end grain core.

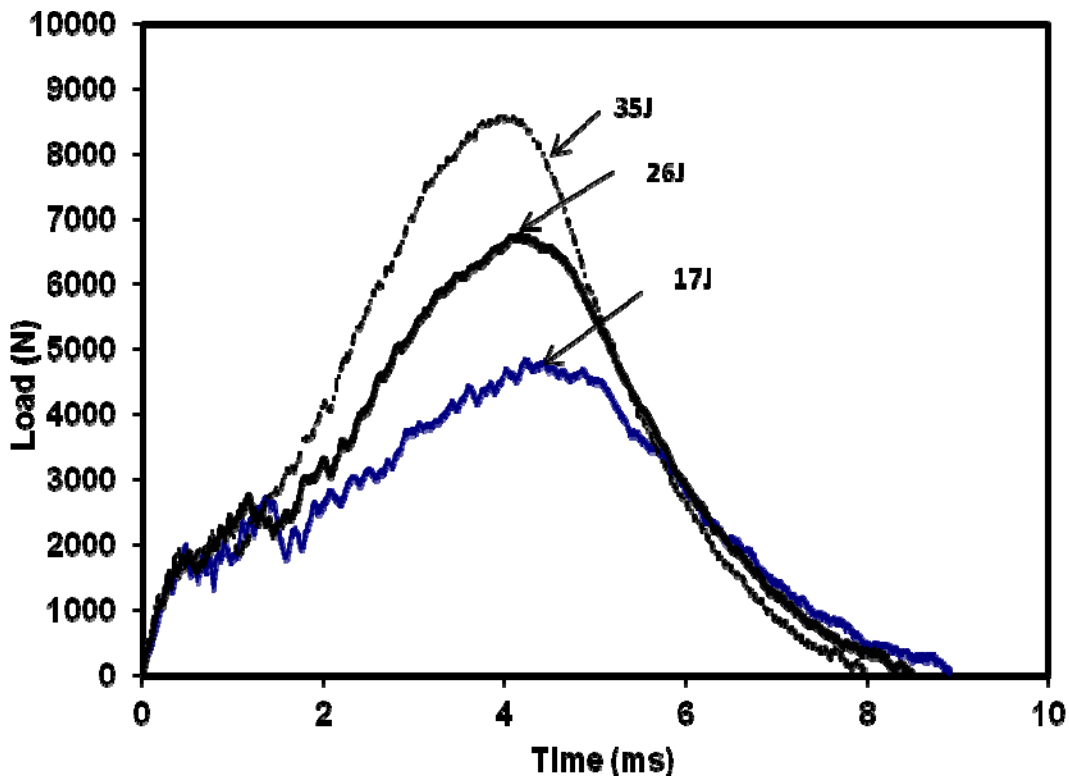


Fig. 5.3: Typical load-time response of sandwich composites with end grain core.



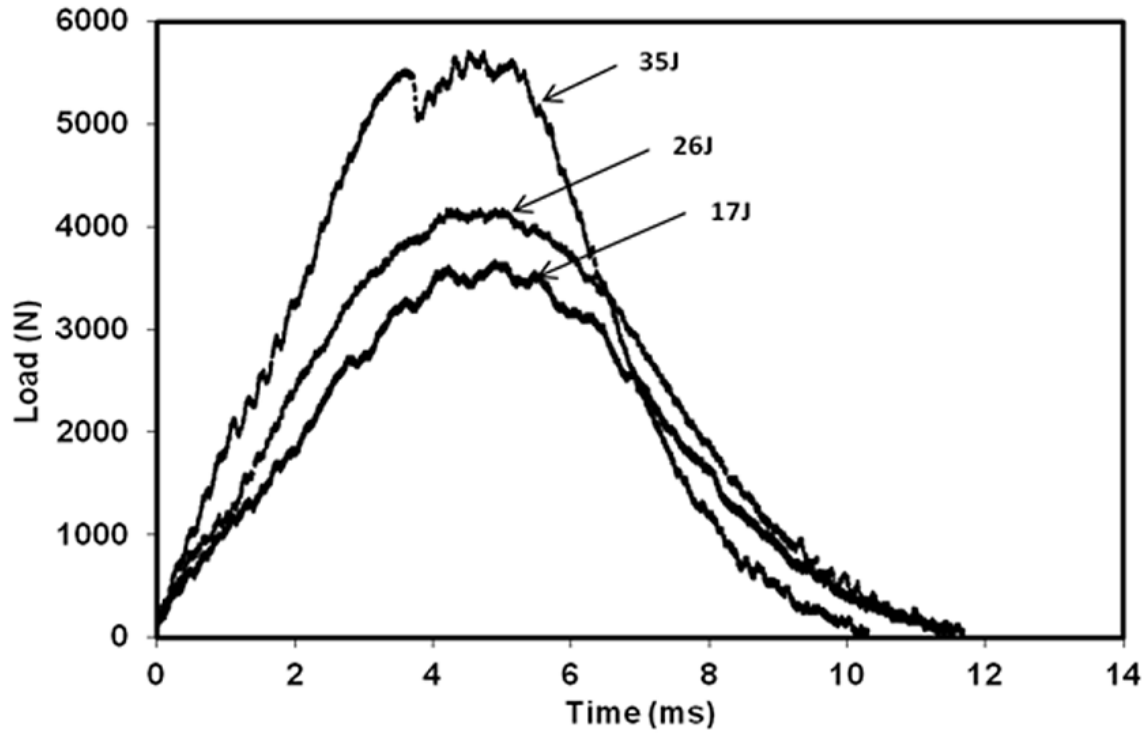


Fig. 5.4: Typical load-time response of sandwich composites with regular balsa core.

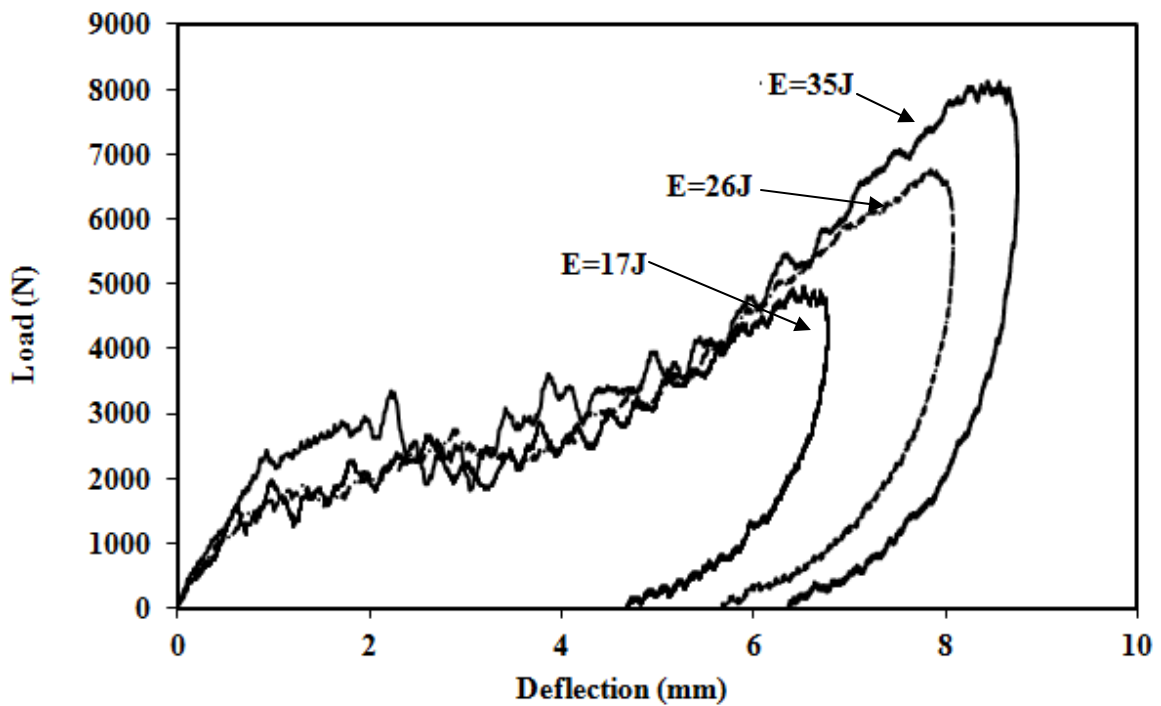


Fig. 5.5: Typical load-deflection response of sandwich composites with end grain core.

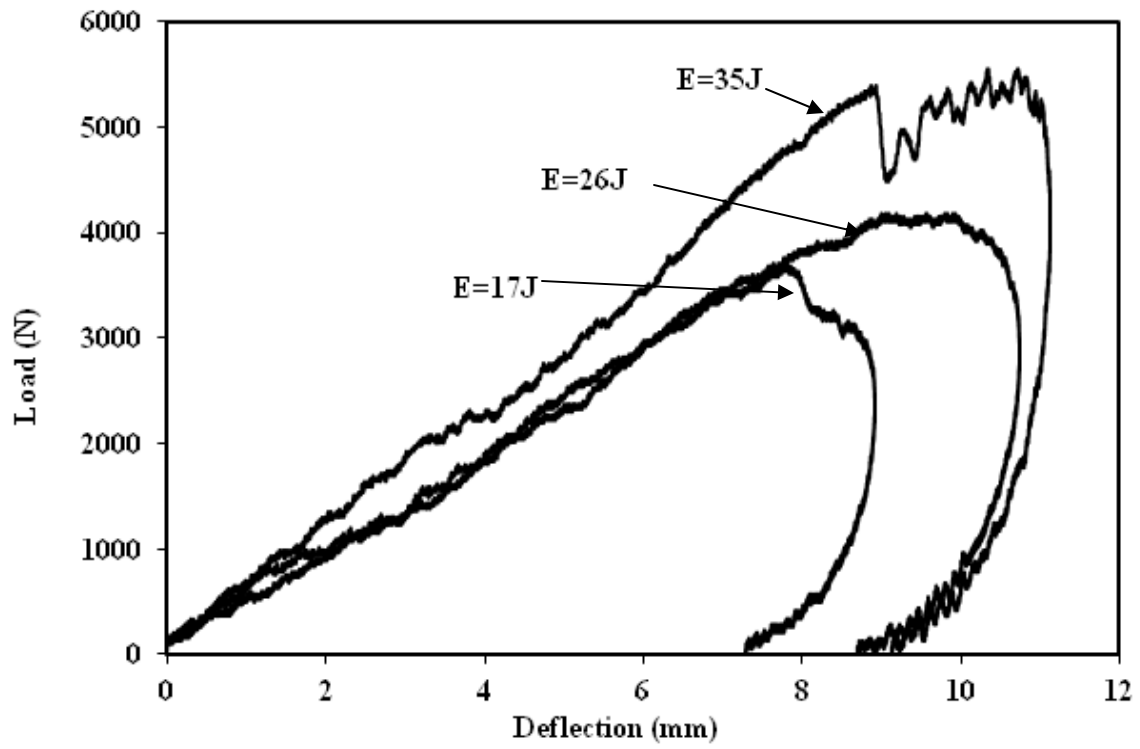
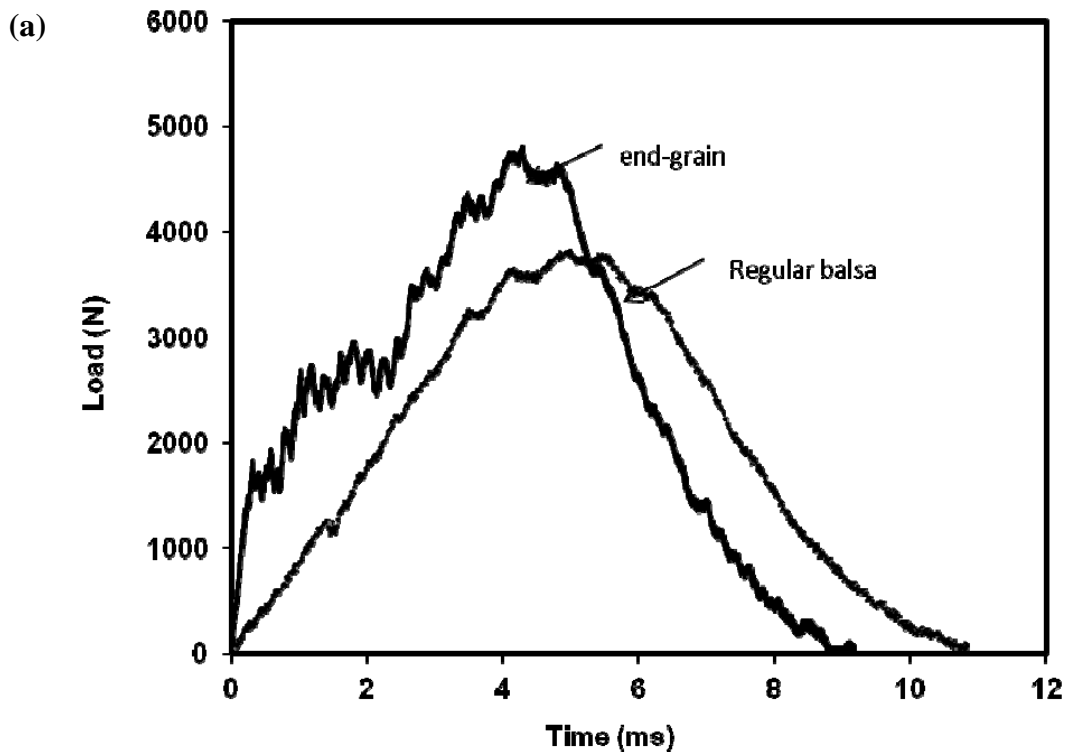
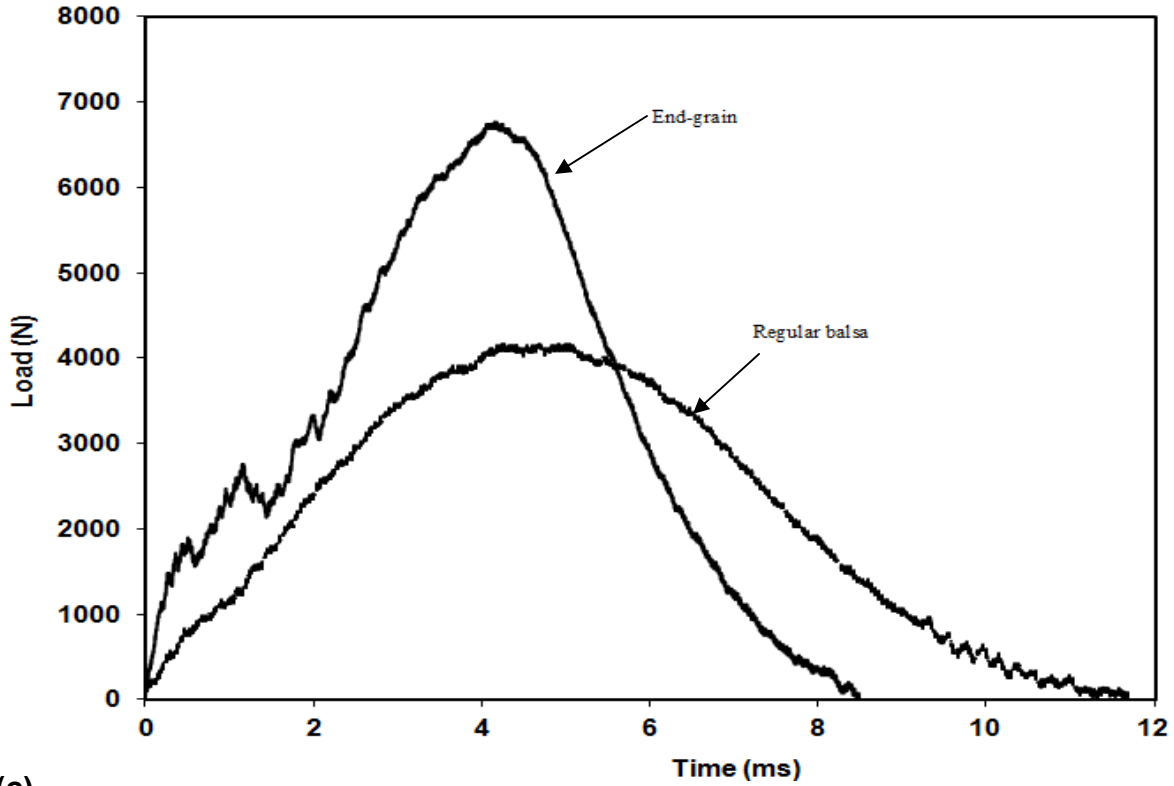


Fig. 5.6: Typical load-deflection response of sandwich composites with regular balsa core.



(b)



(c)

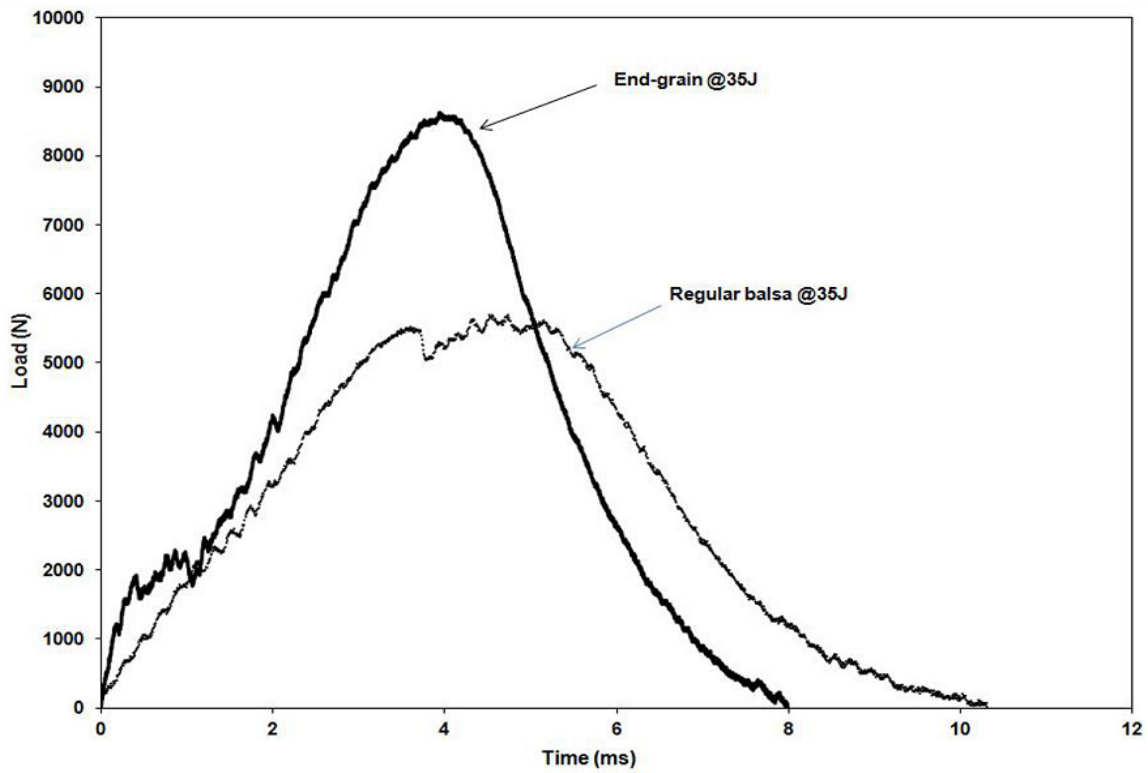
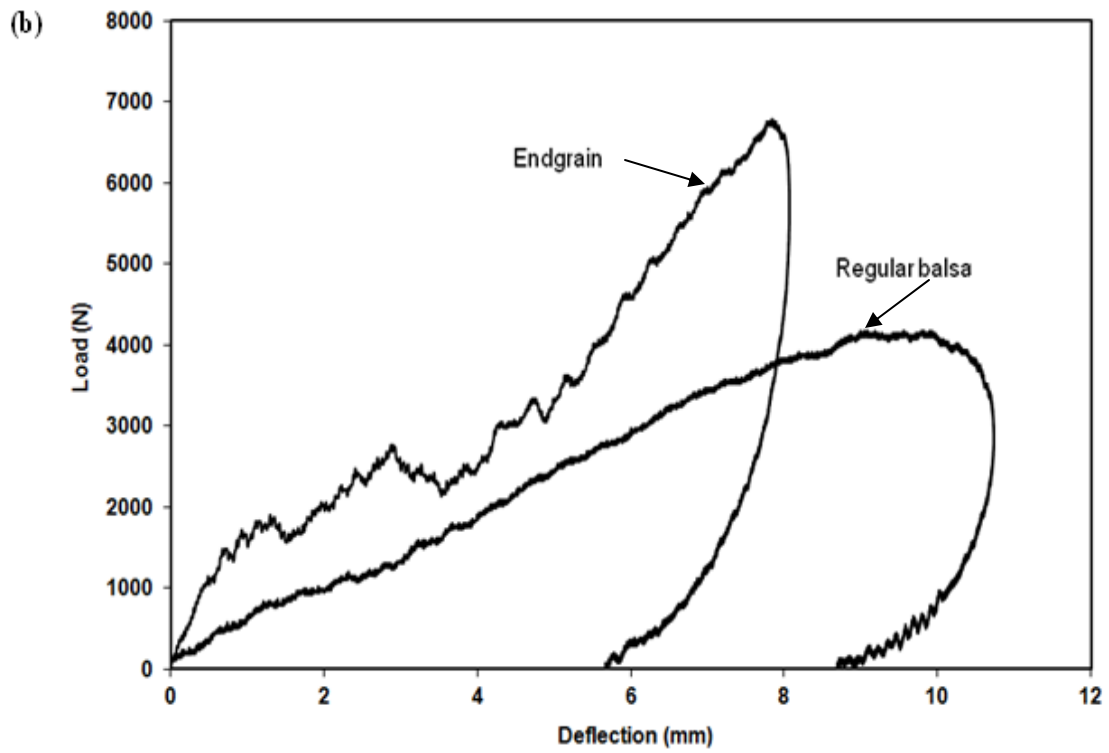
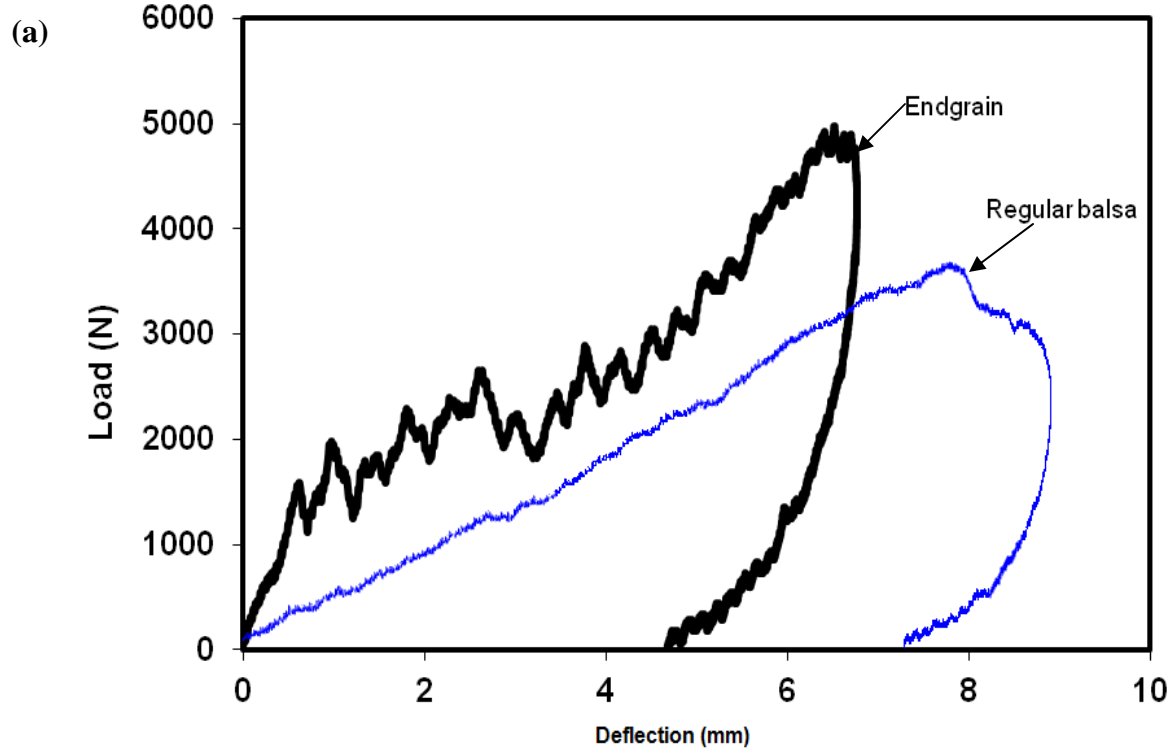


Fig. 5.7: Typical load-time response from impact tests comparison of sandwich composites with end grain and regular balsa cores at (a) 17J (b) 26J (c) 35J.



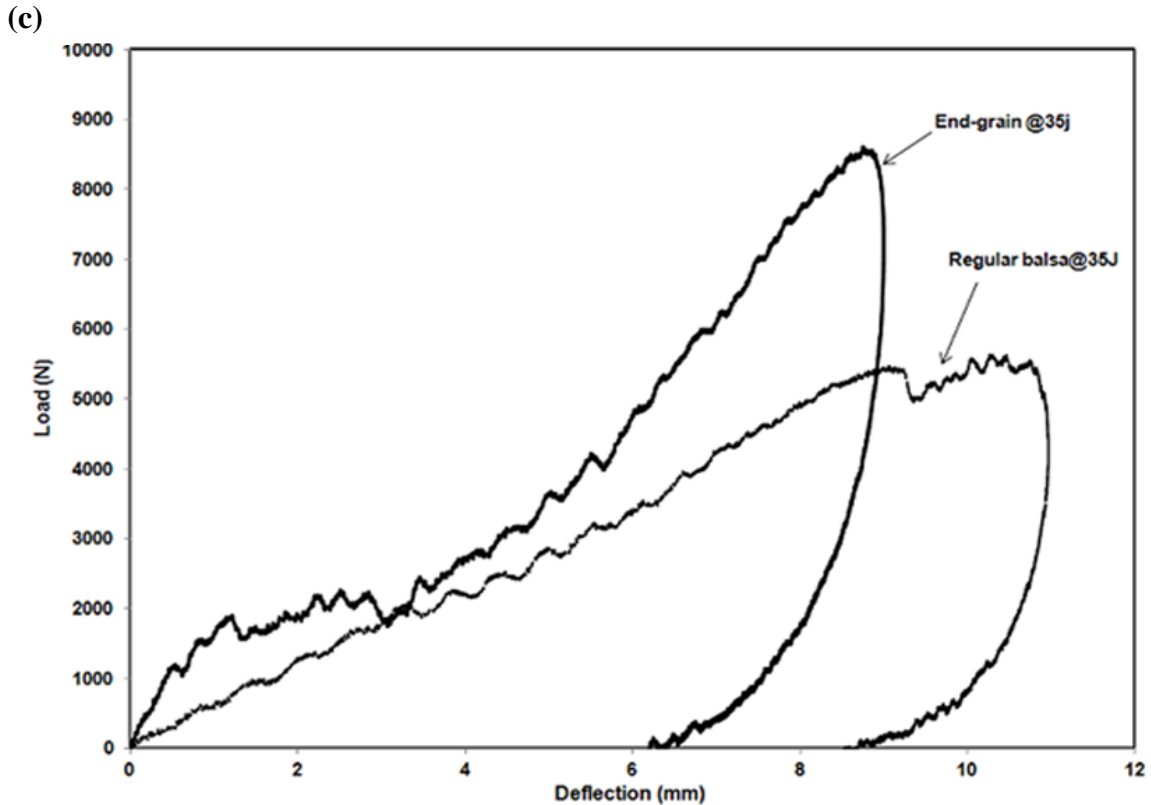


Fig.5. 8: Typical load-deflection comparison of sandwich composites with end grain and regular balsa cores at (a) 17J (b) 26J (c) 35J

The energy absorption of sandwich composites with end-grain and regular balsa cores was determined from the area inside the load- deflection curves that are shown in Fig.5.5 and Fig.5.6 by using ORIGON software. The energy absorption results for the sandwich composites with end grain and regular balsa cores were summarized in table 5.2 and table 5.3 respectively, and the energy absorption comparison results of both sandwich systems were presented in Fig.5.9. Here, it is found that higher impact energy of the impactor causes higher energy absorbed by the sandwich structure. At the highest energy almost 93% of the kinetic energy of the impactor has been absorbed by the regular balsa sandwich structure, while 88% was absorbed by end-grain core

sandwich structure suggesting that these systems offer great potential of use in dynamically load structures.

Figure 5.10 shows a typical velocity vs. time comparison of both sandwich systems which are subjected to 17J impact energy. From the figure, it is clear that the impacting head reached the velocity 2.13 m/s before impacting the specimen. In addition as soon as the sandwich plate is touched, the velocity of impactor decrease continuously until a velocity of 0 m/s has been reached suggesting that a position of rest at maximum displacement has been achieved. Following this, the velocity goes to negative scale reaching 0.71 m/s for end grain core and 0.48 m/s for balsa core as a result of the impactor bouncing back suggesting that a small amount of incident energy was still being carried by the impactor after hitting the target.

Table 5.2: Energy absorption of sandwich composite with end grain core tested by Instron 9250 HV machine

| Damage state (J) | Average peak load (N) | Energy absorption (J) |
|------------------|-----------------------|-----------------------|
| 17J              | 4850                  | 15.1                  |
| 26J              | 6725                  | 23                    |
| 35J              | 8100                  | 31                    |

Table 5.3: Energy absorption of Sandwich composite with regular balsa core

| Damage state (J) | Average peak load (N) | Energy absorption (J) |
|------------------|-----------------------|-----------------------|
| 17J              | 3650                  | 16.2                  |
| 26J              | 4295                  | 24.9                  |
| 35J              | 5645                  | 32.7                  |

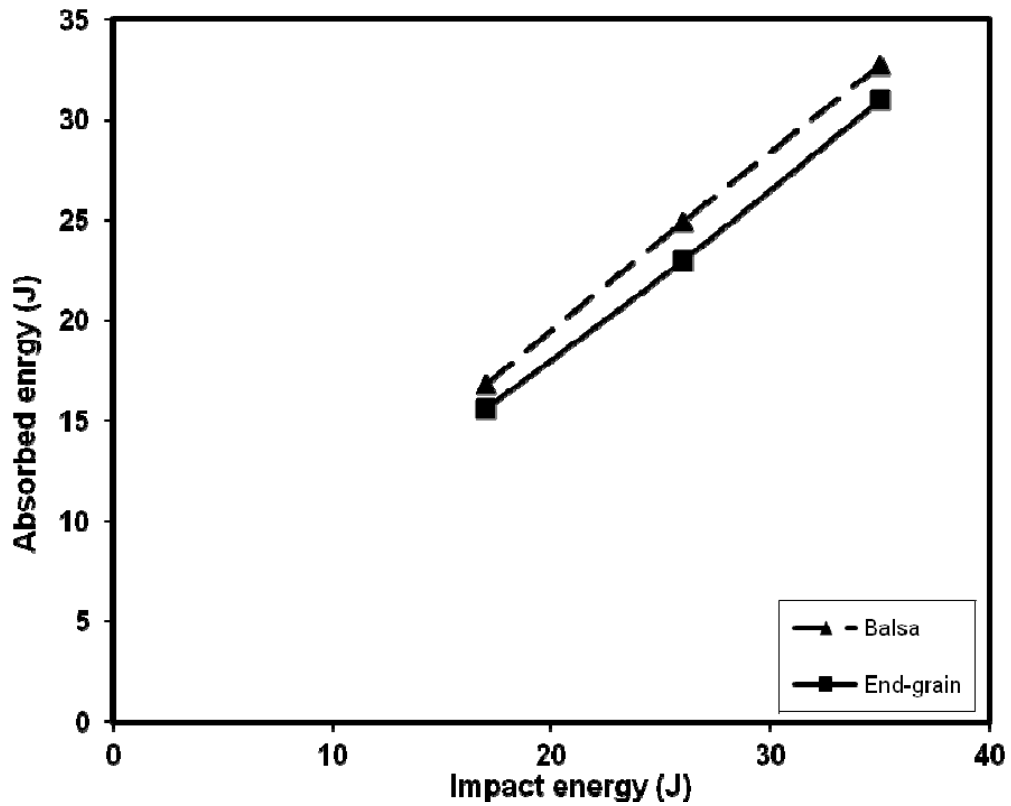


Fig.5.9: Impact energy vs. average absorbed energy comparison of sandwich composites with end grain and regular balsa cores.

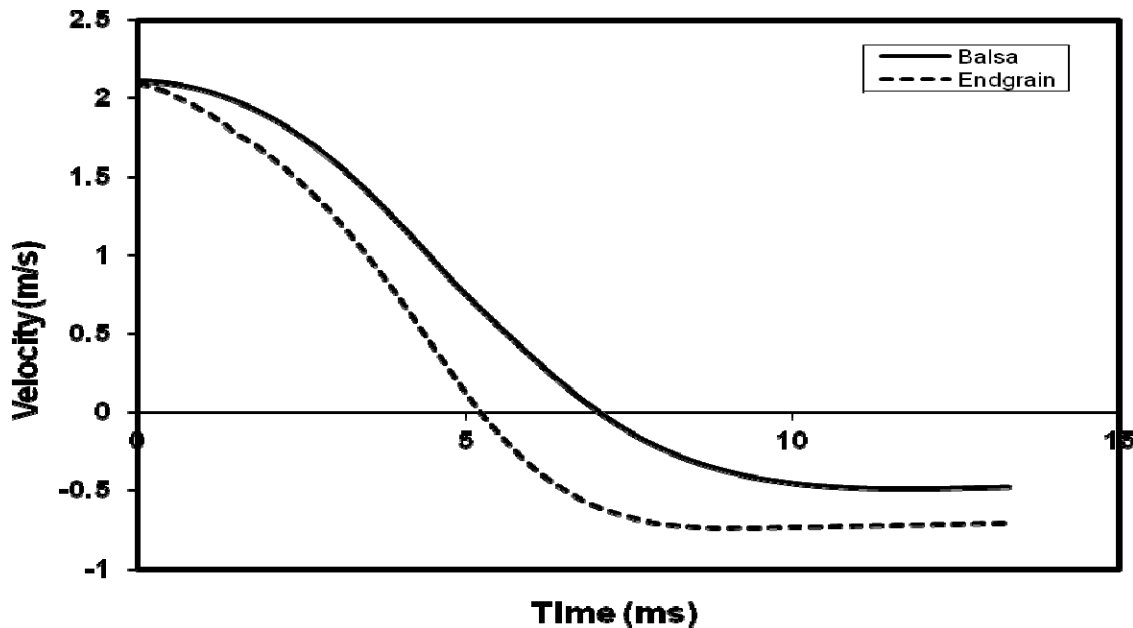


Fig.5.10: typical velocity time comparison of sandwich composite with end grain and regular balsa core at 17J impact energy.

## 5.1.2. Compression after Impact (CAI) Testing

### 5.1.2.1. Failure Modes of Sandwich Composites with End-grain and Regular Balsa Cores

Two different impactor diameters (25.4mm and 50.8 mm) and two different impactor masses (2kg and 7.7kg) were used to impact the sandwich composites with end grain core at three different impact energy levels, 17, 26, and 35J. The failure modes of damaged sandwich composites under compression after impact test which were hit by 25.4 mm impactor diameter are matrix cracking, a rear face sheet failed due to large delamination area and followed by failed damage face sheet and finally core shear occurred. However the failure modes of the same damaged sandwich composites



which were impacted by 50.8 mm impactor diameter are crack matrix, delamination at rear surface and buckling followed by shear core along the thickness. In contrast, the failure modes that were observed for undamaged specimens under compression after impact (CAI) test are matrix cracking, delamination in one side and followed by sandwich buckling. On the other hand, undamaged specimens have another failure mode that was observed during the test, which was fiber fracture and compressive face sheet with core. Damaged and undamaged specimens failure modes for end-grain core comprising with E-glass/epoxy face sheets are presented in Fig.5.11.

The sandwich composites with regular balsa core were impacted just by 50.8 mm impactor diameter. The compression failure modes for this sandwich system were matrix crack, delamination at rear surface followed by buckling and core shear along the length. However, the failure modes of undamaged regular balsa sandwich composites under compression were delamination from both sides and finally core shear. The failure modes for both specimens (damaged and undamaged) are illustrated in Fig.5.12.

#### 5.1.2.2. The Effects of Impact Energy and Damage Area on Residual Strength

The residual strength as function of damage area for the sandwich composite with end grain core which was impacted by 25.4 mm impactor diameter is presented in Fig.5.13. The result shows, as the damaged area increases the residual strength decreases. The effect of impact energy on residual strength of sandwich composite that was described above has been also investigated. Plotting the residual compressive strengths versus impact energy Fig.5.14, shows higher impact energy causes lower

residual strength. For instance, the compressive residual strengths of 15, 12 and 5 MPa were produced at 17, 26 and 35J impact energy levels, respectively.

Also the residual strength as a function of impact energy for the sandwich composites with two different cores, end grain and regular balsa which were impacted by 50.8 mm impactor diameter was presented and discussed. The results for end grain sandwich composite system are illustrated in Fig.5.15. From the plot the same conclusion was obtained as mentioned above when the sandwich system was hit by 25.4 mm impactor diameter, compression after impact depends on the impact energy, larger impact energy leads large reduction in residual strength. However, the residual strengths which were obtained from both cases (different impactor mass and diameter) at the same impact energy were different. Therefore, we can conclude a large mass with low initial velocity may not produce the same residual strength as smaller mass with higher velocity even if the kinetic energies are exactly the same. Figure 5.16 presents the impact energy versus residual strength for regular balsa sandwich composite. The results also show the residual strength decreases as impact energy increases. By comparing end grain and regular balsa cores sandwich composite systems in terms of residual strength at the same impact energy, it is found that the end grain core sandwich system provides higher residual strength than the regular balsa core sandwich composite system because the higher strength of end grain core.

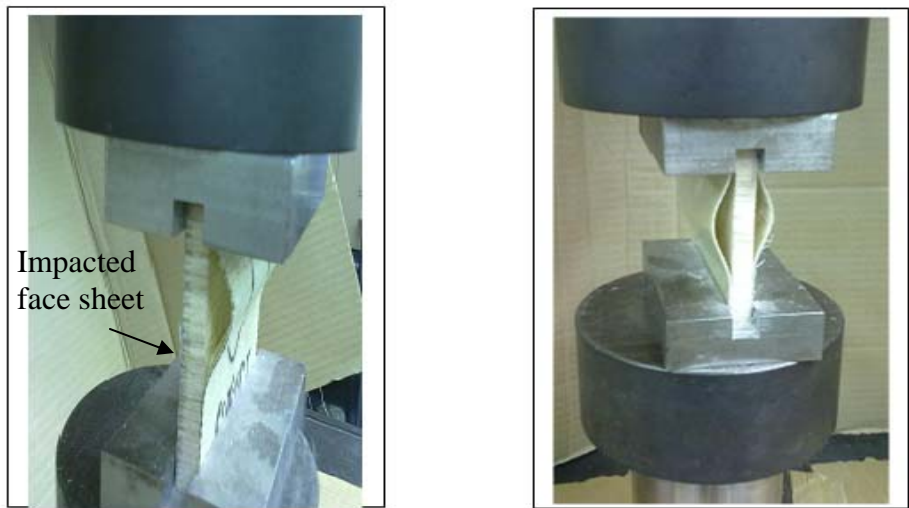
Figure 5.17 illustrates typical compressive stress strain curves for the damaged specimens of end grain sandwich composites, which were hit by 25.4mm impactor diameter at 17J and 26 J impact energies and the undamaged one. To determine the residual strength of the sandwich composites, failure load of the damaged specimen

should be compared with the failure load of the undamaged one. From the figure, it can be seen that the failure load decreases as impact energy increases due to large damage that was introduced during impact. The result of the sandwich composites with end-grain core which were impacted by 50.8 mm impactor diameter is presented in terms of stress vs. strain as shown in Fig.5.18. It exhibits the impactor mass has significant effect on the residual strength of sandwich composites with end grain core; larger impactor mass with larger diameter (50.8mm) produces lower residual strength than that was impacted by smaller impactor mass with smaller diameter (25.4mm) even for exactly the same energy level. This reduction of the strength of the structure is due to delamination impact damage of sandwich face sheets. For example, a 26J impact the strength reduction of end grain core sandwich composite was 37%, when smaller impactor mass was used. However, the strength reduction for the same sandwich composite was 55% when large impactor mass was utilized. Summary of damage state and failure load for end grain sandwich composites which were hit by small and large impactor is tabulated in table 5.4 and table 5.5 respectively. A typical stress strain relationship for sandwich composite with regular balsa core, which was hit by 50.8 mm impactor diameter, is presented in Fig.5.19. From the figure, it is found that the strength reduction of the sandwich composite after compression are 52%,53% and 66%, when the sandwich composites were subjected to 17J, 26J, and 35J respectively. The summary of damage state and failure load for the sandwich composite with regular balsa core is presented in table 5.6. By comparing the residual compressive strength of sandwich composites with end grain core with regular balsa core which were subjected to the same energy level 26J and 35J, it is found that the residual strength of the end grain core sandwich composite system is

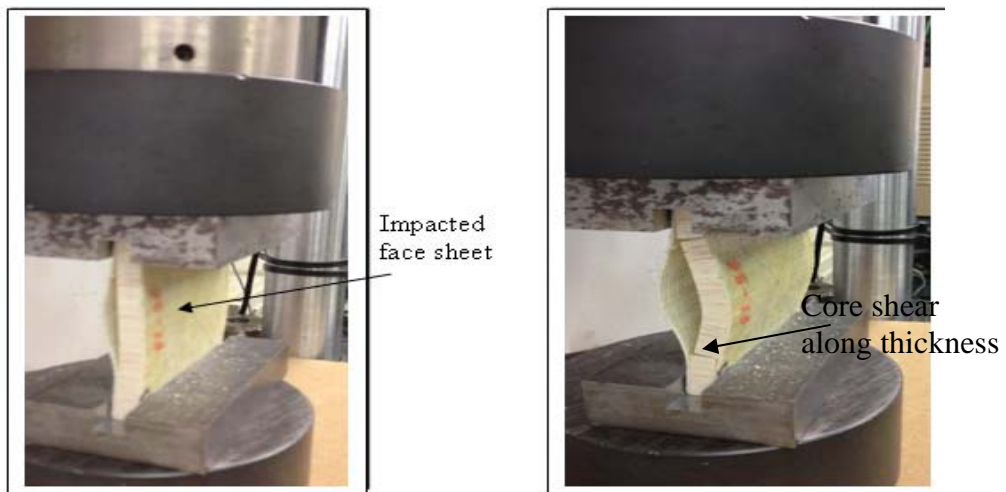
only slightly higher than that of the regular balsa core sandwich composite system due to more impact resistance of end grain sandwich composite and less damage was introduced during impact.



Undamaged specimen failure modes

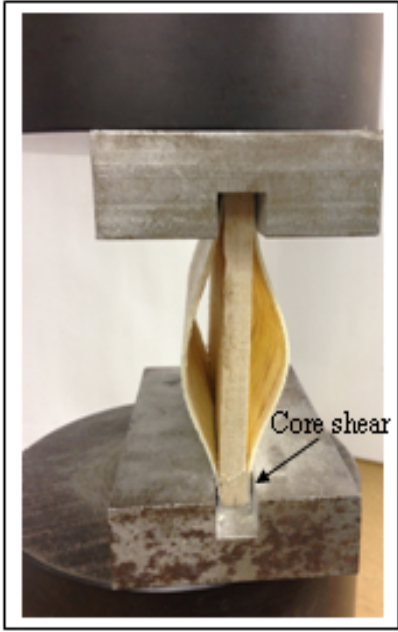


Damage failure modes by using 25.4 mm impactor diameter

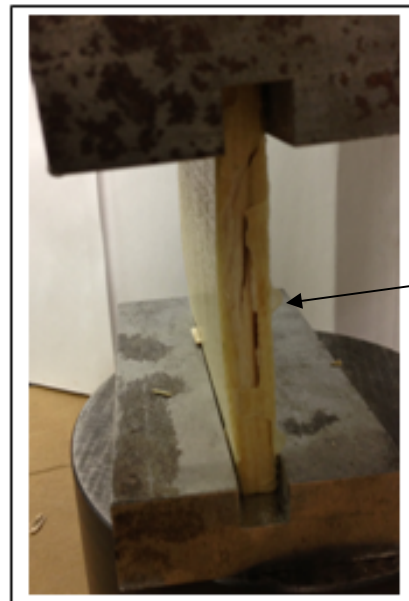
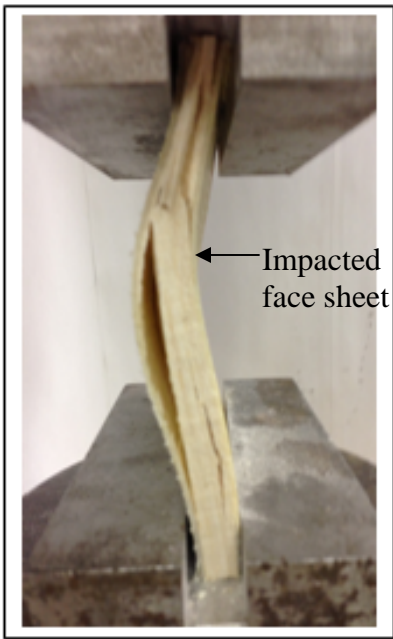


Damage failure modes by using 50.8 mm impactor diameter

Fig.5.11: Sandwich composite with end grain failure modes under compression



Undamaged specimen failure modes



Damaged specimen failure modes

Fig.5.12: Compression failure modes for sandwich composite with regular balsa core

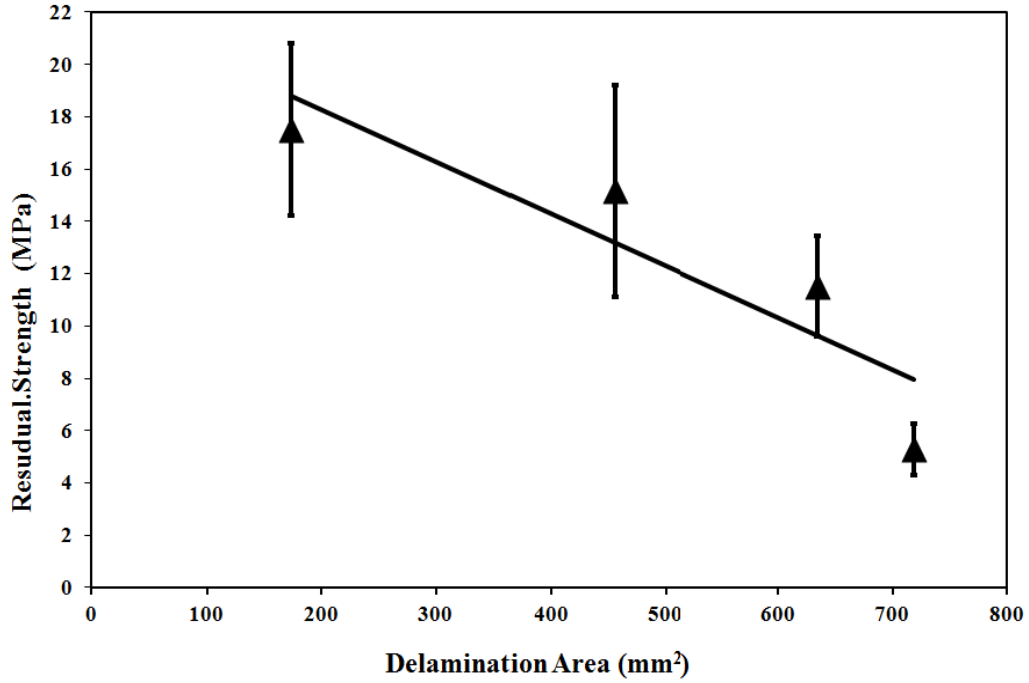


Fig.5.13: Residual strength versus delamination area for end grain sandwich composite structures.

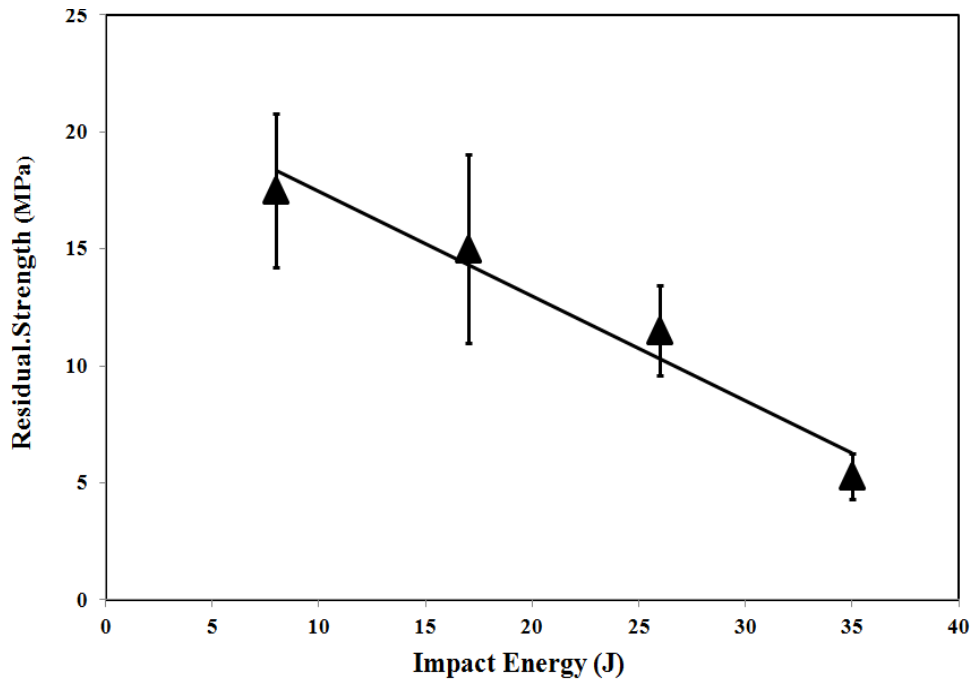


Fig. 5.14: Residual strength versus impact energy for end grain sandwich composite structures. The error bars show variation in data.

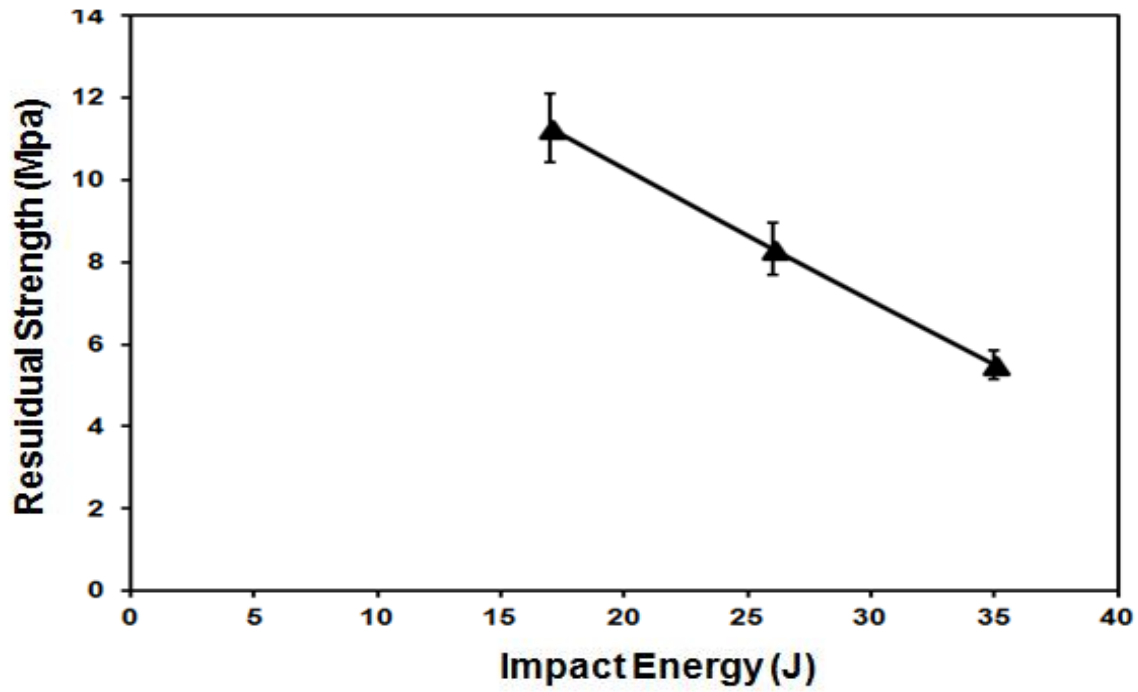


Fig. 5.15: Residual strength versus impact energy for end grain sandwich composite subjected to 50.8 mm impactor diameter. The error bars show variation in data.

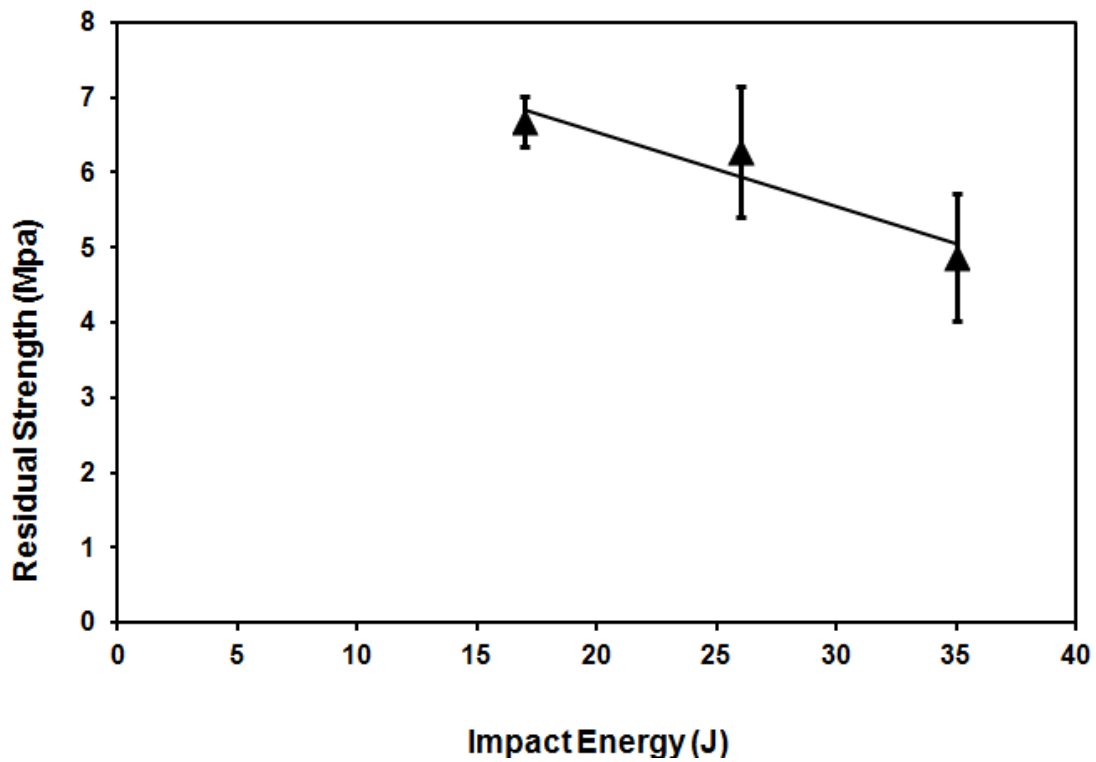


Fig. 5.16: Residual strength versus impact energy for regular balsa sandwich composite subjected to 50.8 mm impactor diameter. The error bars show variation in data.



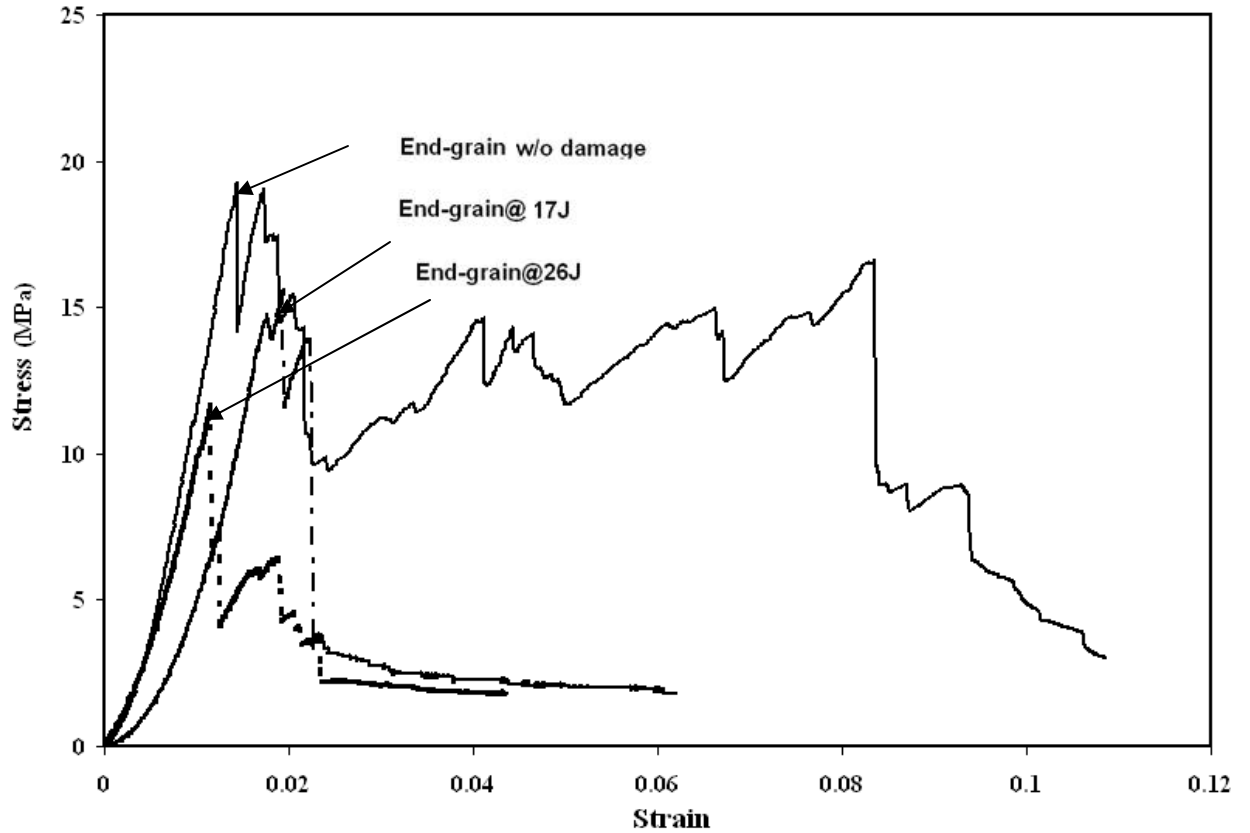


Fig.5.17: Average compressive stress strain curves for damaged and undamaged specimens (CAI ).

Table 5.4: Summary of damage state and average failure load of end grain sandwich composite

| *Damage state (J) | Average failure load (MPa) | Residual load carrying capacity |
|-------------------|----------------------------|---------------------------------|
| undamaged         | 19                         | -                               |
| 17                | 15                         | 79 %                            |
| 26                | 12                         | 63%                             |

\*damaged specimens were hit by 25.4mm impactor diameter

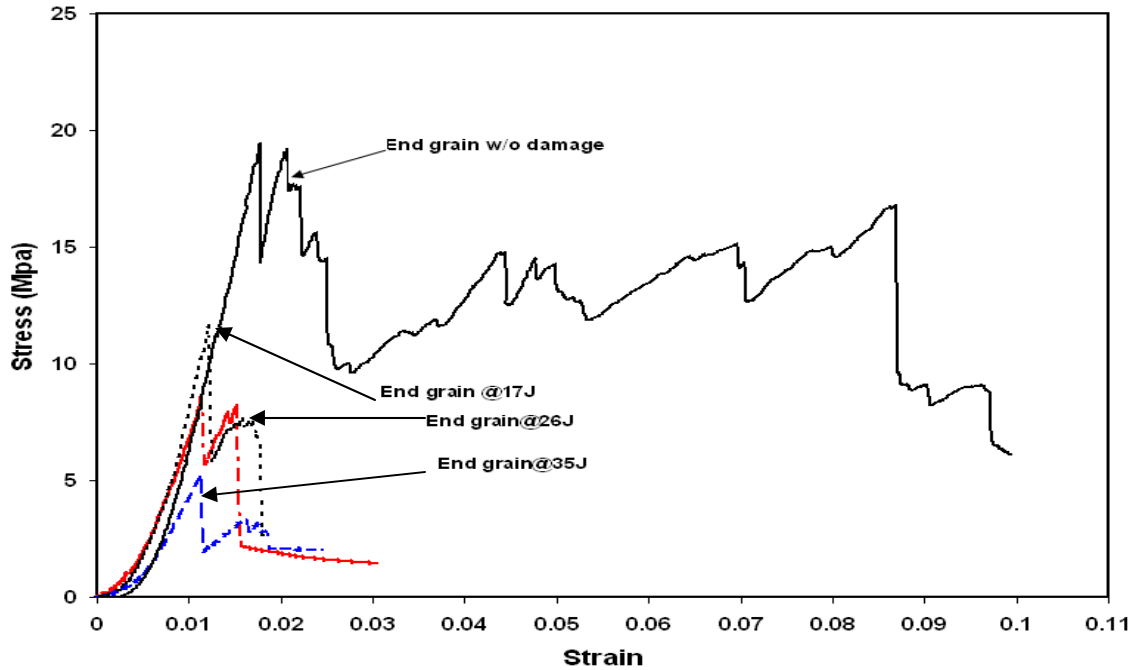


Fig.5.18: Average compressive stress- strain curves along length for sandwich Composite with end grain core

Table 5.5: Summary of damage state and failure load of end grain sandwich composite

| *Damage state (J) | Average failure load (MPa) | Residual load carrying capacity |
|-------------------|----------------------------|---------------------------------|
| undamaged         | 19                         | -                               |
| 17                | 11.5                       | 60%                             |
| 26                | 8.5                        | 45%                             |
| 35                | 5                          | 26%                             |

\*damaged specimens were hit by 50.8mm impactor diameter

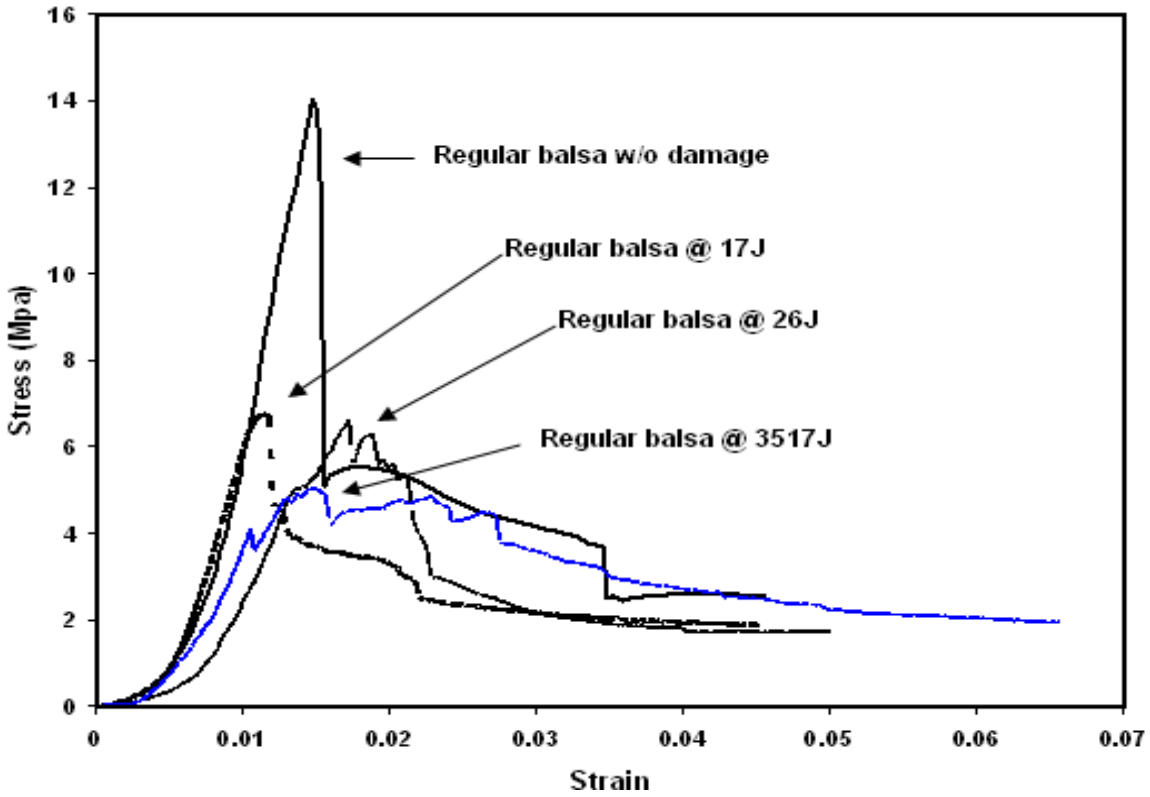


Fig.5.19: Average compressive stress-strain curves along length for sandwich composite structure with regular balsa core

Table 5-6: Summary of damage state and average failure load of regular balsa sandwich composite

| Damage state (J) | Average failure load (MPa) | Residual load carrying capacity |
|------------------|----------------------------|---------------------------------|
| undamaged        | 14                         | -                               |
| 17               | 6.7                        | 48%                             |
| 26               | 6.6                        | 47%                             |
| 35               | 4.8                        | 34%                             |

### 5.1.3. Compression after Impact (CAI) Testing for Through Thickness specimens

Damaged and undamaged specimens were tested and the results from the CAI tests were presented. Fiber breakage and delamination between skins and core were observed during tests. A typical stress-strain curve from the CAI of end grain core sandwich composite test is plotted in terms of average and maximum load for both damaged and undamaged specimens as shown in Fig.5.20 and Fig. 5.21, respectively. The stress was calculated by dividing the compressive load by the in-plane cross section area of sandwich composite specimen, where as the strain was calculated by dividing displacement by the original sandwich composite thickness. It is found that impacted specimens produced higher contact force than undamaged one because the core was densified after impact and became more compact. It was very obvious that the densification of the core was independent of the impact energy levels as shown in figure (5.20) where the 17J impact energy provides higher contact force than 26J impact energy. However, we couldn't conclude that higher impact energy produces higher contact force. The residual strength of the sandwich composite versus the impact energy is given in Fig 5.22. It can be seen from the plot, the undamaged sandwich composite plate was provided less residual strength than the damaged one because the core of the damaged specimen became more compact after impact. However, it was difficult to understand influence of the impact energy on the residual strength for the damaged sandwich plate from the plot. For example, the specimen which was subjected to 17J impact energy gives higher residual strength than that specimen was subjected to 26J, even though higher impact energy causes higher core densification. A summary

of damage state, failure load and energy absorption of end grain core sandwich composite is tabulated in table 5.7

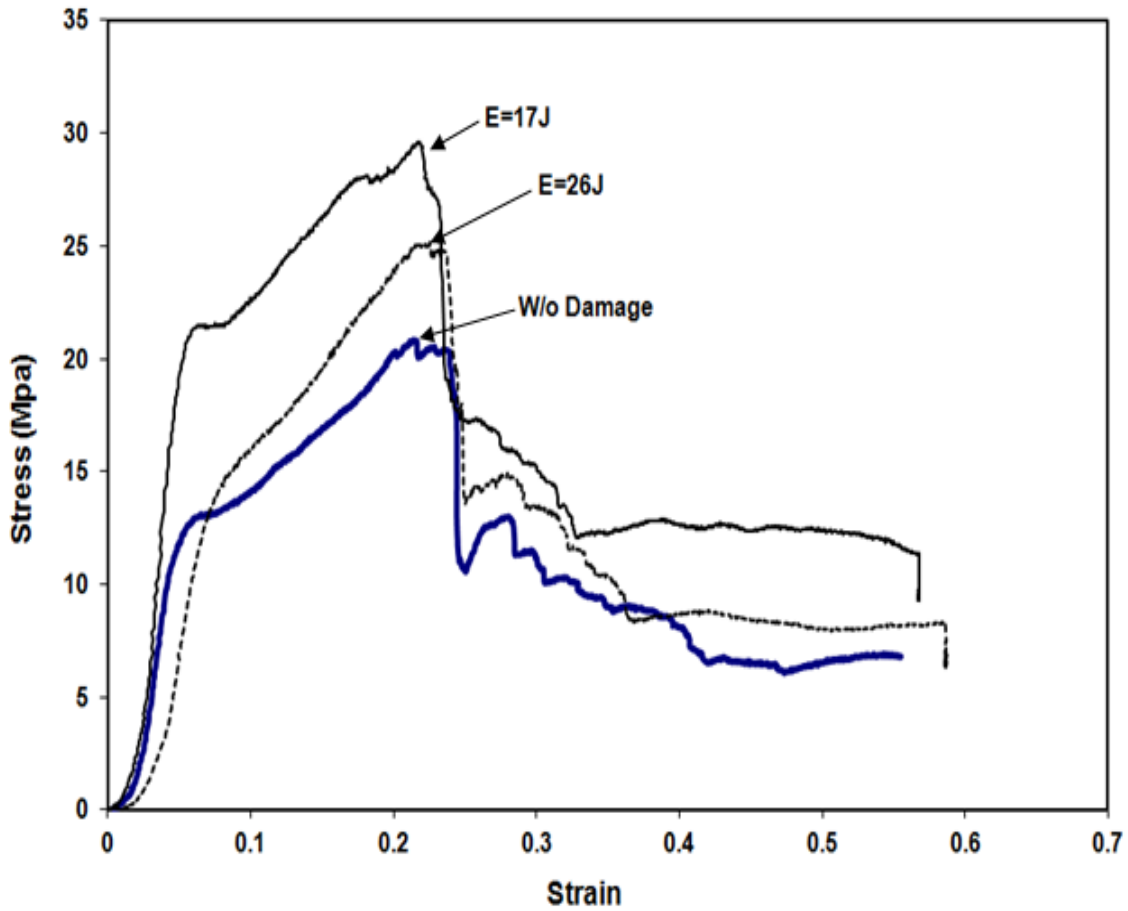


Fig.5.20: Through thickness compression after impact average failure stress comparison of damaged and undamaged sandwich composite with end grain core (typical stress-strain results)

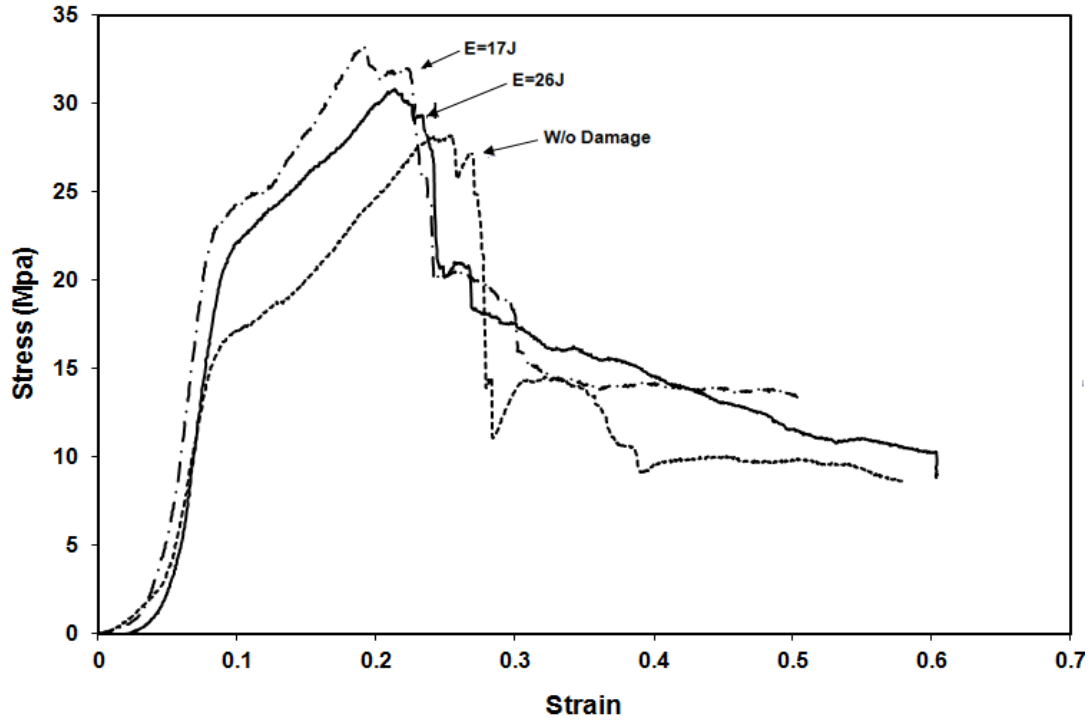


Fig.5.21: Through thickness compression after impact maximum failure stress comparison of damaged and undamaged sandwich composite with end grain core

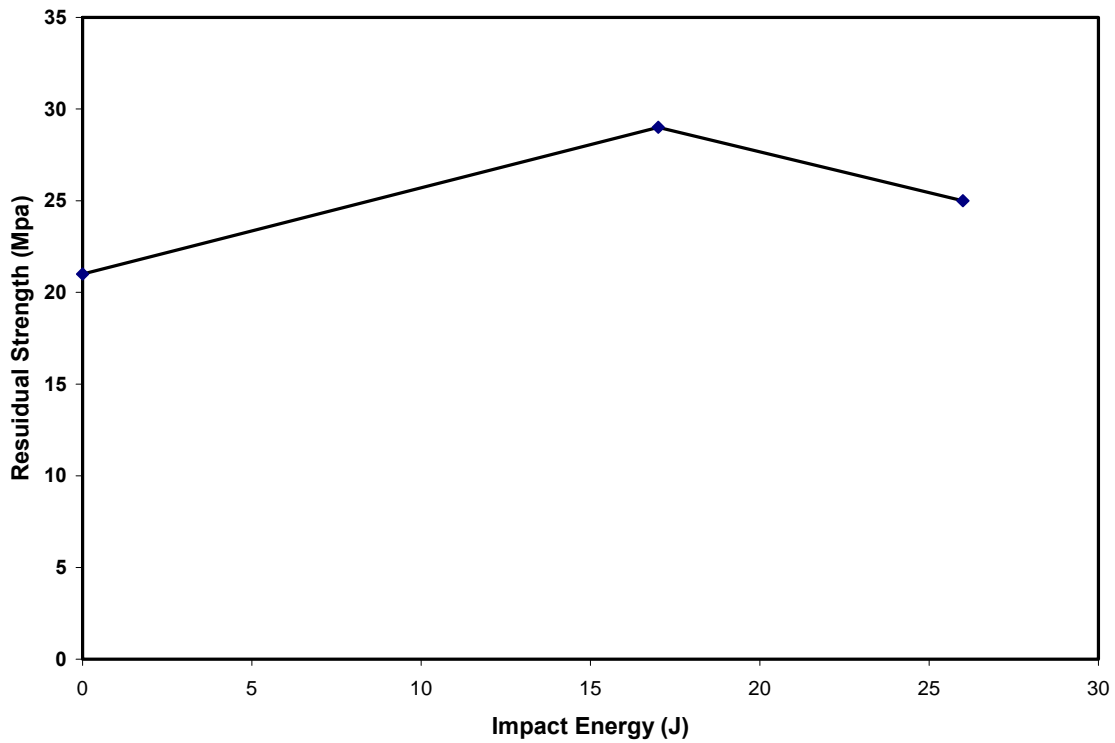


Fig. 5.22: Average residual strength versus impact energy for end grain sandwich composite after compression through thickness.

Table 5.7: Summary of damage state and failure load of end grain sandwich composite after compressed through thickness

| Damage state (J) | Average failure load (MPa) | Residual load carrying capacity | Energy absorption |
|------------------|----------------------------|---------------------------------|-------------------|
| undamaged        | 21                         | -                               | -                 |
| 17               | 27                         | 128 %                           | 16.3              |
| 26               | 23                         | 109%                            | 25.4              |

## 5.2. Finite Element Results

### 5.2.1. Quarter End grain Sandwich System Simulation

Fig. 5.23 and Fig. 5.24 show the results of the contact force history between the 1 caliber impactor and the end grain core sandwich plate as a function of time predicted by LS-DYNA code were correlated with experimental data at 17 J and 26 J impact energies. Good agreement was obtained for the peak load; but, the agreement was less in duration time in the unloading portion. The reason of this difference is that the clamped boundary conditions might not have been completely realized in the impact test [26, 45]. This difference can also be due to lack of sophisticated progressive material damage model in LS-DYNA. Nature of complex damage in sandwich composite requires considerable attention. Comparisons of results predicted by LS-DYNA with experimental data for the sandwich plate deflection history along z-axis were

made in figures 5.25 and 5.26 at two different energy levels, 17J and 26J, and good agreements were obtained. For example, the maximum deflection in the experimental and numerical at 17J impact energy was 4.8 and 4.2 mm respectively. Also impactor kinetic energy from the point of contact with the target until bounce back history is presented numerically and experimentally at 26 J impact energy as shown in figure 5.27.

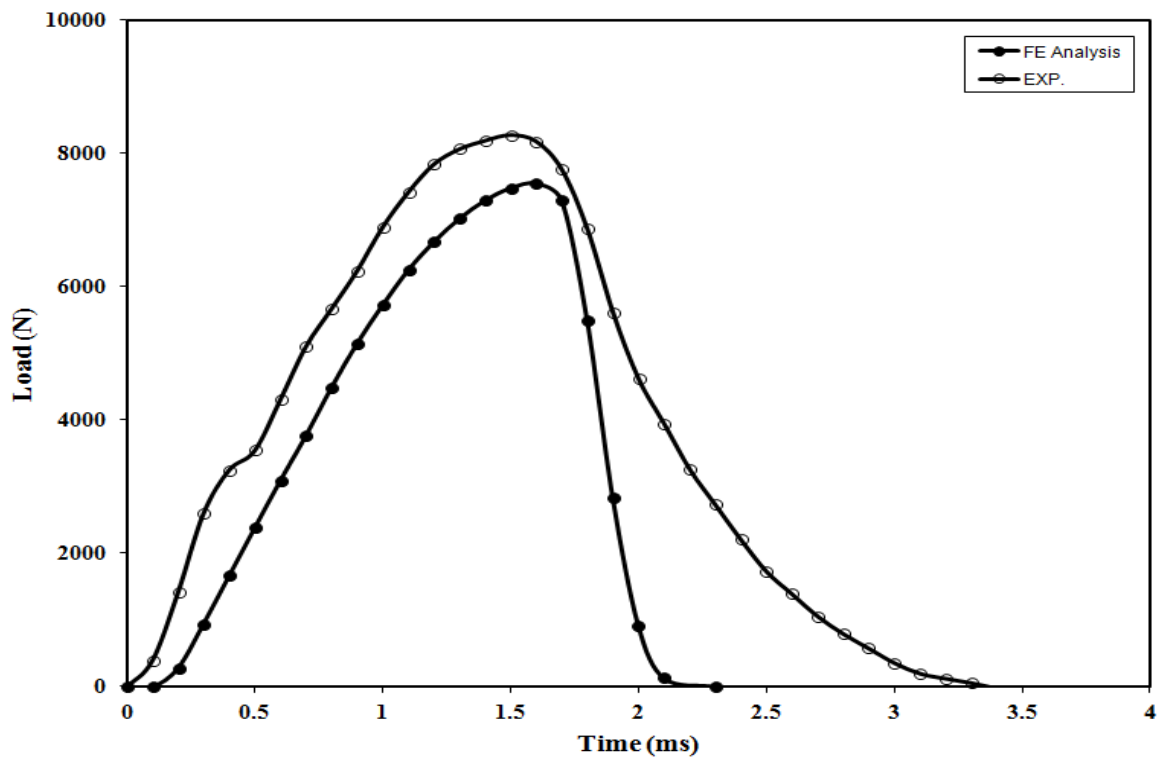


Fig. 5.23: Comparison of experimental and FEA load- time histories of sandwich composites with end grain core at 17 J.



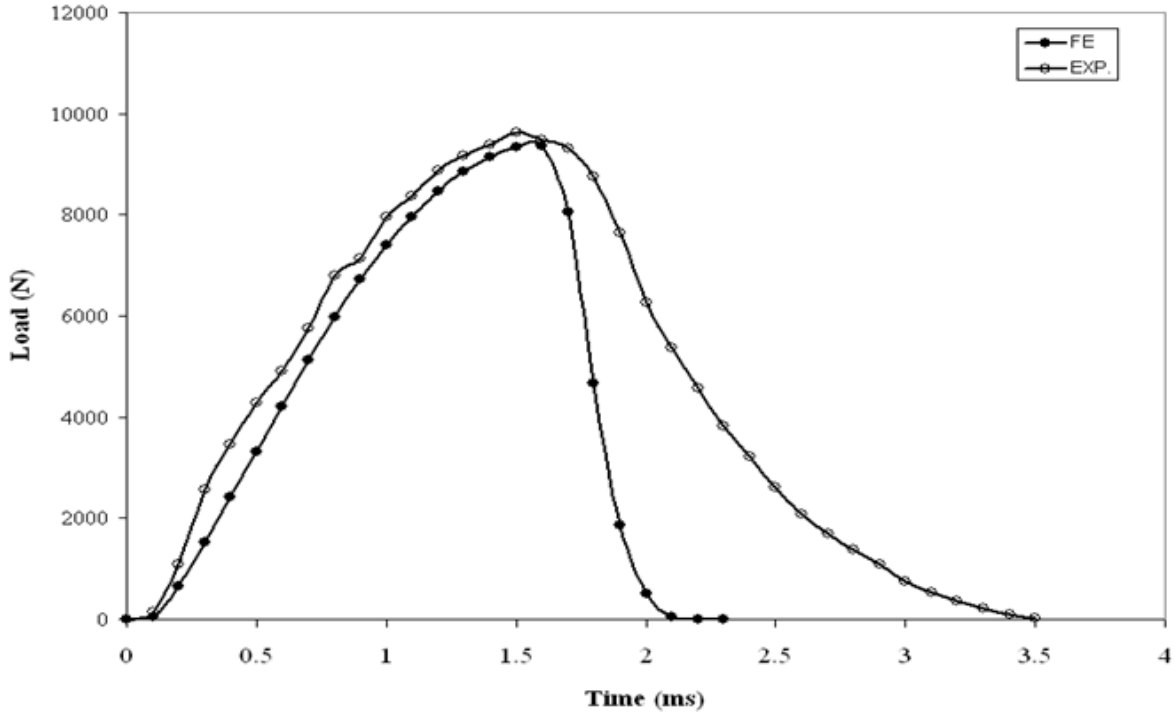


Fig.5.24: Comparison of experimental and FEA load- time histories of sandwich composites with end grain core at 26 J.

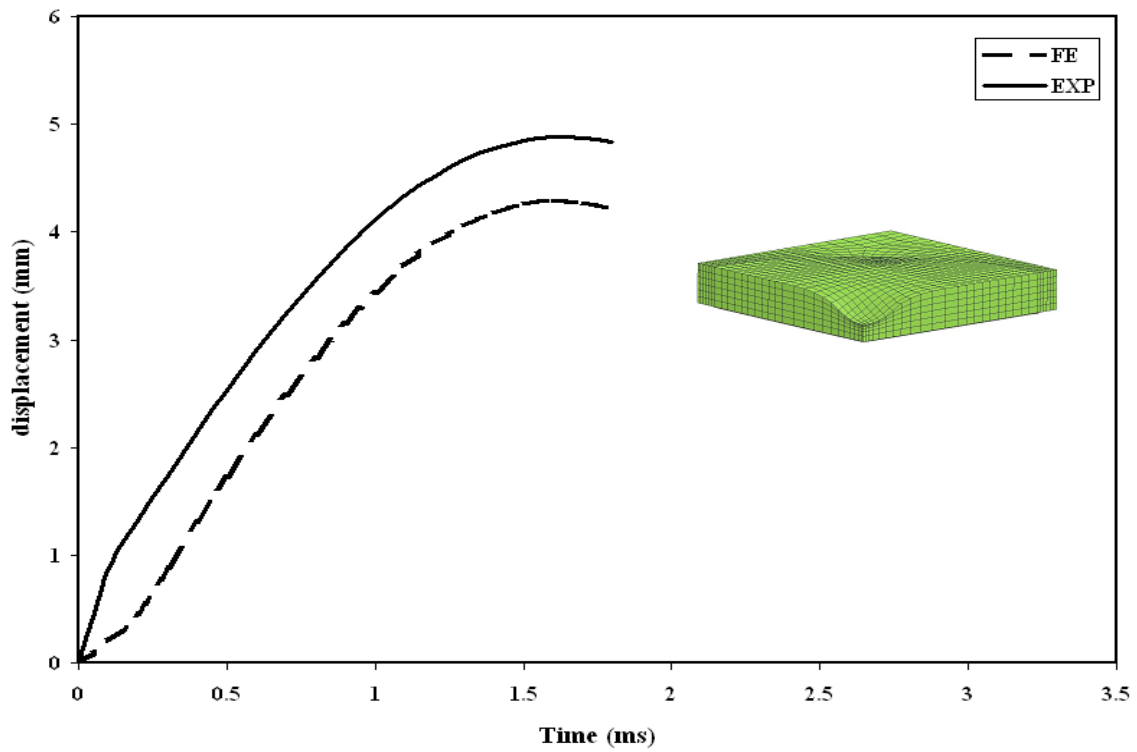


Fig.5.25: Comparison of experimental and FEA deflection- time histories of sandwich composites with end grain core at 17J.

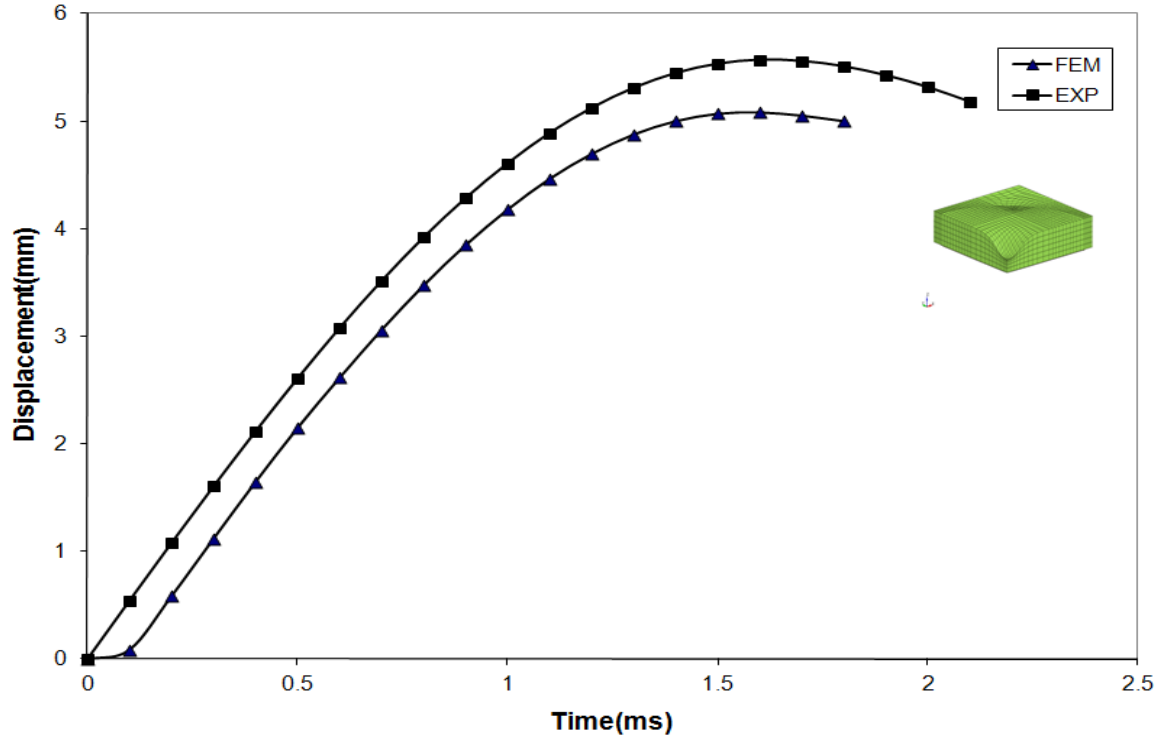


Fig.5.26: Comparison of experimental and FEA deflection- time histories for sandwich composites with end grain core at 26J.

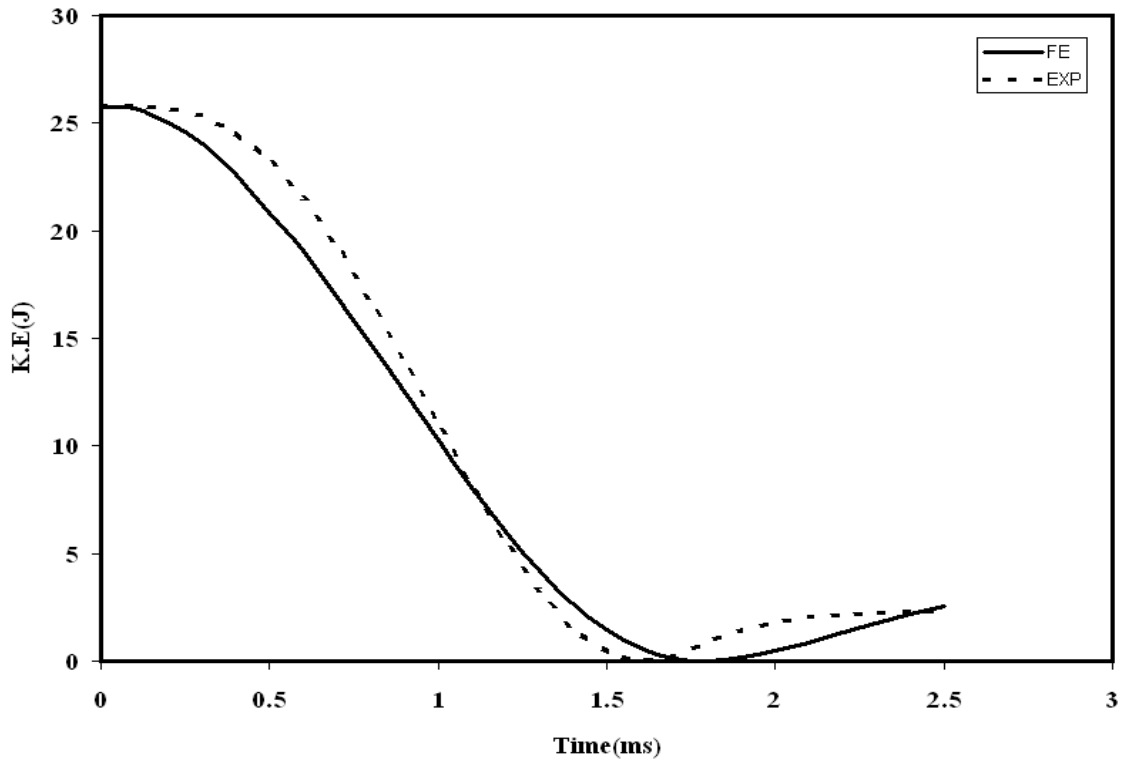


Figure 5.27: Comparison of experimental and FEA impactor kinetic energy histories for sandwich composites with end grain core at 26J.

### 5.2.2. End Grain and Regular Balsa Sandwich Systems Simulation

In Fig. 5.28 the contact force history between the impactor and the end grain core of sandwich plate as a function of time was predicted by LS-DYNA code and compared with the experimental data. Good agreement was obtained for the peak load; but, the agreement was less in duration time in the unloading portion. The reason of this difference was explained in section 5.2.1. Also the experimental data of regular balsa wood core was compared with FE analysis in terms of contact force-time histories. The results were presented in Fig. 5.29 and they show the peak value of contact force that predicted by FE was a little bit higher and short duration. That is probably due to the slight local crash of the core during the impact. A comparison of the experimental results with LS-DYNA for both sandwich systems (end grain and regular balsa cores) deflection history along z-axis is illustrated in Fig. 5.30. The agreement between the two curves for each sandwich system is good. For example, 6.6 mm and 6.7 mm values were recorded experimentally and numerically, respectively, for end grain core sandwich composite at 17J impact energy. However, the experimental and numerical displacements for regular balsa sandwich composite were 8.2mm and 8.7mm at 17J impact energy.

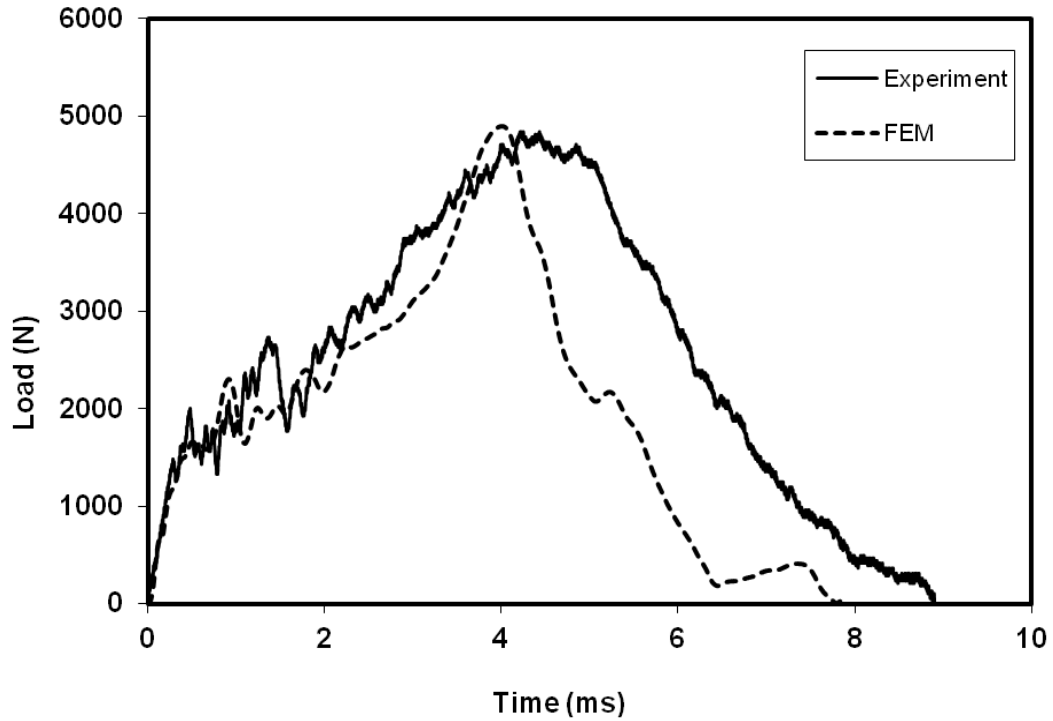


Fig. 5.28: Sandwich composite with end-grain core comparison of experimental (typical) and FEA load-time histories at 17J.

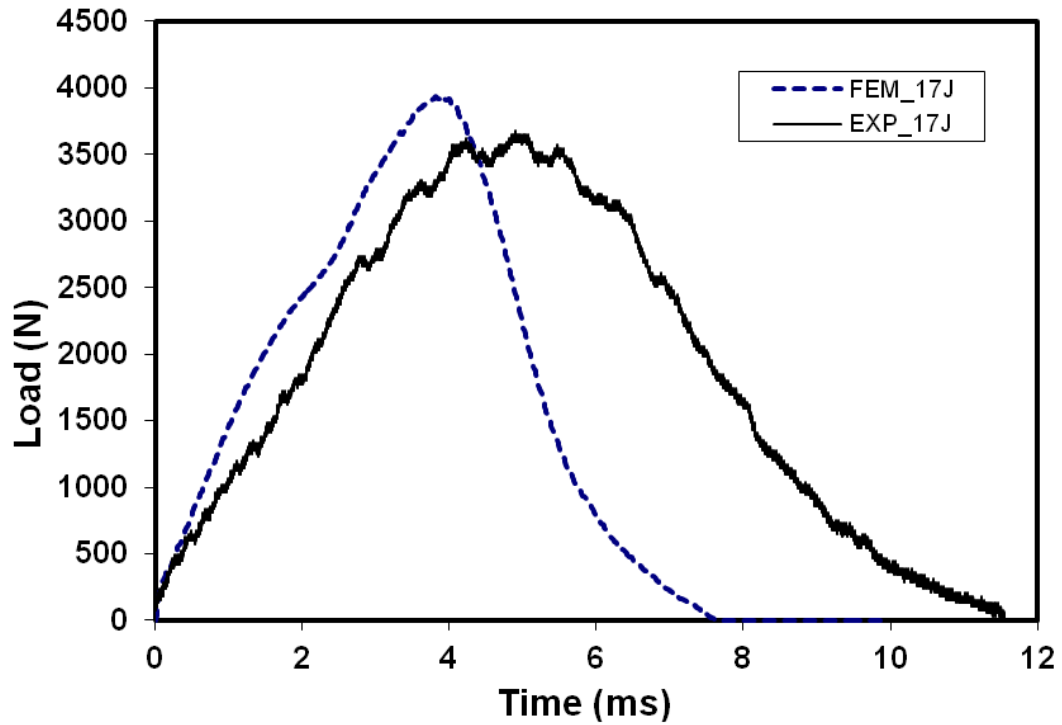


Fig. 5.29: Sandwich composite with regular balsa core comparison of experimental (typical) and FEA load-time histories at 17J.

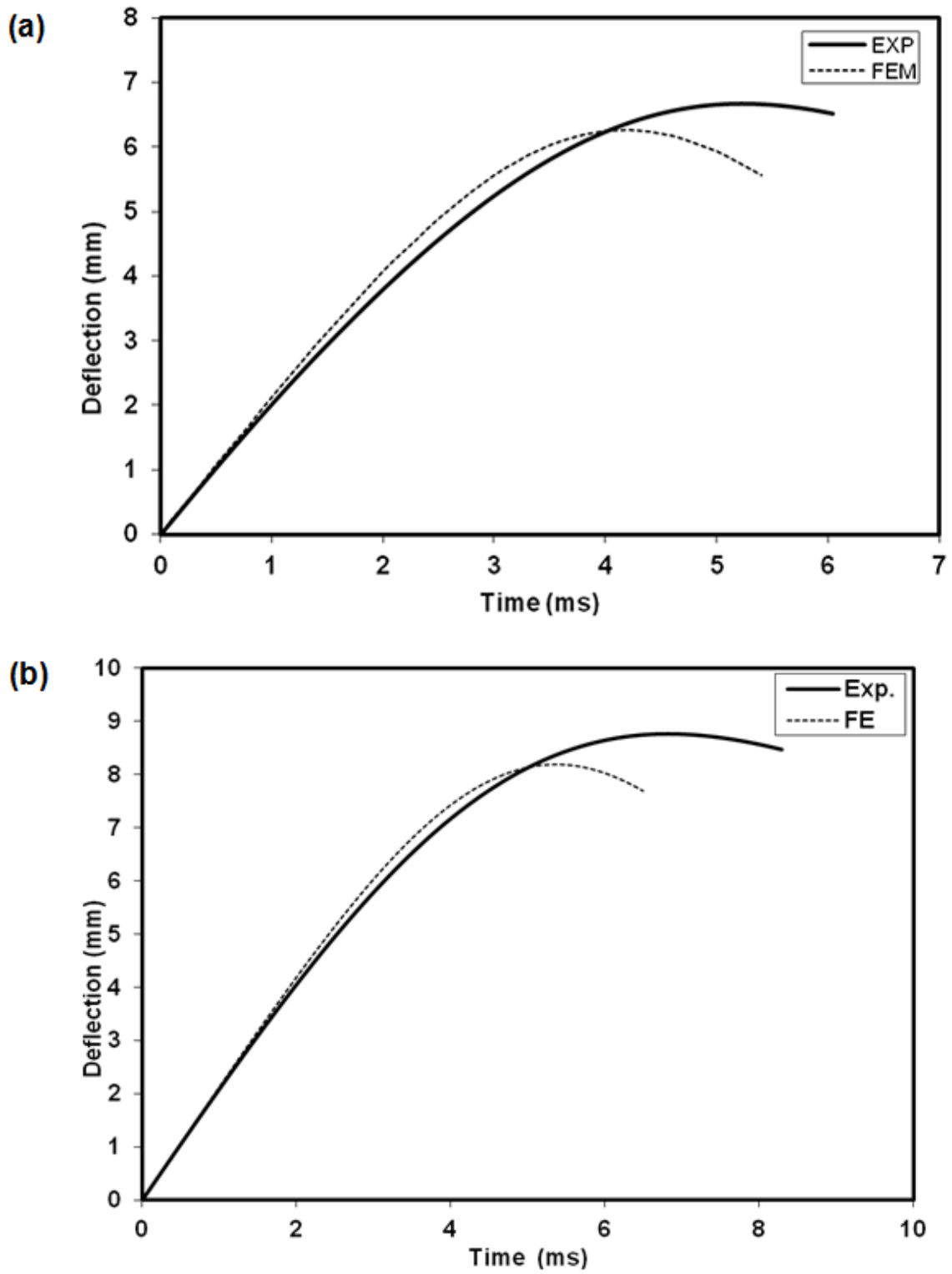


Fig. 5.30: Comparison of experimental (typical) and FEA deflection- time histories of sandwich composites with (a) end-grain (b) regular balsa at 17J.

## CHAPTER 6

### CONCLUSIONS AND RECOMENDATIONS

#### 6.1. Conclusions

Sandwich structures with end grain and regular balsa cores were fabricated, tested, and modeled to understand the behavior of sandwich composite under low velocity impact.

#### **DAMAGE MECHANISMS:**

- A. Impact on the sandwich composite results in upper skin cracks and shear failure of the core and multiple cracks due to this core damage.
- B. Inspection of the skin damage and delamination at core/skin interface can be better observed through visual inspection for the end-grain balsawood composite.

#### **EFFECT OF GRAIN ORIENTATION**

- A. Low velocity impact tests were carried out at different impact energy; only three energy levels (17J, 26J and 35J) were thoroughly investigated. The damage area increases with impact energy for both regular and end grain balsawood sandwich composites.
- B. The experimental results show that the sandwich structures with end grain core are able to withstand *higher impact loads* compared with regular balsa core because the higher stiffness of end grain core.

C. However, sandwich panels with regular balsa core offer *higher energy* absorption than end grain core sandwich composite structures.

#### ■ RESIDUAL STRENGTH

A. Compression after impact (CAI) test was conducted and residual strength was estimated which showed that end grain sandwich composite retained higher residual strength.

B. It is found that higher impact energy (17J) causes large reduction in the residual strength for both sandwich systems in the range of 40-52%.

#### ■ COMPUTATIONAL MODELING

A. LS\_DYNA code was utilized to simulate the impact test for both sandwich systems. The results of load-deflection history of experimental and finite element results were matched and showed good agreement for both composite systems.

B. The experimental and finite element results were matched better for maximum load. However, progressive damage accumulation could not be predicted well due to lack of sophisticated material damage models in FEA codes that can account for complex damage state during impact.

## 6.2. Recommendations

1. In the current study semi spherical impactor was used, in the future work are needs to investigate the effect of projectile shape on the balsa wood sandwich composite structure.
2. Investigate the role of adhesive bonding of core to face sheets.
3. Studying the effect of core thickness on the behavior of sandwich composites under low velocity impact should be studied.
4. Damage accumulative and post-impact damage models are inadequate for sandwich composites. Constitutive models need to be developed.



**REFERENCES**

- 1- Zenkert D. An Introduction to Sandwich Construction. EMAS; 1995 [ISBN 0947817778].
2. Achilles P. (1998). "Design of Sandwich Structures". Ph.D. Thesis, Cambridge University. UK.
- 3- Saito H, Kimpara I. "Evaluation of impact damage mechanism of multi-axial stitched CFRP laminate", Composites Part A, Volume 37, 2006.
- 4- Gibson RF. Principles of composite material mechanics, second edition. CRC Press; 2007 [ISBN 0824753895].
- 5- Muthyala V. Composite Sandwich Structure with Grid Stiffened Core, Osmania University, Hyderabad, India, December 2007
- 6- Office of Aviation Research. Review of damage tolerance for composite sandwich Airframe Structures ,1990.
- 7- Vlot A. Low-velocity impact loading on fibre reinforced aluminium laminates (arall) and other aircraft sheet materials, Ph.D. Thesis, Delft University of Technology, Delft, The Netherlands; October 1991.
- 8- Zhang X, Davies G, Hitchings D. Impact damage with compressive preload and post-impact compression of carbon composite plates. Int J Impact Eng 1999; 22:485–509.
- 9- Strait L, Karasek M, Amateau M. Effects of stacking sequence on the impact resistance of carbon fiber reinforced thermoplastic toughened epoxy laminates. J Compos Mater 1992; 26(12):1725–40.

- 10- Wu HYT, Chang FK. Transient dynamic analysis of laminated composite plates subjected to transverse impact. *Comput Struct* 1989;31:453–66.
- 11- Choi H, Chang F. A model for predicting damage in graphite/epoxy laminated composites resulting from low-velocity point impact. *J composite Materials* 1992; 26(14:2134-69).
- 12- Dost E, Ilcewiz L, Avery W, Coxon B. Effects of stacking sequence on impact damage resistance and residual strength for quasi-isotropic laminates. In: O'Brien T, editor. *Composites materials: fatigue and fracture*, vol. 3. American Society for Testing and Materials; 1997. p. 476–500 [ASTM STP 1110].
- 13- Caprino G, Lopresto V, Scarponi C, Briotti G. Influence of material thickness on the response of carbon-fabric/epoxy panels to low velocity impact. *Compos Sci Technol* 1999; 59:2279–86.
- 14- Caprino G, Lopresto V. The significance of indentation in the inspection of carbon fibre-reinforced plastic panels damaged by low-velocity impact. *Compos Sci Technol* 2000; 60 (7):1003–12.
- 15- Luo R, Green R, Morrison C. An approach to evaluate the impact damage initiation and propagation in composite plates. *Composites: Part B*: 2001;32:513-520.
- 16- Sadasivam B, Mallick P. Impact damage resistance of random fiber reinforced automotive composites. *J Thermoplast Compos Mater* 2002;15:181–91.
- 17- Cho C, Zhao G. Effects of geometric and material factors on mechanical response of laminated composites due to low velocity impact. *J Compos Mater* 2002;36:1403–28.

- 18- Aslan Z, Karakuzu R, Sayman O. Dynamic characteristics of laminated woven E-glass–epoxy composite plates subjected to low velocity heavy mass impact. *J Compos Mater* 2002; 36(21):2421–42.
- 19- Aslan Z, Karakuzu R, Okutan B. The response of laminated composite plates under low velocity impact loading. *Compos Struct* 2003; 59:119–27.
- 20- Datta S, Krishna A, Rao R. Low velocity impact damage tolerance studies on glass–epoxy laminates – effects of material, process and test parameters. *J Reinf Plast Compos* 2004; 23(3):327–45.
- 21- Hosur M, Adbullah M, Jeelani S. Studies on the low-velocity impact response of woven hybrid composites. *Compos Struct* 2005; 67:253–62.
- 22- Saez S, Barbero E, Zarea R, Navarro C. Compression after impact of thin composite laminates. *Composite Science and Technology* 2005; 65:1911-1919.
- 23- Hosseinzadeh R, Shokrieh M, Lessard L. Damage behavior of fiber reinforced composite plates subjected to drop weight impacts. *Composites Science Technology* 2006; 66 :61-68.
- 24- Tiberkak R, Bachene M, Rechak S, Necib B. Damage prediction in composite plates subjected to low velocity impact. *Compos Struct* 2008;83:73–82.
- 25- Ulven C, Vaidya U, Hosur M. Effect of projectile shape during ballistic perforation of VARTM carbon/epoxy composite panels. *Compos Struct* 2003; 61:143-150.
- 26- Aslan Z, Karakuzu R. (2002). Transient dynamic analysis of laminated composite plate subjected to low velocity impact. *Mathematical and computational applications*, vol.7,No.,pp.73-82.

- 27- Kim C, Jun E. Impact resistance of composite laminated sandwich plates. *J Comp Mater* 1992; 26 (15):2247–62.
- 28- Abrate S. Localized impact on sandwich structures with laminated facings. *Appl Mech Rev* 1997;50(2): 69–82.
- 29- Anderson T, Madenci E. Experimental investigation of low-velocity impact characteristics of sandwich composites. *Compos Struct* 2000; 50 (3):239–47.
- 30- Hosur M, Abdullah M, Jeelani S. Manufacturing and low-velocity impact characterization of foam filled 3-D integrated core sandwich composites with hybrid face sheets. *Compos Struct* 2005; 69: 167–81.
- 31- Schubel P, Luo J, Daniel I. Low velocity impact behavior of composite sandwich panels. *Composites: Part A* 2005; 36 :1389–98.
- 32- Schubel P, Luo J, Daniel I. Impact and post impact behavior of composite sandwich panels. *Composites: Part A* 2007; 38: 1051–7.
- 33-Vaidya U, Selvam P, Shane B, Chad U, Dana G, Biji M. Impact and post impact vibration response of protective metal foam composite sandwich plates. *Material Science and Engineering A* 2006 : 428: 59-66.
- 34- Imielinska K, Guillaumat L, Wojtyra R, Castaings M. Effects of manufacturing and face/core bonding on impact damage in glass/polyester–PVC foam core. *Composites: Part B* 2008; 39: 1034–1041.
- 35- Ulven C, Vaidya K. Impact response of fire damaged polymer-based composite materials. *Composites: Part B* 2008; 39: 92–107.
- 36- Deka J, Vaidya K. LS-DYNA® Impact Simulation of Composite Sandwich Structures with Balsa Wood Core.conf.2008.

- 37- Leijten J, Bersee H, Bergsma O, Beukers A. Experimental study of the low velocity impact behavior of primary sandwich structures in aircraft. *Composites Part A* 2009;40:164-175.
- 38- Atas C, Sevim C. On the impact response of sandwich composites with cores of balsa wood and PVC foam. *Composites* :2010; 93:40-48.
- 39- Wing B, Wu L, Li F. Low velocity characteristics and residual tensile strength of carbon fiber composite lattice core sandwich structures. *Composites : part B*(2011).
- 40- Avinash S. P. (2012). Flexural analysis of balsa core sandwich composite: failure mechanisms, core grain orientation and padding effect. Wayne State University Theses. pp. 164.
- 41- Schweizerof K, Weimar K, Munz T, Rottner T. Crashworthiness Analysis with Enhanced Composite Material Models in LS-DYNA-Merits and Limits. *LS-Dyna World Conference*,1998.
- 42- Tabiei A and Wu. Three dimensional non linear orthotropic finite element material model for wood, *Composite structure* 50 (2000), pp.143-149.
- 43- Murray Y, Reid J, Faller R, Bielenberg B, and Paulsen T. Evaluation of LS-DYNA Wood Material model 143, US Department of Transportation, FHWA-HRT-04-096, August 2005.
- 44- LS- DYNA Theoretical Manual. Version 970, Livermore Software Tech. Corp., April 2003.
- 45- Luo R, Green E, Morrison C. (2001). An approach to evaluate the impact damage initiation and propagation in composite plates. *Composite: part B* , 32: 513-520.

**ABSTRACT****IMPACT DAMAGE ANALYSIS OF BALSAWOOD SANDWICH COMPOSITE MATERIALS**

by

**SUOF OMRAN ABDALSLAM**

August 2013

**Advisor:** Prof. Golam Newaz**Major:** Mechanical Engineering**Degree:** Doctor of Philosophy

In this study, a new composite sandwich structure with a balsa wood core (end grain and regular balsa) in conjunction with E-glass/epoxy face sheets was proposed, fabricated, impact tested, and modeled. The behavior of the sandwich structure under low velocity impact and compression after impact was investigated. Low velocity impact tests were carried out by drop-weight impact tower at different energy levels (8J-35J) to evaluate the impact response of the sandwich structure. Visual inspection, destructive and non destructive evaluation methods have been conducted. For the sandwich plate with end grain core, the damage was very clear and can be visually detected. However, the damage in regular balsa core was not clearly visible and destructive evaluation method was used. Compression testing was done after subjecting the specimens to impact testing. Impact test results; load-time, load-deflection history and energy absorption for sandwich composites with two different cores, end grain and regular balsa were compared and they were investigated at three different impact energies. The results show that the sandwich structures with end grain core are able to withstand impact loading better than the regular balsa core because the higher stiffness of end

grain core informs of sustaining higher load and higher overall energy. The results obtained from compression after impact testing show that the strengths of sandwich composites with end grain and regular balsa cores were reduced about 40% and 52%, respectively, after impact. These results were presented in terms of stress-strain curves for both damaged and undamaged specimens. Finite element analysis was conducted on the sandwich composite structure using LS-DYNA code to simulate impact test. A 3-D finite element model was developed and appropriate material properties were given to each component. The computational model was developed to predict the response of sandwich composite under dynamic loading. The experimental and finite element results were matched better for maximum load. However progressive damage accumulation could not predicted well due to lack of sophisticated material damage models in FEA codes.

**AUTOBIOGRAPHICAL STATEMENT****SUOF OMRAN ABDALSLAM**

Souf Abdalslam earned a Bachelor's degree in Mechanical Engineering from Tripoli University in Tripoli, Libya in 1991, a Master's degree in Mechanical Engineering from Kazan State University in Kazan -Tatarstan, Russia in 2002, and he has been at Wayne State University since 2009. From 1991-2008, Suof Abdalslam was working as engineer in the department of design at the Central Agency for Research in Tripoli, Libya. Suof is a member in a variety of professional and engineering organizations such as American Society of Mechanical Engineers and Society of Plastic Engineers.